Failure Analysis of RC Structures using Volume Control Technique

-COE Intensive Course-

Feb. 3, 2005

Hokkaido University, Sapporo, Japan

Ha-Won Song

School of Civil and Environmental Engineering

Concrete Materials, Mechanics and Engineering Lab.
YONSEI UNIVERSITY

Outline

- Introduction
  - Characteristic of failure in concrete structures
  - Homogenized crack model
  - Volume control method
- Modeling for cracked RC and ECC
  - Constitutive equations of RC/ Layered shell element
  - Modeling of ECC as re-strengthening material
- Analysis results and comparison
  - RCCV subjected to internal pressure
  - RC tank , RC slab, and RC box culvert subjected to various loading
  - RC hollow column subjected to lateral loading
  - Verification with PCCV
- Conclusion and future work

Performance of deteriorated/repaired RC structures ?

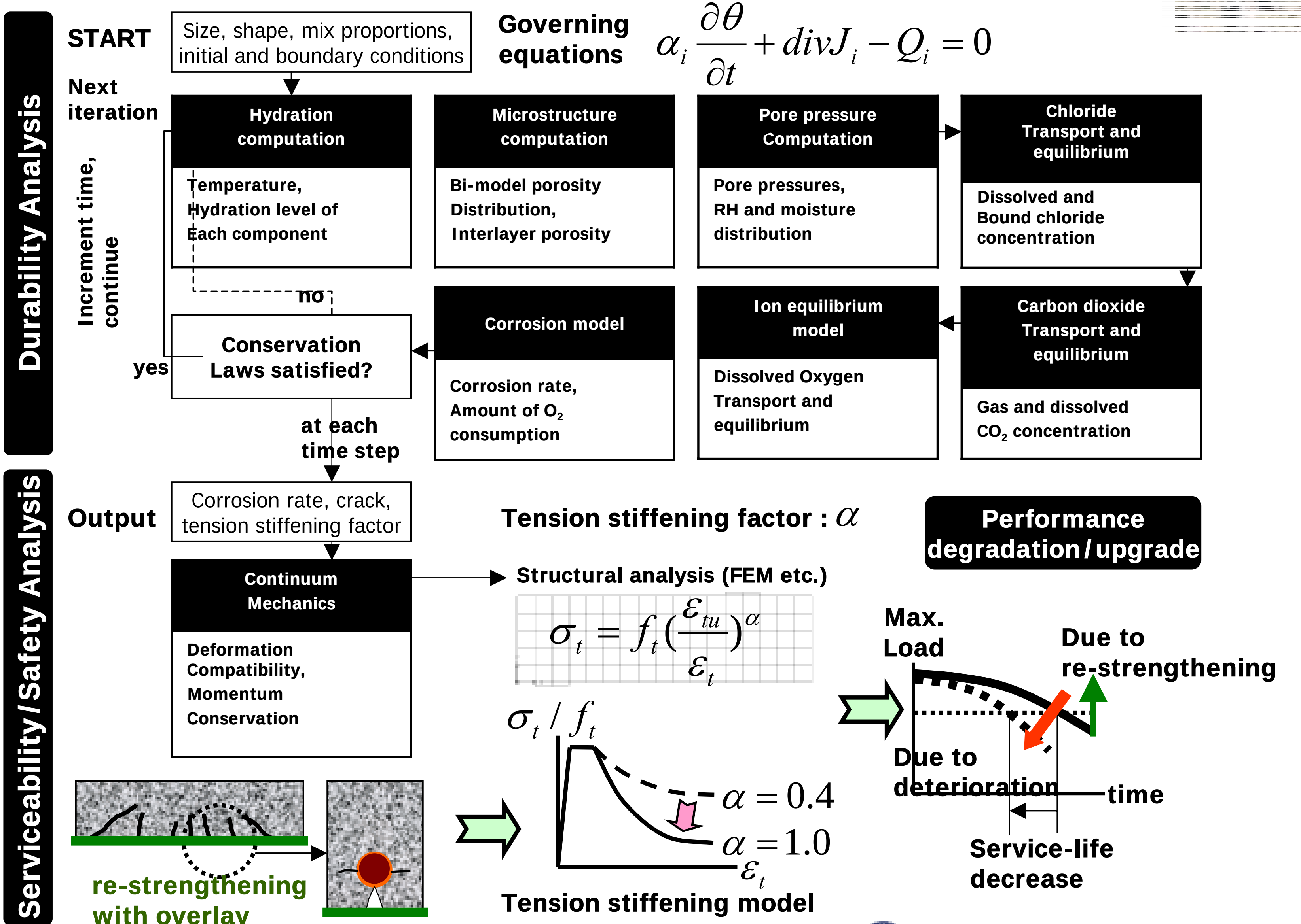

Characteristics of concrete fracture and analysis

- Material instability

Micro cracks → localize → **Major macro cracks**

Softening behavior

- Decreased load resistant capacity after peak
- Localized strain

Numerical problem in concrete fracture analysis :

- Loss of ellipticity of governing equation
- Ill-posed boundary value problem

Numerical drawback (Mesh sensitivity)

Structural instability

Sources of Non-linearity ; Material, Geometrical, Boundary and Contact

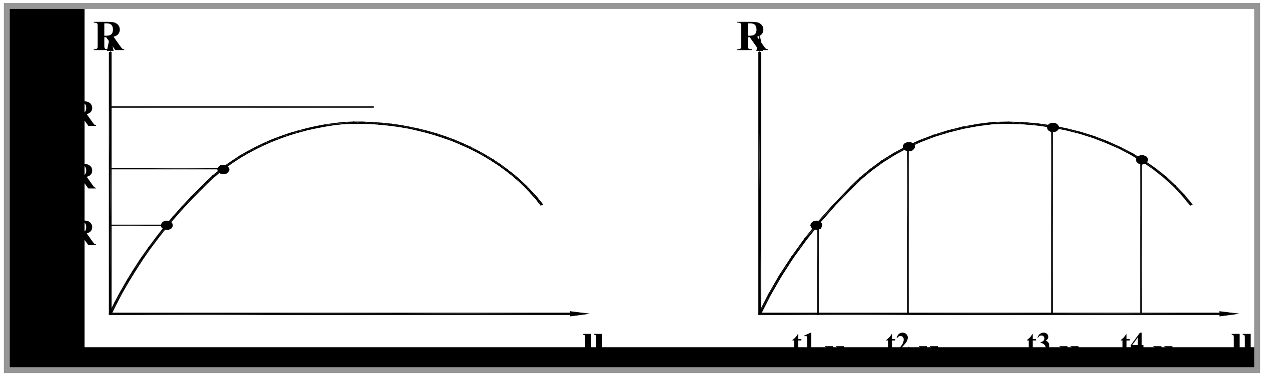

Load control

Displacement control

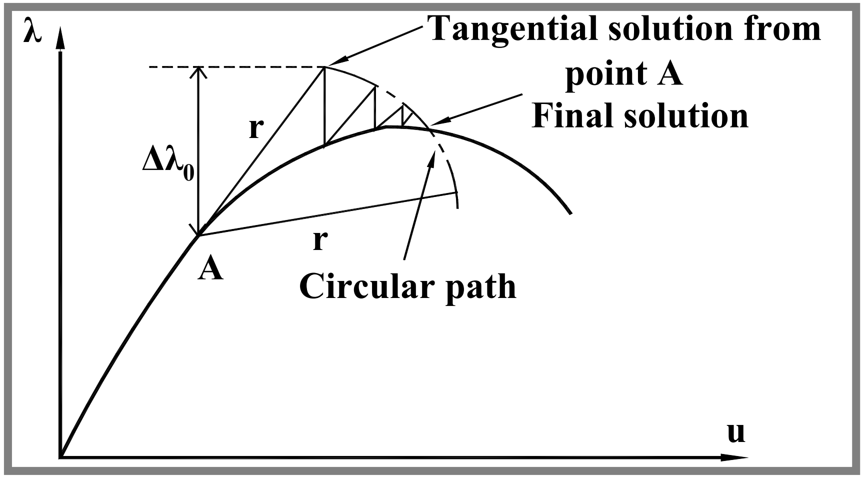

Arc-length control method

Effort to solve material instability in progressive fracture analysis of concrete using FEM

Discrete crack model and smeared crack model (in 1980's)

Embedded discontinuities approximations (in 1990's)

Continuum approximation

- Strain-stress relationship
- Discontinuity : strain localization zone

Discrete approximation

- Displacement jump-traction
- Discontinuity : crack

Weak discontinuities

- Strain localization band width is finite ($k \gg 0$)

Strong discontinuities

- Strain localization band width is very small ($k \to 0$)

Homogenized crack model

Effort to solve structural instability in progressive failure of concrete shell structures using FEM

Failure analysis of RC shell structures subjected to various loadings

Load Control Method : difficulty to obtain post-peak ultimate behavior of RC structures

Displacement Control Method : difficulty to select a representative point for displacement control in 3D

Layered shell utilizing in-plane constitutive models of RC

- **Remove the drawback of load control method**
- **overcome the limitation for displacement control method**

Volume Control Method

Volume Control Method with Pressure Node

- **Pressure Node : the uniform change of applied pressure on the shell element (Δp) (Song and Tassoulas, IJNME, 1993)**

$$\Delta V = \int_{b^e} \boldsymbol{n}^T \cdot \Delta \boldsymbol{u} \, \mathrm{d} b^e = \left(\int_{b^e} \boldsymbol{n}^T \cdot N \, \mathrm{d} b^e \right) \Delta \boldsymbol{U}$$

$$\int_{b^e} N^T (\boldsymbol{t} + \Delta \boldsymbol{t}) \, \mathrm{d} b^e = -(\boldsymbol{p} + \Delta \boldsymbol{p}) \int_{b^e} N^T \boldsymbol{n} \, \mathrm{d} b$$

$$\boldsymbol{K}_e \Delta \boldsymbol{U} = -(\boldsymbol{p} + \Delta \boldsymbol{p}) \int_{b^e} N^T \boldsymbol{n} \, \mathrm{d} b^e - \boldsymbol{F}_e$$

$$\begin{bmatrix} \boldsymbol{K}_e & \int_{b^e} N^T \boldsymbol{n} \, \mathrm{d} b^e \\ \int_{b^e} N^T \boldsymbol{n} \, \mathrm{d} b^e & 0 \end{bmatrix} \begin{bmatrix} \Delta \boldsymbol{U} \\ \Delta \boldsymbol{p} \end{bmatrix} = \begin{bmatrix} \boldsymbol{p} \int_{b^e} N^T \boldsymbol{n} \, \mathrm{d} b^e - \boldsymbol{F}_e \\ \Delta V \end{bmatrix}$$

Path dependant pseudo-volume control technique

- **Pseudo Volume (Song et. al, J. Str. Eng. 2002)**

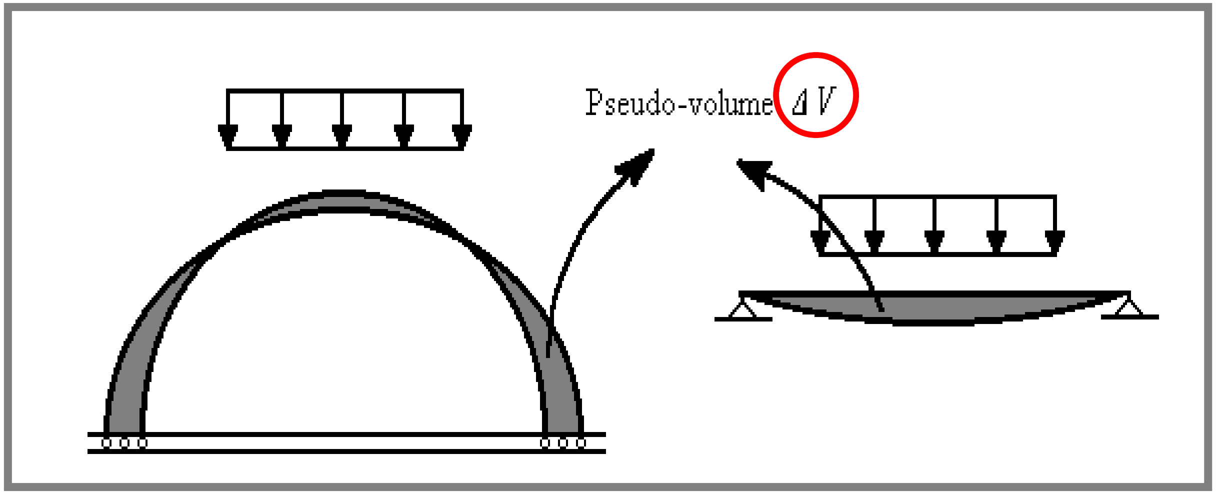

- **Path-dependent Volume (Song et. al, Nuclear Eng. and Design, 2003)**

Algorithm for path dependant volume control technique

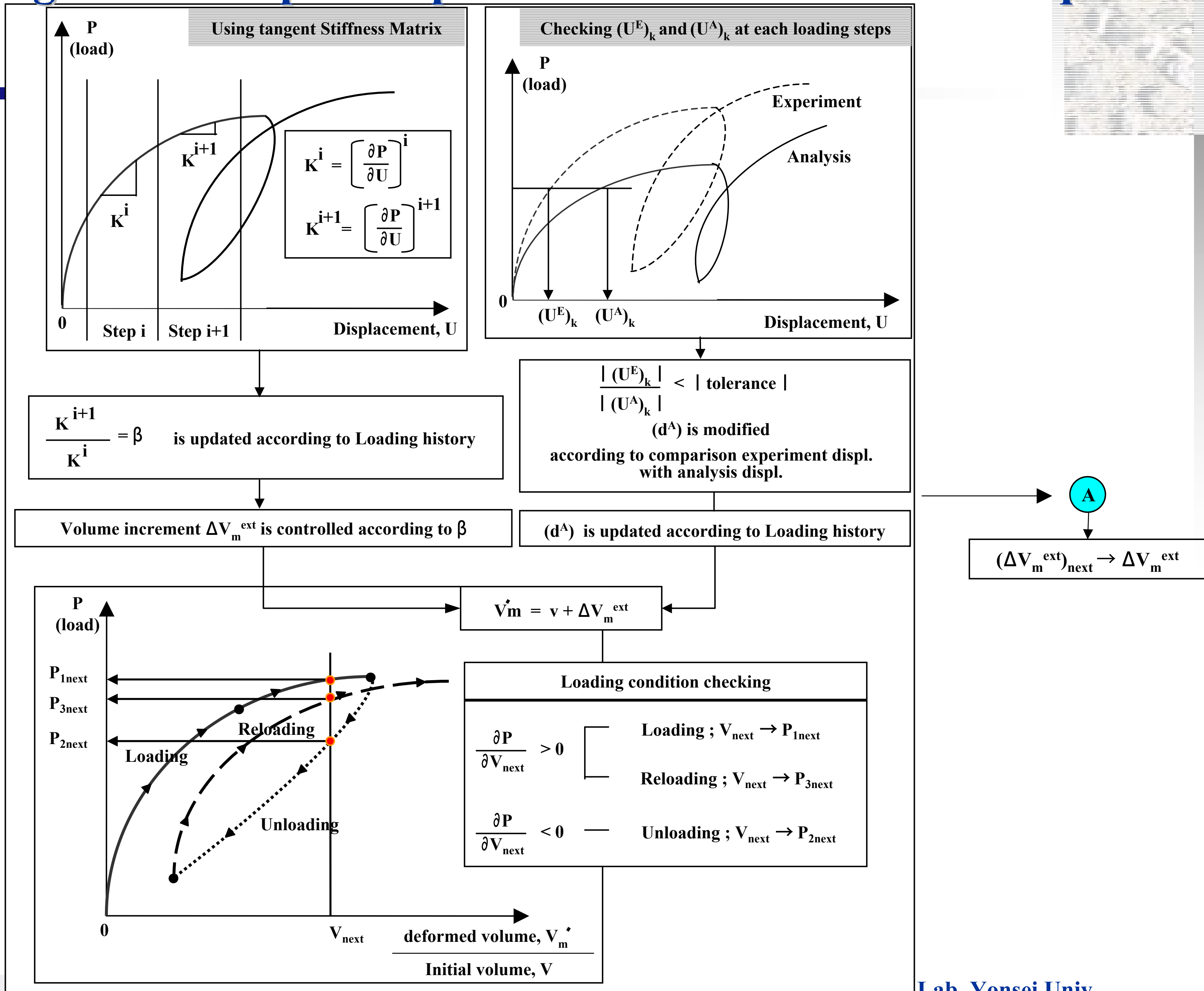

Solution procedure path-dependant volume control method

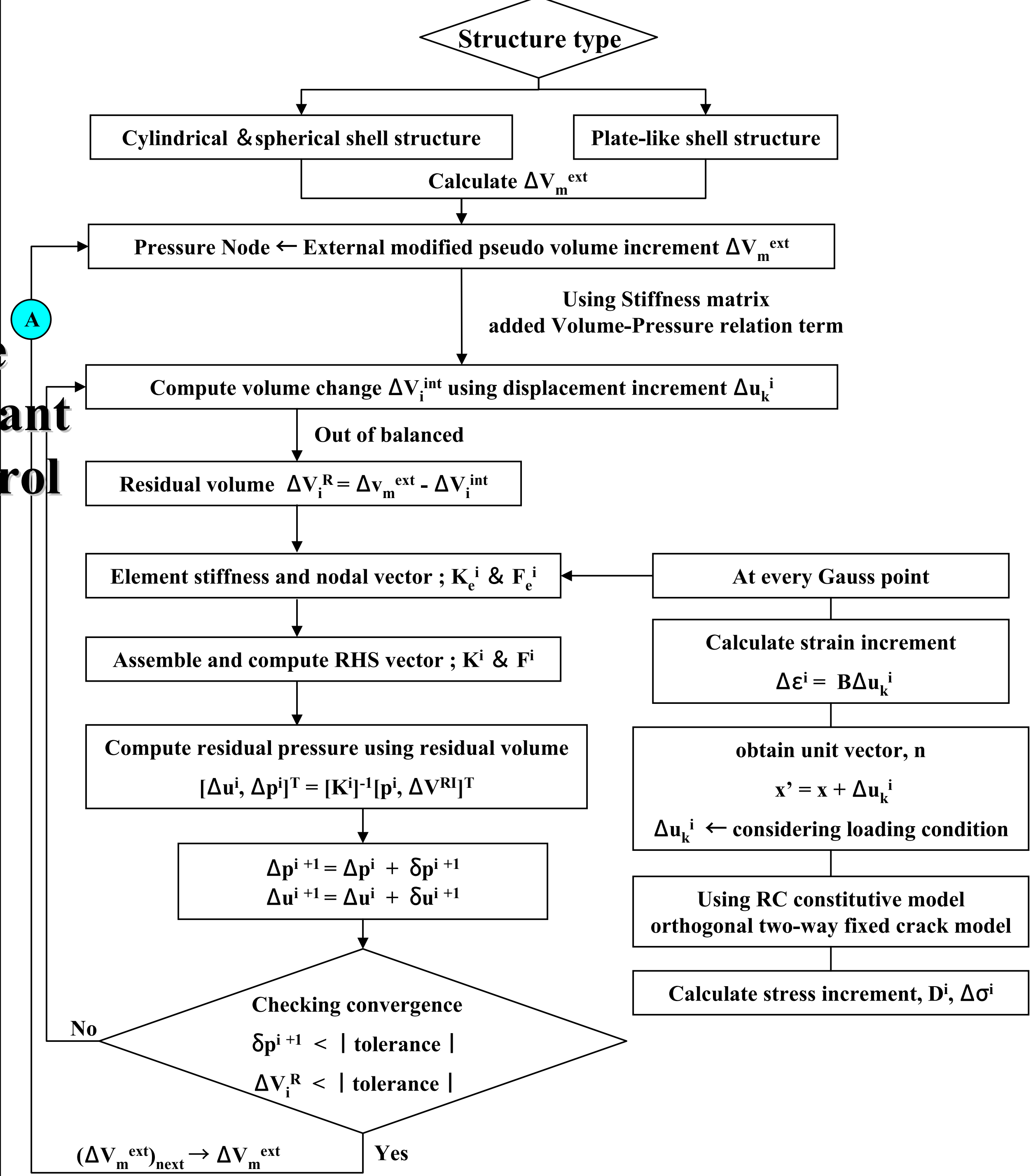

Layered shell element

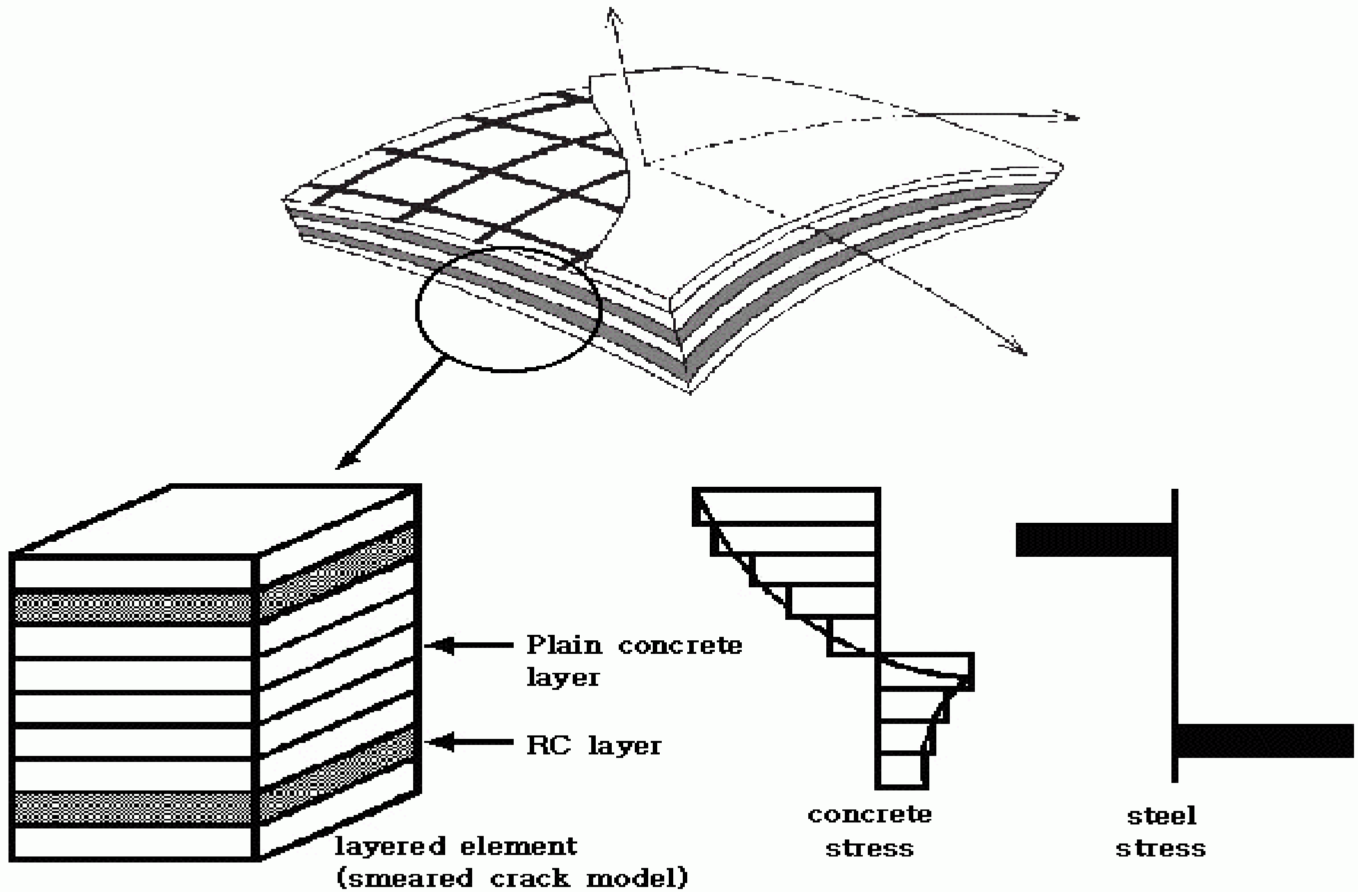

- Degenerated, isoparametric, serendipity, quadratic shell element with drilling degree of freedom
- Geometrical nonlinearity is considered by adopting total Lagrangian formulation
- In plane constitutive laws applied to each layer of element consists of RC layers and PL layers

Constitutive law for each layer

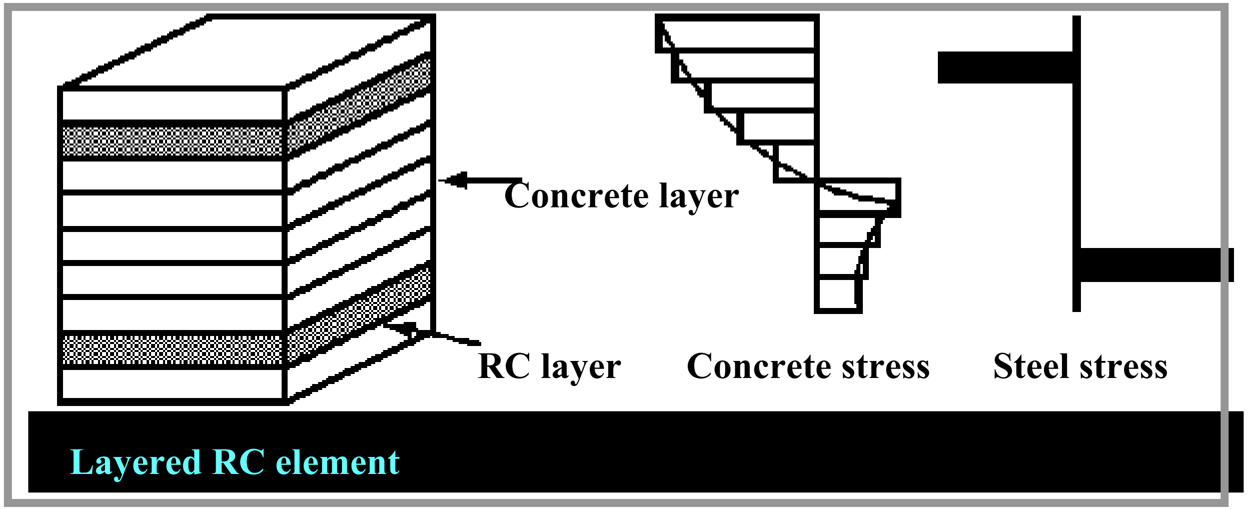

— Concrete under compression : Elasto-plastic fracture model (Maekawa et. al)

— Cracked concrete : Smeared fixed crack model

— Concrete under shear : Crack density model (Maekawa and Li)

Shear locking + Membrane locking

↓

Reduced integration (2 x 2 Gaussian quadrature)

In-plane constitutive models of cracked concrete

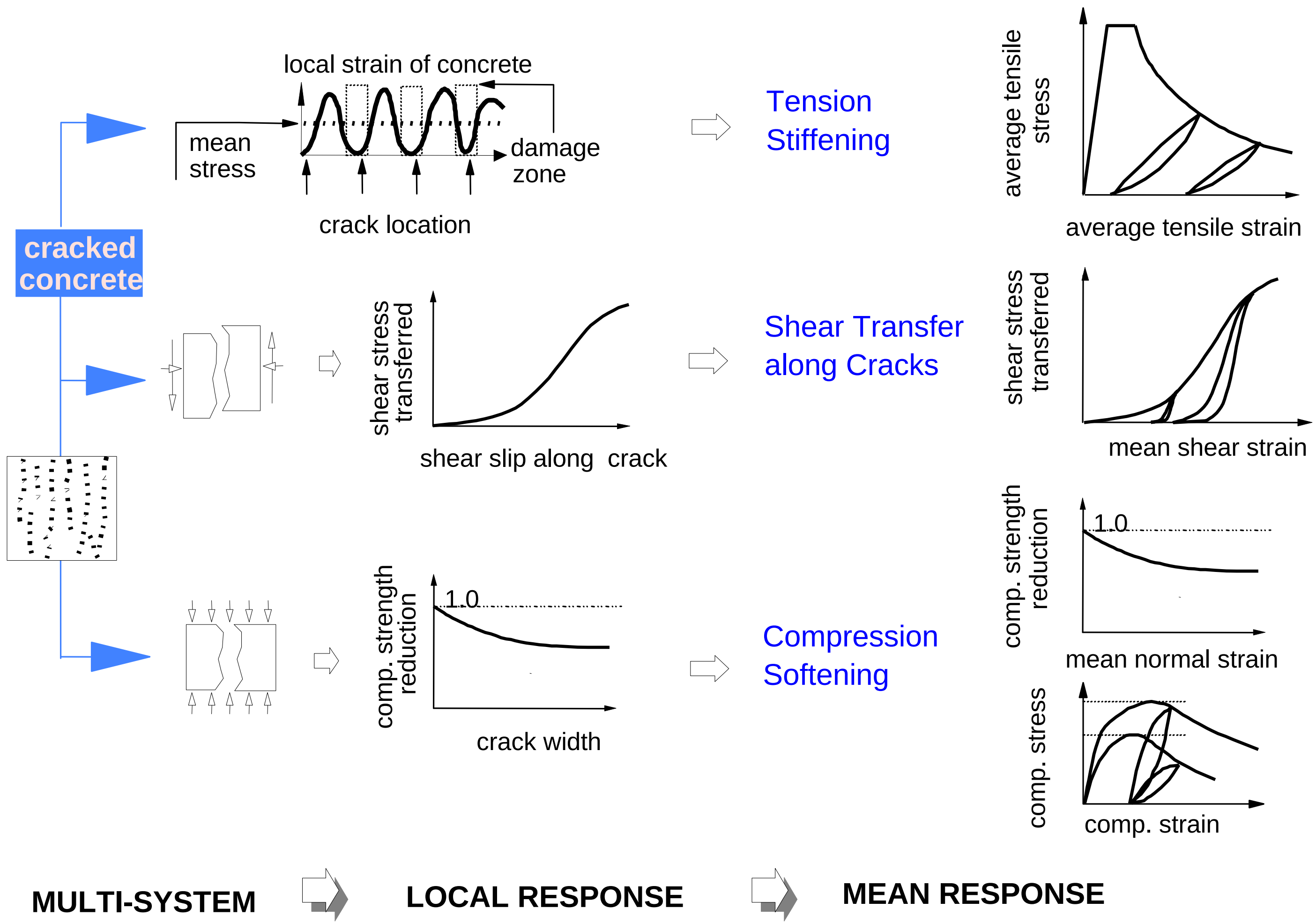

Cracking criteria of concrete

Cracking is affected by past loading history.

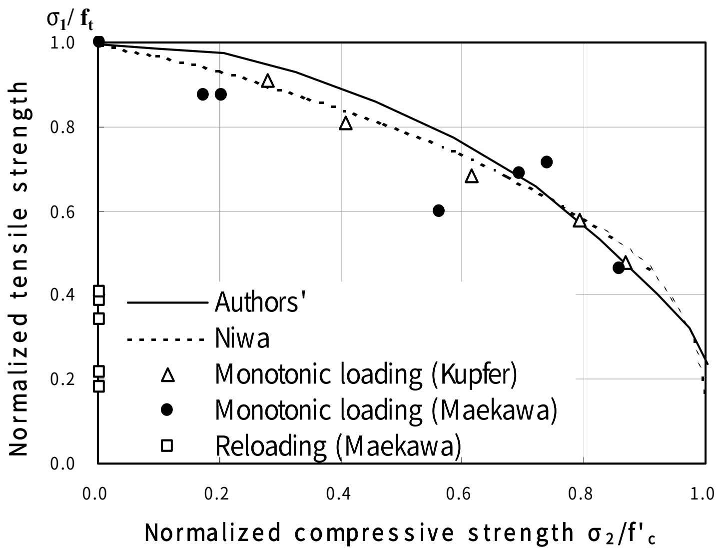

< Failure envelope in tension-compression domain >

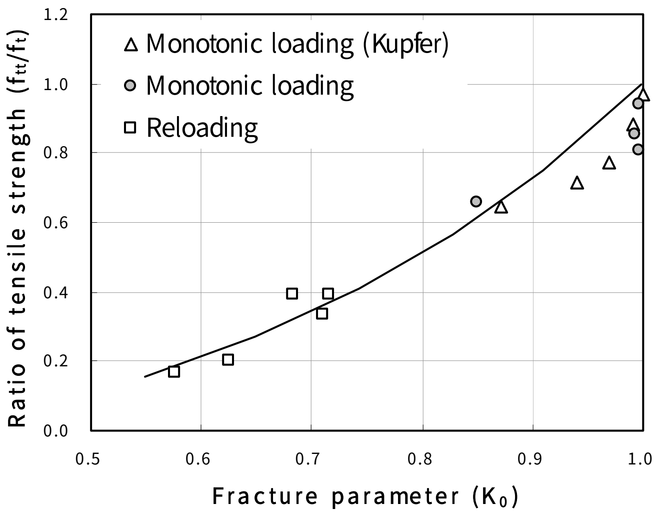

< Normalized tensile strength and fracture parameter >

By taking account influence of continuum fracture in past compression, cracking criterion can be defined in the space of biaxial principal stresses

$$\frac{\sigma_1}{(R_f \cdot f_t)} = 1.0$$ Compression-tension domain

$$\left(\frac{\sigma_1}{(R_f \cdot f_t)}\right) + 0.26\left(\frac{\sigma_2}{\sigma_1}\right) = 1.0$$ Tension-tension domain

Where, σ_1, σ_2 : principal stress ($\sigma_1 > \sigma_2$)

f_t : uniaxial tensile strength

R_f : tensile strength reduction factor

Tension stiffening model

Concrete model under tensile stress is unrelated to spacing of cracks, direction of reinforcing bars and reinforcement ration.

Tension stiffening effect is known to increase overall stiffness of RC in tension compared with that of single reinforcing bar.

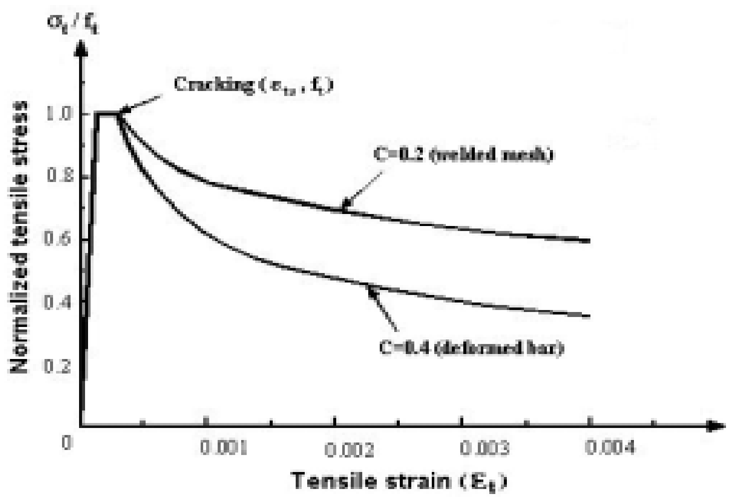

< Tension stiffening model for deformed bars (c=0.4) and welded meshes (c=0.2) >

$$\sigma_t = f_t \left(\frac{\varepsilon_{tu}}{\varepsilon_t} \right)^c$$

Where, σ_t : average tensile stress, ε : average tensile strain

f_t : uniaxial tensile strength, ε_{tu} : cracking strain

c : stiffening parameter

Steel model

Reinforcing bar model is based on the assumed cosine distribution of bar stress and concrete tension stiffening.

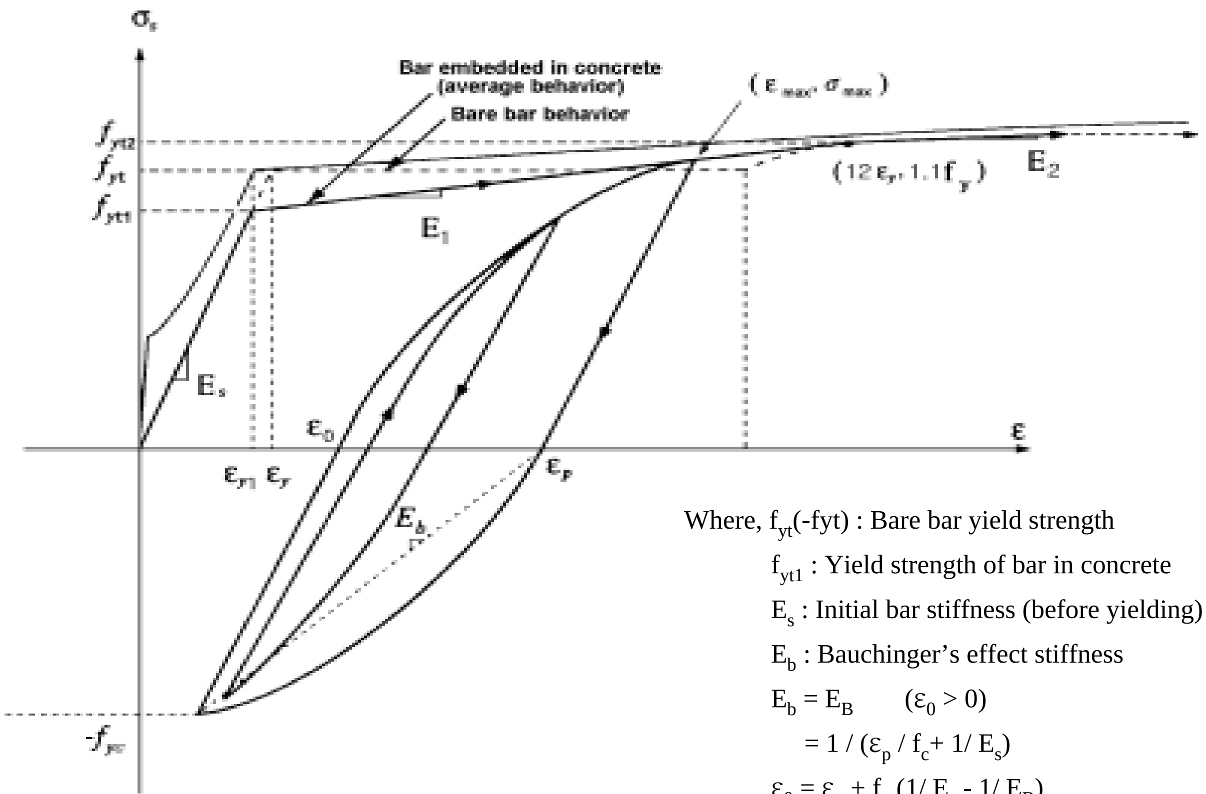

Where, f_{yt}(-fyt) : Bare bar yield strength

f_{yt1} : Yield strength of bar in concrete

E_s : Initial bar stiffness (before yielding)

E_b : Bauchinger's effect stiffness

$E_b = E_B \quad (\varepsilon_0 > 0)$

$= 1 / (\varepsilon_p / f_c + 1/ E_s)$

$\varepsilon_0 = \varepsilon_p + f_c (1/ E_s - 1/ E_B)$

$E_B = - E_s \log_{10}(10\, \varepsilon_p)/6$

Multi-directional smeared crack approach

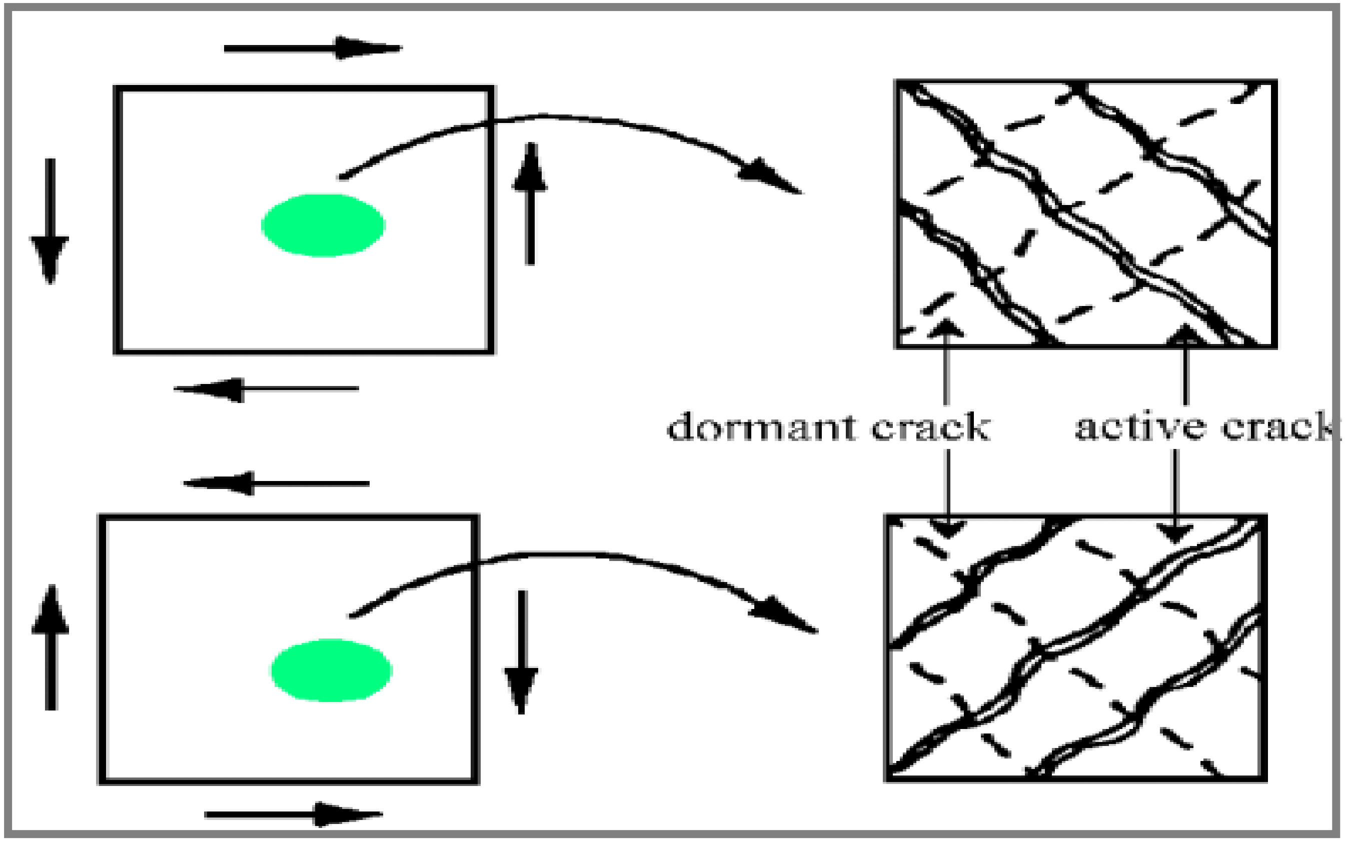

One-way active crack governs the overall nonlinearity as for in-plane cyclic shear

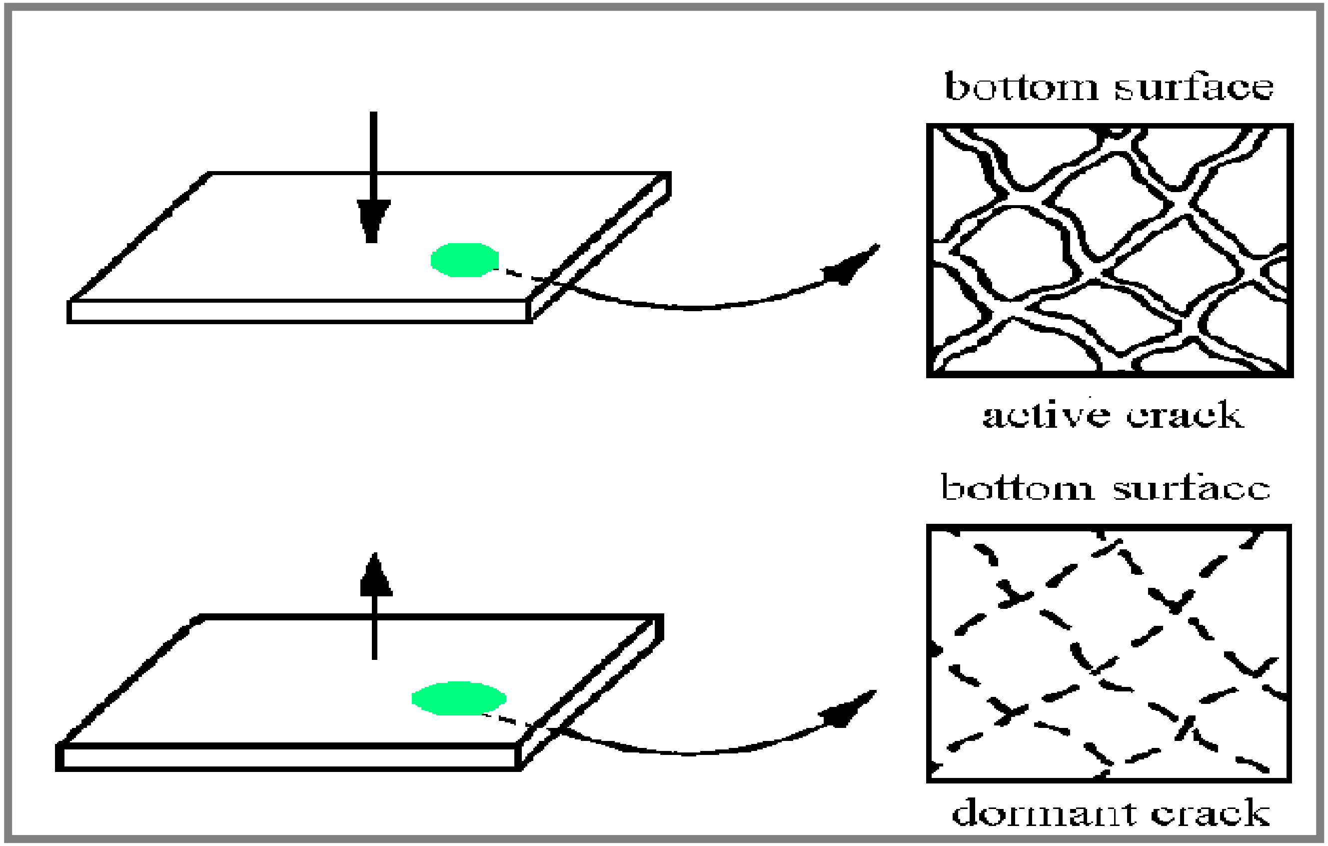

Two-way active cracks may control the overall nonlinearity as for out of plane cyclic action

Orthogonal two-way fixed crack model

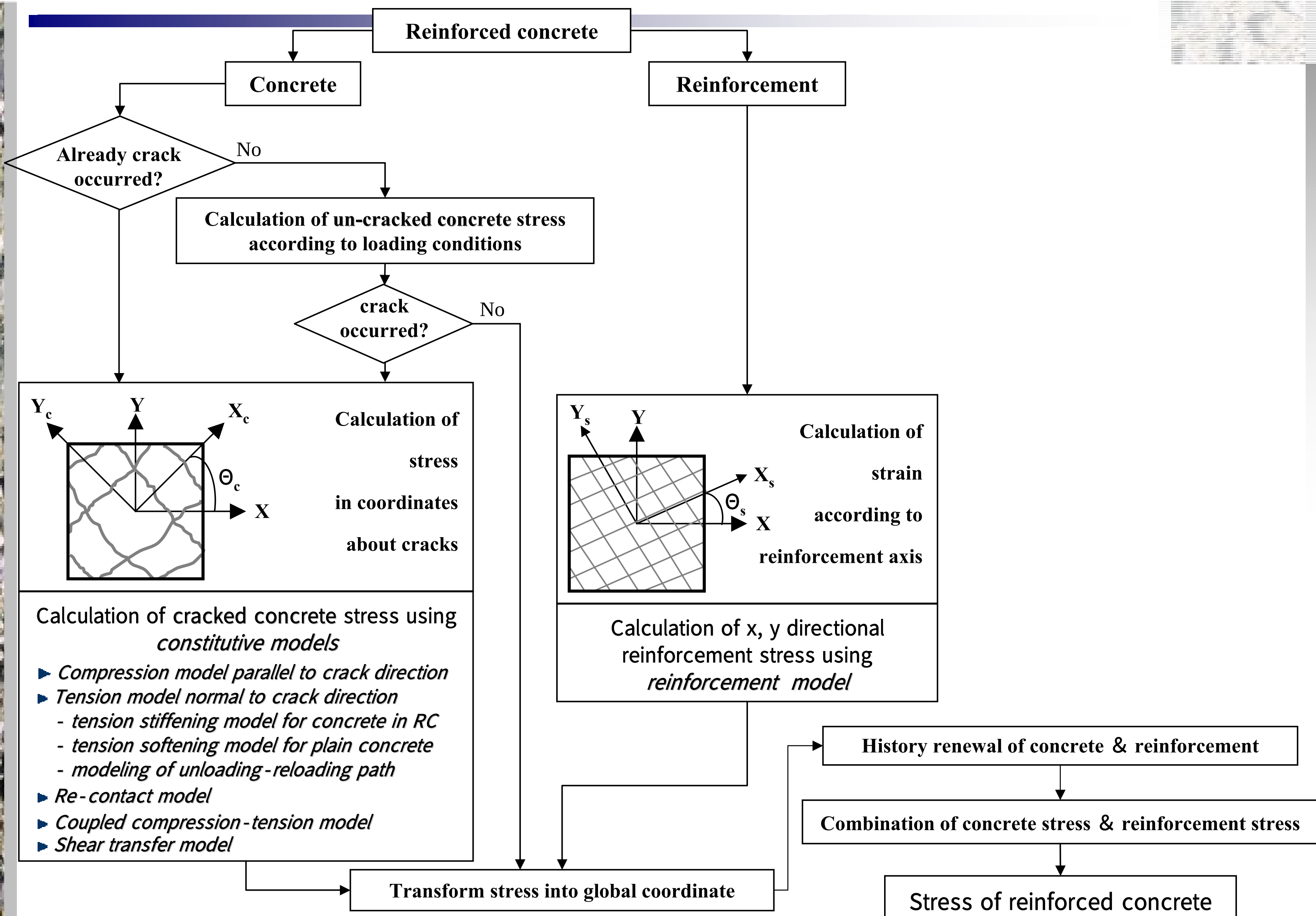

ECC as durable overlays and repair layers

Engineered_Cementitious Composites (ECC)

V.C. Li et al. 1992~

- cementitious matrix + short random fibers
- conscious micromechanics-based design of material composition … Performance Driven Design Approach
- high performance with low fiber content (~2%)

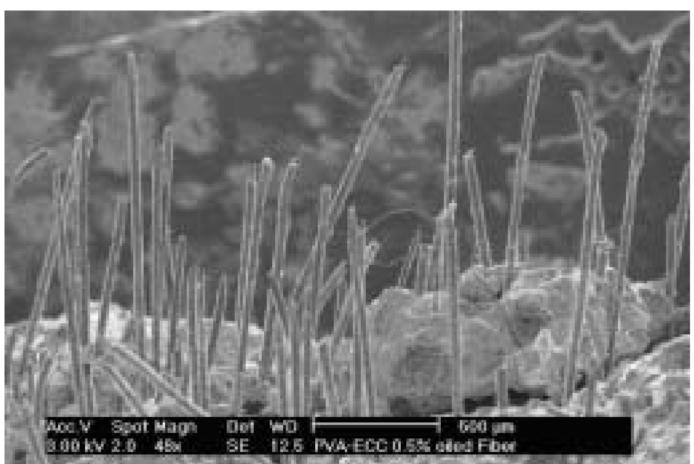

High performance cementitious composites

- cementitious matrix + fibers
- multiple cracking

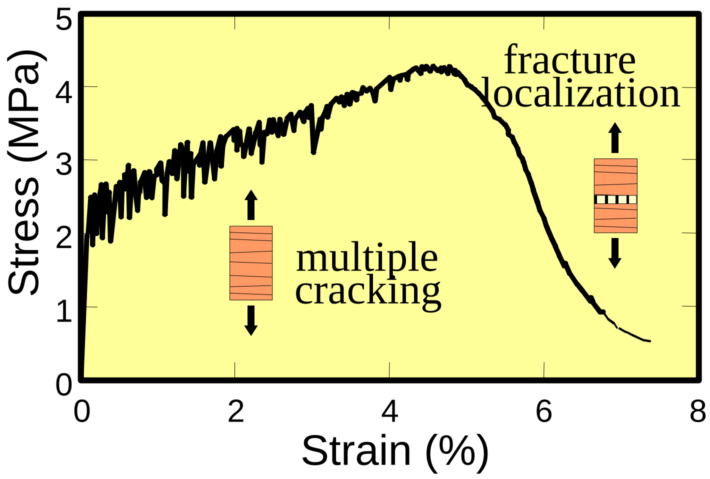

- high overall ductility in tension and shear

  with ease of processing

  and variability of shaping

- damage tolerance, durability, ...

Characteristic of ECC behavior

mechanical properties:

- high tensile strain capacity (~5%)
- small crack width O(10~100 μm)

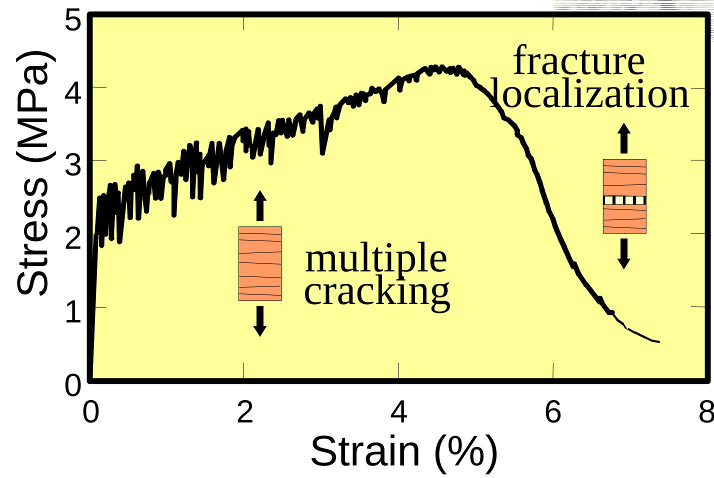

- Strain hardening
- Multiple cracking
- Localized failure

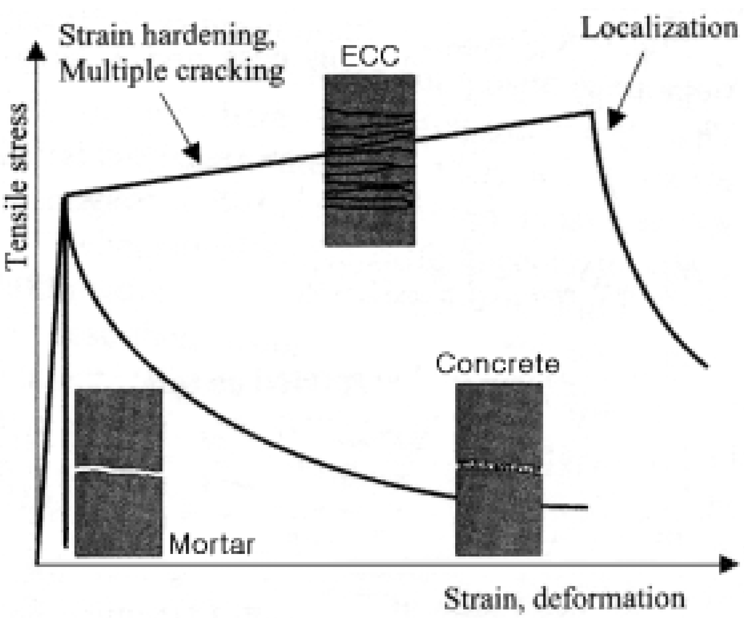

3-d homogenized crack model

- 3-D formulation of homogenized crack model

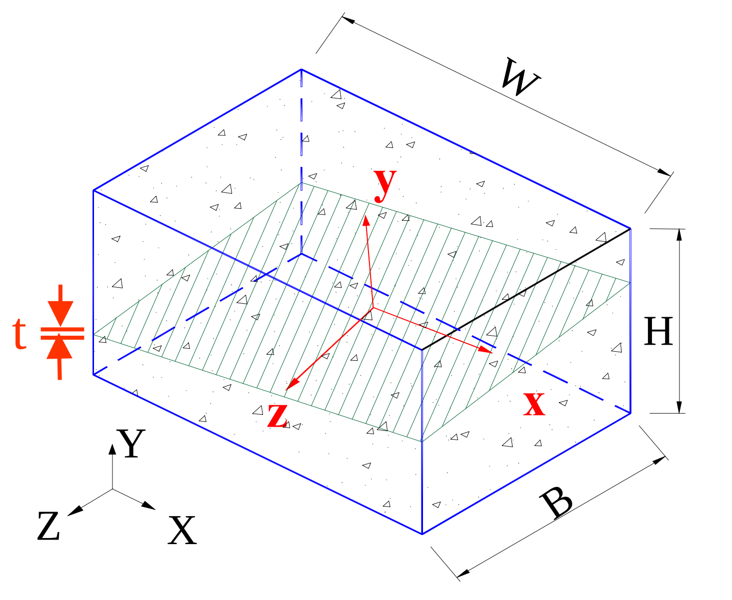

Representative elementary volume (REV)

σ_i , ε_i: *concrete*

σ_j , ε_j: *crack*

σ, ε : *concrete with crack*

- Mixture rule (R.E.V)

$$\sigma = \mu_i \sigma^i + \mu_j \sigma^j \qquad \varepsilon = \mu_i \varepsilon^i + \mu_j \varepsilon^j$$

$$\mu_i + \mu_j = 1$$

- Equilibrium & compatibility

$$\sigma_{yy} = \sigma^i_{yy} = \sigma^j_{yy} \qquad \varepsilon_{xx} = \varepsilon^i_{xx} = \varepsilon^j_{xx}$$

$$\tau_{xy} = \tau^i_{xy} = \tau^j_{xy} \qquad \varepsilon_{zz} = \varepsilon^i_{zz} = \varepsilon^j_{zz}$$

$$\tau_{yz} = \tau^i_{yz} = \tau^j_{yz} \qquad \gamma_{zx} = \gamma^i_{zx} = \gamma^j_{zx}$$

- Velocity discontinuity at crack surface

$$g = \{g_y, g_x, g_z\}^T \qquad [\delta]\,\sigma^j = [K]\,g$$

$$[\delta] = \begin{bmatrix} 0 & 1 & 0 & 0 & 0 & 0 \\ 0 & 0 & 0 & 1 & 0 & 0 \\ 0 & 0 & 0 & 0 & 1 & 0 \end{bmatrix}$$

$$[K] = \begin{bmatrix} K_{11} & K_{12} & K_{13} \\ K_{21} & K_{22} & K_{23} \\ K_{31} & K_{32} & K_{33} \end{bmatrix} \qquad [K] = [K^e] = \begin{bmatrix} K_N & 0 & 0 \\ 0 & K_{S1} & 0 \\ 0 & 0 & K_{S2} \end{bmatrix}$$

If $t \ll H$,

$$\mu_i = \frac{BW(H - t)}{HBW} \cong 1$$

$$\mu_j = \frac{BWt}{HBW} \cong \frac{t}{H}$$

$$\underbrace{\frac{1}{t}\boldsymbol{g}}_{\text{averaged crack strain}} = [\boldsymbol{\delta}]\boldsymbol{\varepsilon}_i$$

Let μ be the ratio of the crack area and REV., i.e. ($\mu := \dfrac{1}{H}$)

Then, $\boldsymbol{\varepsilon} = \mu_i \boldsymbol{\varepsilon}_i + \mu_j \boldsymbol{\varepsilon}_j$ can be written as

$$[\boldsymbol{\delta}]\boldsymbol{\varepsilon} = \mu_i [\boldsymbol{\delta}]\boldsymbol{\varepsilon}_i + \mu_j [\boldsymbol{\delta}]\boldsymbol{\varepsilon}_j$$

$$= 1 \cdot [\boldsymbol{\delta}]\boldsymbol{\varepsilon}_i + \frac{t}{H} \cdot \frac{1}{t}\boldsymbol{g}$$

$$= [\boldsymbol{\delta}]\boldsymbol{\varepsilon}_i + \mu\, \boldsymbol{g}$$

- Structural relationship

$$\{\boldsymbol{\sigma}^{i}\} = [\boldsymbol{D}]\{\boldsymbol{\varepsilon}^{i}\} \qquad \{\boldsymbol{\sigma}\} = \mu_i\{\boldsymbol{\sigma}^{i}\} + \mu_j\{\boldsymbol{\sigma}^{j}\}$$

$$[\boldsymbol{\delta}]\{\boldsymbol{\varepsilon}\} = [\boldsymbol{\delta}]\{\boldsymbol{\varepsilon}^{i}\} + \mu\{\boldsymbol{g}\}$$

$$[\boldsymbol{\delta}]\{\boldsymbol{\varepsilon}^{i}\} = [\boldsymbol{A}]\{\boldsymbol{\varepsilon}\} + [\boldsymbol{B}]\{\boldsymbol{g}\}$$

$$[\boldsymbol{A}] = \begin{bmatrix} \frac{-D_{21}}{C_1} & \frac{-K_{11}}{\mu C_1} & \frac{-D_{23}}{C_1} & \frac{-D_{24}}{C_1} & \frac{-D_{25}}{C_1} & \frac{-D_{26}}{C_1} \\ \frac{-D_{41}}{C_2} & \frac{-D_{42}}{C_2} & \frac{-D_{43}}{C_2} & \frac{-K_{22}}{\mu C_2} & \frac{-D_{45}}{C_2} & \frac{-D_{46}}{C_2} \\ \frac{-D_{51}}{C_3} & \frac{-D_{52}}{C_3} & \frac{-D_{53}}{C_3} & \frac{-D_{54}}{C_3} & \frac{-K_{33}}{\mu C_3} & \frac{-D_{56}}{C_3} \end{bmatrix}$$

$$[\boldsymbol{B}] = \begin{bmatrix} 0 & \frac{K_{12}+\mu D_{24}}{C_1} & \frac{K_{13}+\mu D_{25}}{C_1} \\ \frac{K_{21}+\mu D_{42}}{C_2} & 0 & \frac{K_{23}+\mu D_{45}}{C_2} \\ \frac{K_{31}+\mu D_{52}}{C_3} & \frac{K_{32}+\mu D_{54}}{C_3} & 0 \end{bmatrix}$$

$$C_1 = D_{22} + \frac{K_{11}}{\mu}$$

$$C_2 = D_{44} + \frac{K_{22}}{\mu}$$

$$C_3 = D_{55} + \frac{K_{33}}{\mu}$$

- **Structural relationship of (tensile) crack**

$$[\delta]\{\varepsilon\} = [\delta]\{\varepsilon^{i}\} + \mu\{g\}$$

$$\{\varepsilon^{i}\} = [S_1]\{\varepsilon\} \quad \textbf{or} \quad [\delta]\{\varepsilon^{i}\} = [S]\{\varepsilon\}$$

i.e , $$[\delta]\{\varepsilon\} = [S]\{\varepsilon\} + \mu\{g\}$$

$$\therefore\ \mu\{g\} = ([\delta] - [S])\{\varepsilon\}$$

$$\{g\} = \frac{1}{\mu}([\delta] - [S])\{\varepsilon\}$$

Let $$[S_2] = \frac{1}{\mu}([\delta] - [S])$$

then $$\{g\} = [S_2]\{\varepsilon\}$$

- Total strain relationship

$$[\delta]\{\varepsilon^{i}\} = [S]\{\varepsilon\}$$

$$[S] = ([I] + \frac{1}{\mu}[B])^{-1}([A] + \frac{1}{\mu}[B][\delta])$$

$$\{\varepsilon^{i}\} = [S_1]\{\varepsilon\}$$

$$[S_1] = \begin{bmatrix} 1 & 0 & 0 & 0 & 0 & 0 \\ S_{11} & S_{12} & S_{13} & S_{14} & S_{15} & S_{16} \\ 0 & 0 & 1 & 0 & 0 & 0 \\ S_{21} & S_{22} & S_{23} & S_{24} & S_{25} & S_{26} \\ S_{31} & S_{32} & S_{33} & S_{34} & S_{35} & S_{36} \\ 0 & 0 & 0 & 0 & 0 & 1 \end{bmatrix}$$

- Homogenized constitutive equation

$$\boldsymbol{\sigma} = \mu_i \boldsymbol{\sigma}^i + \mu_i \boldsymbol{\sigma}^j$$

$$\approx \boldsymbol{\sigma}^i$$

$$= [\boldsymbol{D}][\boldsymbol{S}_1]\boldsymbol{\varepsilon}$$

$$\boldsymbol{\sigma} = [\boldsymbol{D}^{eq}]\boldsymbol{\varepsilon} \qquad [\boldsymbol{D}^{eq}] = [\boldsymbol{D}][\boldsymbol{S}_1]$$

Remark

Crack width, t, is removed in the final constitutive equation only expressed with μ. This is a solution for the mesh sensitivity problem without the introduction of additional length scale such as a characteristic length.

→ Regularization of the continuum model

Constitutive equation for crack

$$\boldsymbol{t} = \{\, t_n^{\;cr},\; t_{S_1}^{\;cr},\; t_{S_2}^{\;cr} \,\}^T$$

$$\sigma_{yy} \qquad \tau_{xy} \qquad \tau_{yz}$$

$$= [\boldsymbol{\delta}\,]\,\boldsymbol{\sigma} = [\,\boldsymbol{K}\,]\,\boldsymbol{g}$$

➢ Compression

- Bifurcation analysis for crack initiation

$$F(\boldsymbol{n}) = \det\left(n_i\, D^{eq}{}_{ijkl}\, n_l \right)$$

$$[\boldsymbol{K}] = \begin{bmatrix} K_N^{ep} & 0 & 0 \\ 0 & K_{S1}^{ep} & 0 \\ 0 & 0 & K_{S2}^{ep} \end{bmatrix}$$

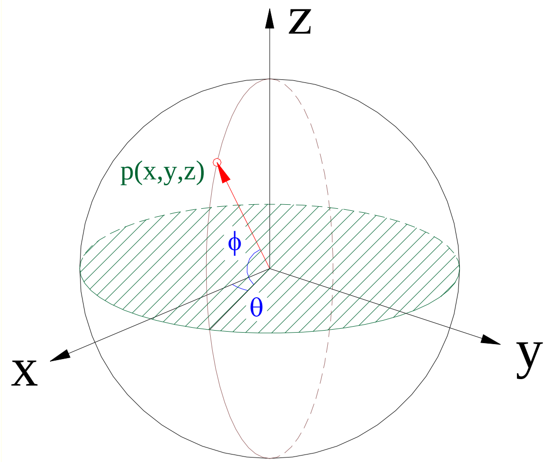

Failure criteria and softening curve (compression)

Drucker-Prager type

$$F = \alpha I_1 + \sqrt{J_2} - k(\bar{\sigma}, \bar{\varepsilon}^p) = 0$$

Hardening and softening function

1) Song and Na (1997)

$$k(\bar{e}^p, \bar{\sigma}) = \sigma_0 + \bar{\sigma}\bar{e}^p + (\sigma_\infty - \sigma_0)[1 - e^{-\beta \bar{e}}] - \sqrt{\frac{3}{2}}\alpha p$$

2) Song et al (2003), Farahat et al.(1995)

$$k(W^p) = k_0 e^{-[(\beta W^P)^\gamma - \xi]^2}$$

3) Barcelona model

- k(ε^p) (J. Lubliner, 1996)

$$k(\varepsilon^p) = f_{N0}[(1 + a_N)\exp(-b_N \varepsilon^p) - a_N \exp(-2b_N \varepsilon^p)]$$

- k(W^p) (Modified Barcelona Model, MBM)

$$k(W^p) = f_{N0}[(1 + a_N)\exp(-b_N W^p) - a_N \exp(-2b_N W^p)]$$

Failure criteria and softening function (tension)

- **Failure criterial (Gopalaratnam and Shah, 1985)**

$$F = \sigma_1 - k(\cdot)$$

- **Hardening and softening function**

1) Gopalaratnam and Shah (1985)

$$k(t) = f_t(e^{-\kappa t^{\lambda}})$$

2) Song et al. (2003)

$$k(g_y^p) = f_t(e^{-\kappa(\eta g_y^p)^{\lambda}})$$

3) Barcelona model

- $k(\varepsilon^p)$ (J. Lubliner, 1996)

$$k(\varepsilon^p) = f_{t0}[(1+a_t)\exp(-b_t\varepsilon^p) - a_t\exp(-2b_t\varepsilon^p)]$$

- $k(g_y^p)$ (MBM)

$$k(g_y^p) = f_{t0}[(1+a_t)\exp(-b'_t\, g_y^p) - a_t\exp(-2b'_t\, g_y^p)]$$

유한 요소 해석 흐름도

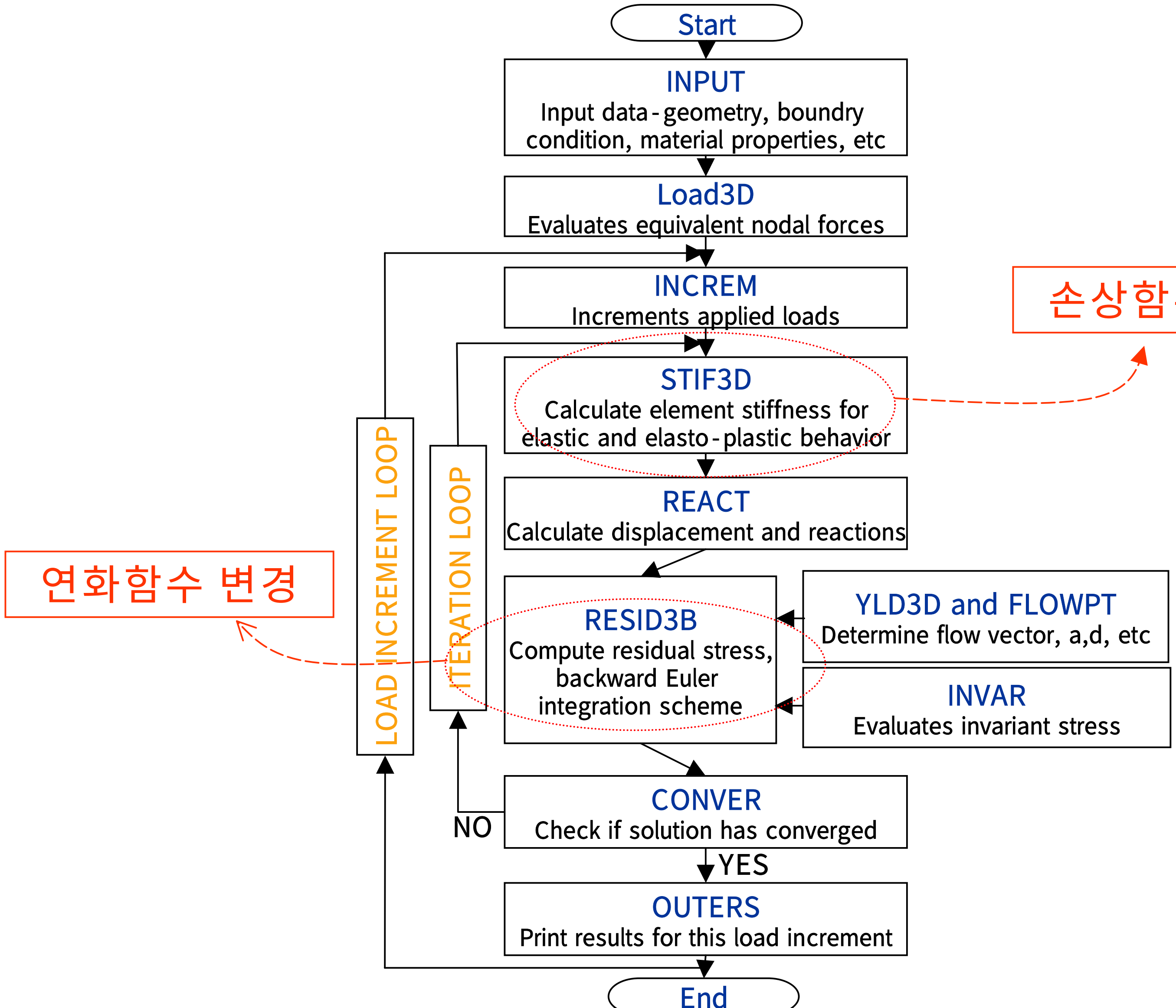

Start
INPUT
Input data - geometry, boundry condition, material properties, etc
Load3D
Evaluates equivalent nodal forces
INCREM
Increments applied loads
STIF3D
Calculate element stiffness for elastic and elasto - plastic behavior
손상함수 도입
REACT
Calculate displacement and reactions
RESID3B
Compute residual stress, backward Euler integration scheme
연화함수 변경
YLD3D and FLOWPT
Determine flow vector, a,d, etc
INVAR
Evaluates invariant stress
LOAD INCREMENT LOOP
ITERATION LOOP
CONVER
Check if solution has converged
NO
YES
OUTERS
Print results for this load increment
End

Hardening and softening curve for concrete and ECC (tension)

- **J. Lubliner (1996)**

$$k(g_y^p) = f_{t0}[(1 + a_t)\exp(-b'_t\, g_y^p) - a_t \exp(-2b'_t\, g_y^p)]$$

① $a_t < 1$ ⟹ Concrete

② $a_t > 1$ ⟹ ECC

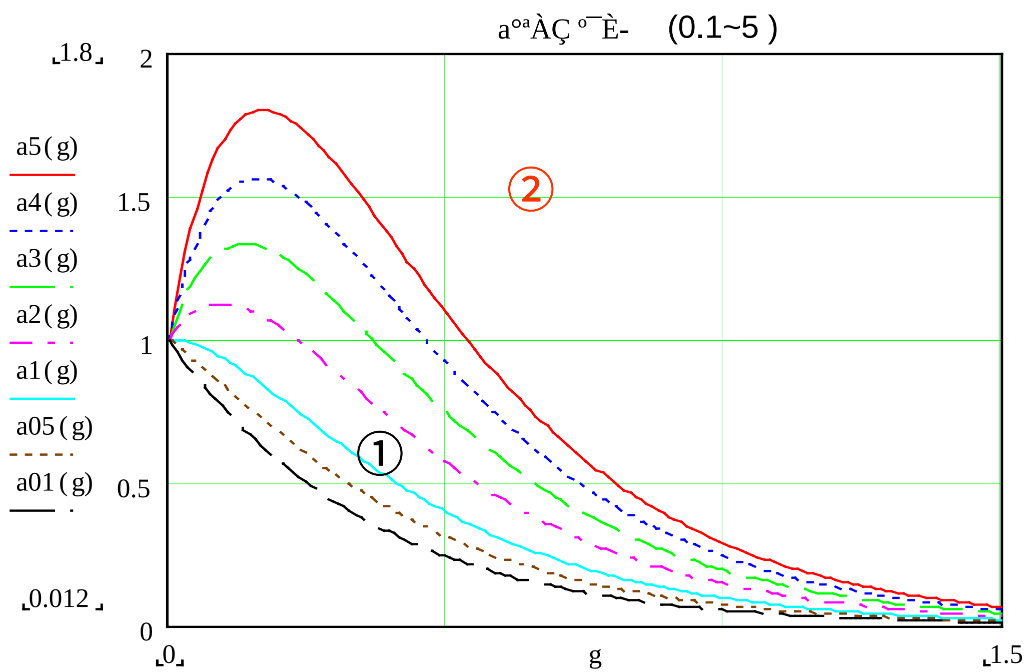

➤ Result for 2% polyetylane fiber contained ECC

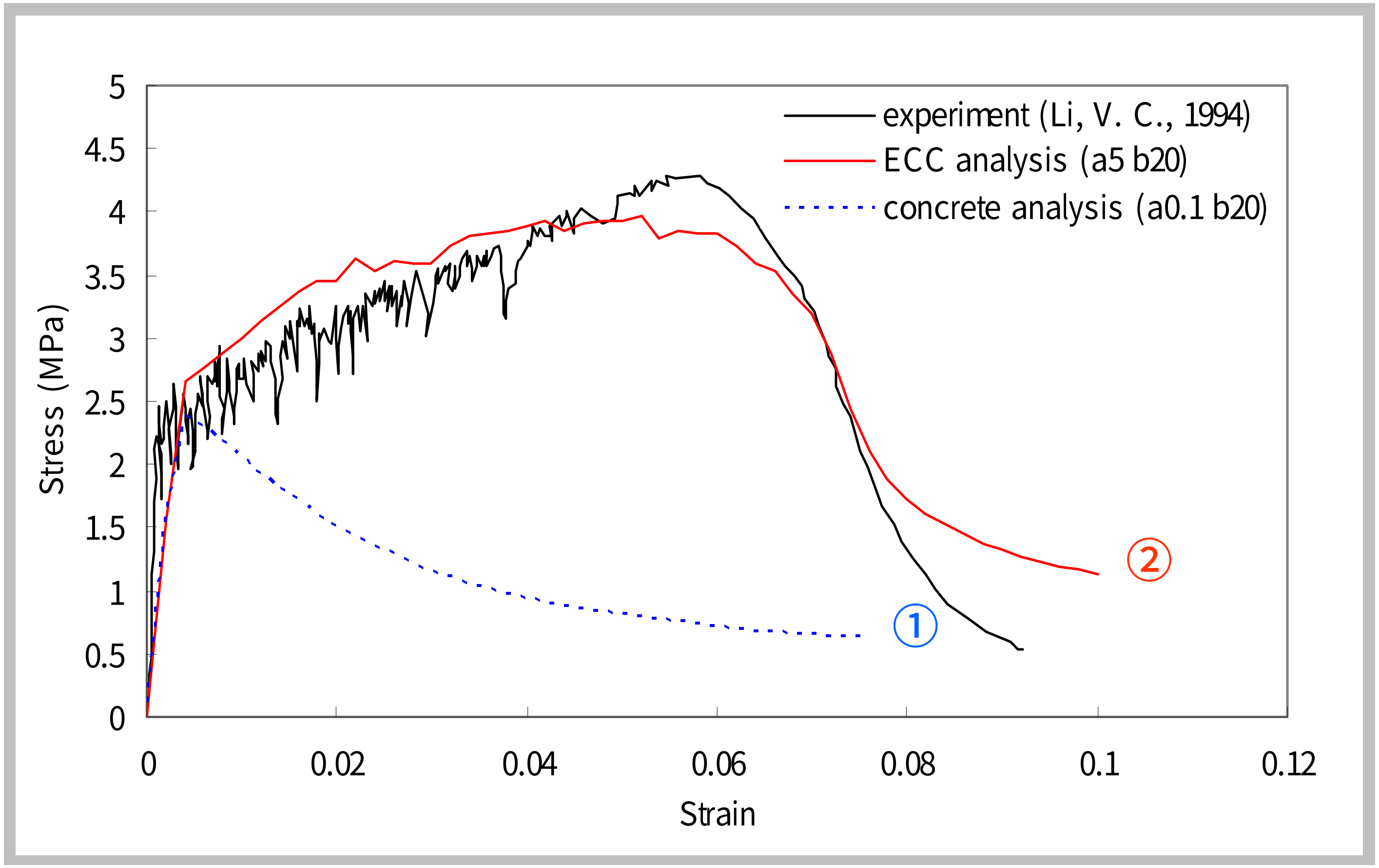

① ⇒ $a_t = 0.1$: Concrete

② ⇒ $a_t = 5$: ECC

- Experimental result (Tetsushi Kanda, 1998)
- polyetylane fiber : 0.75% , 1% , 1.25%

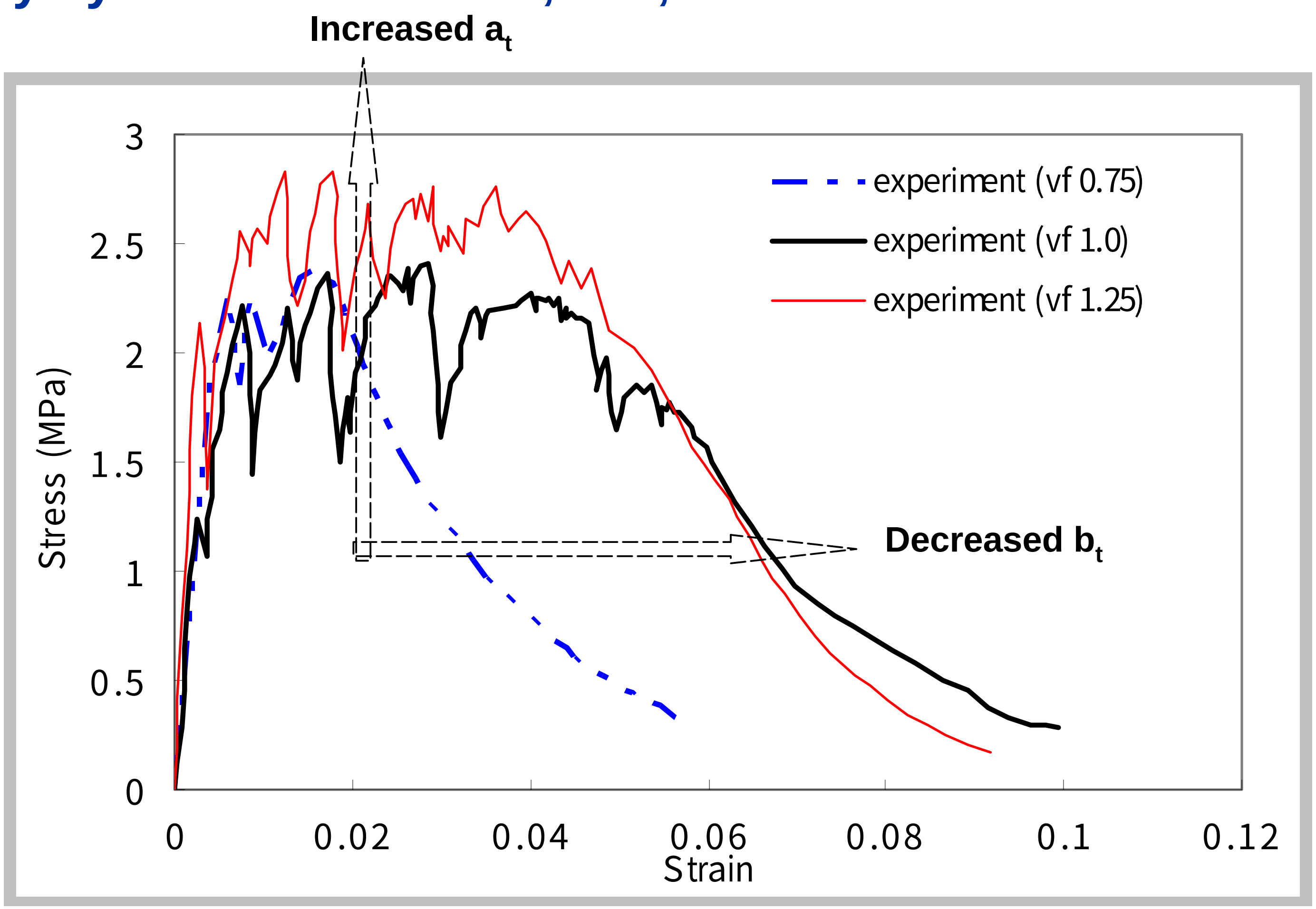

- 0.75% ECC

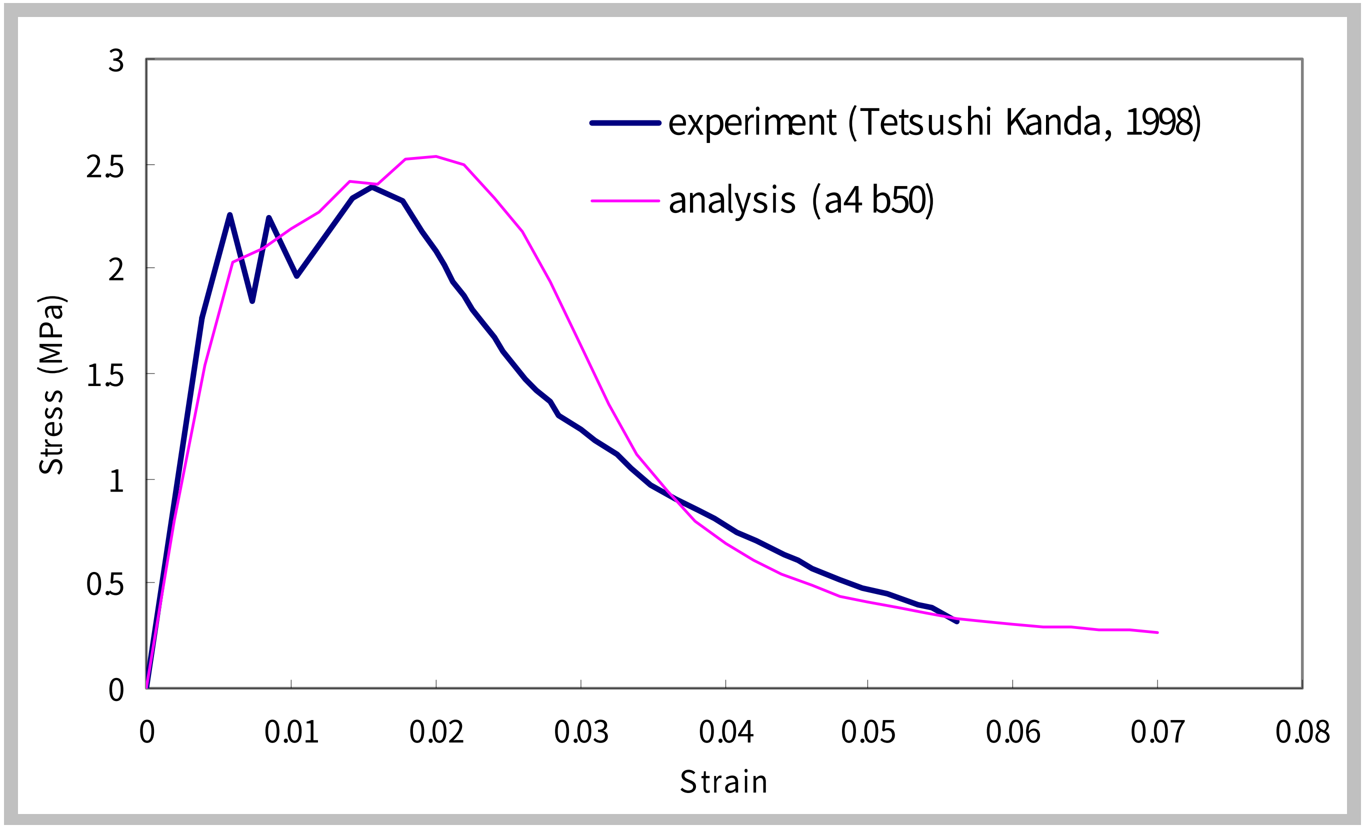

experiment (Tetsushi Kanda, 1998)
analysis (a4 b50)
Stress (MPa)
Strain
0
0.5
1
1.5
2
2.5
3
0
0.01
0.02
0.03
0.04
0.05
0.06
0.07
0.08

- 1% ECC

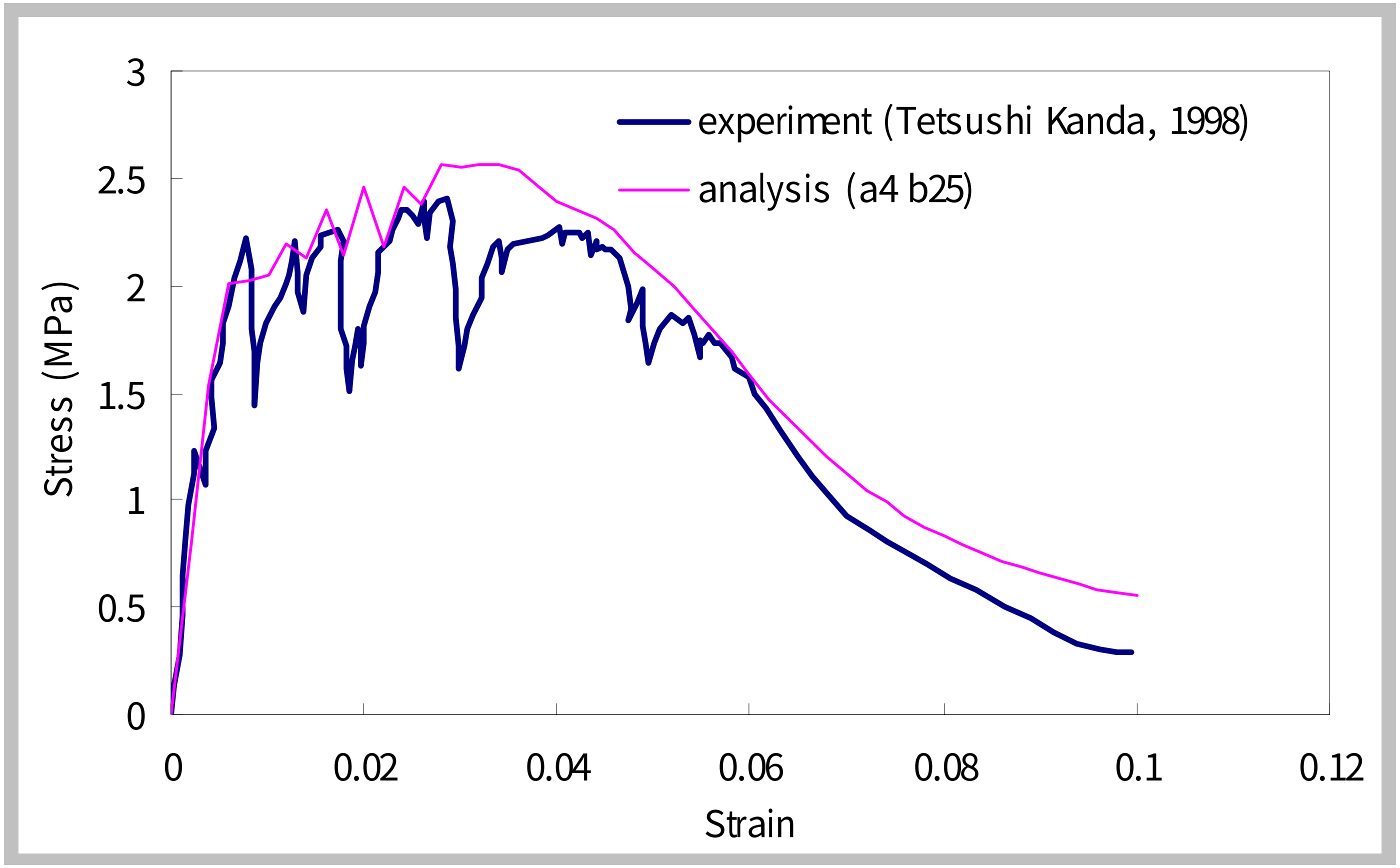

experiment (Tetsushi Kanda, 1998)
analysis (a4 b25)
Stress (MPa)
3
2.5
2
1.5
1
0.5
0
0
0.02
0.04
0.06
0.08
0.1
0.12
Strain

- 1.25% ECC

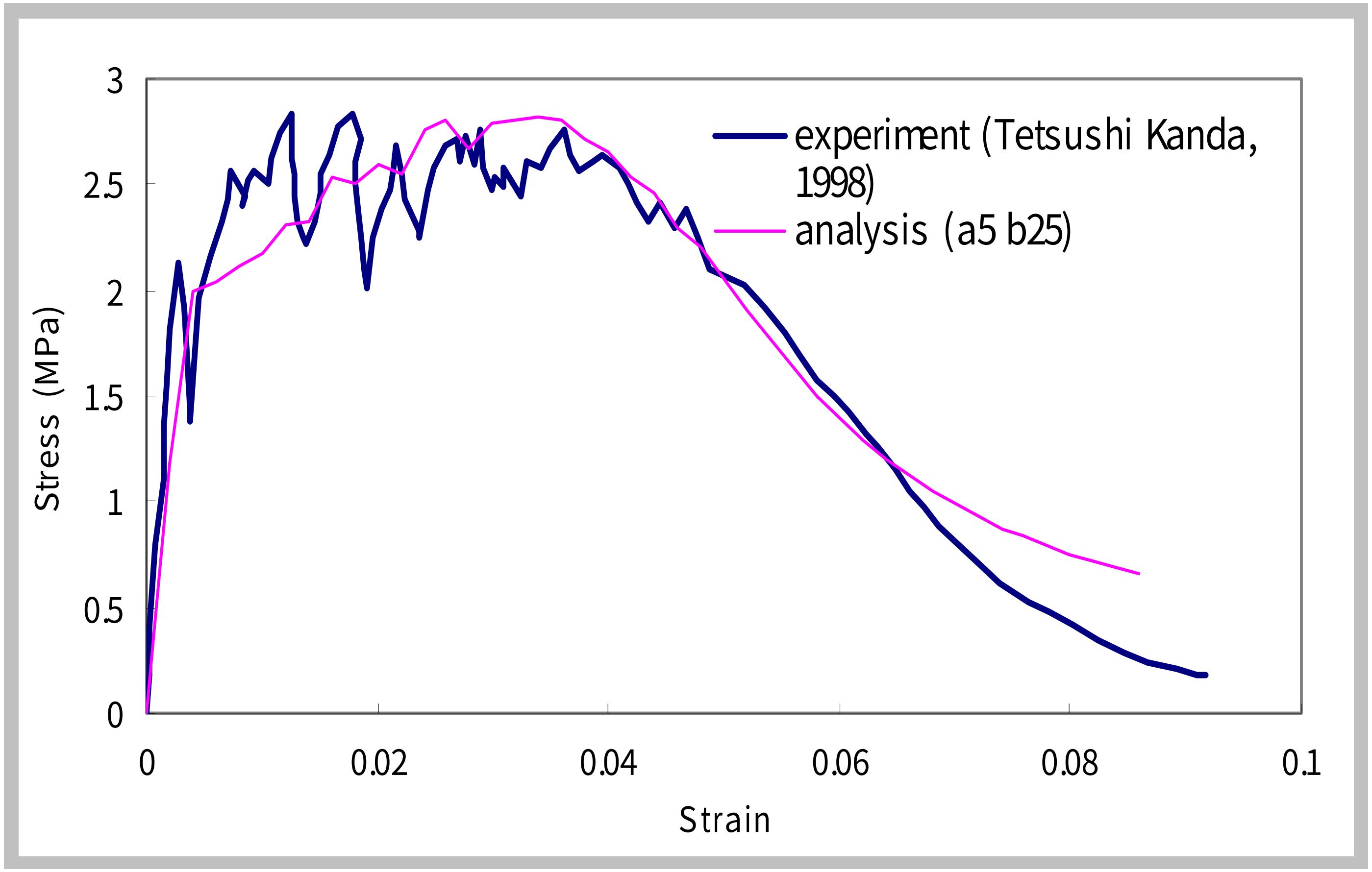

Stress (MPa)
3
2.5
2
1.5
1
0.5
0
0
0.02
0.04
0.06
0.08
0.1
Strain
experiment (Tetsushi Kanda, 1998)
analysis (a5 b25)

- Mesh sensitivity check on softening behavior

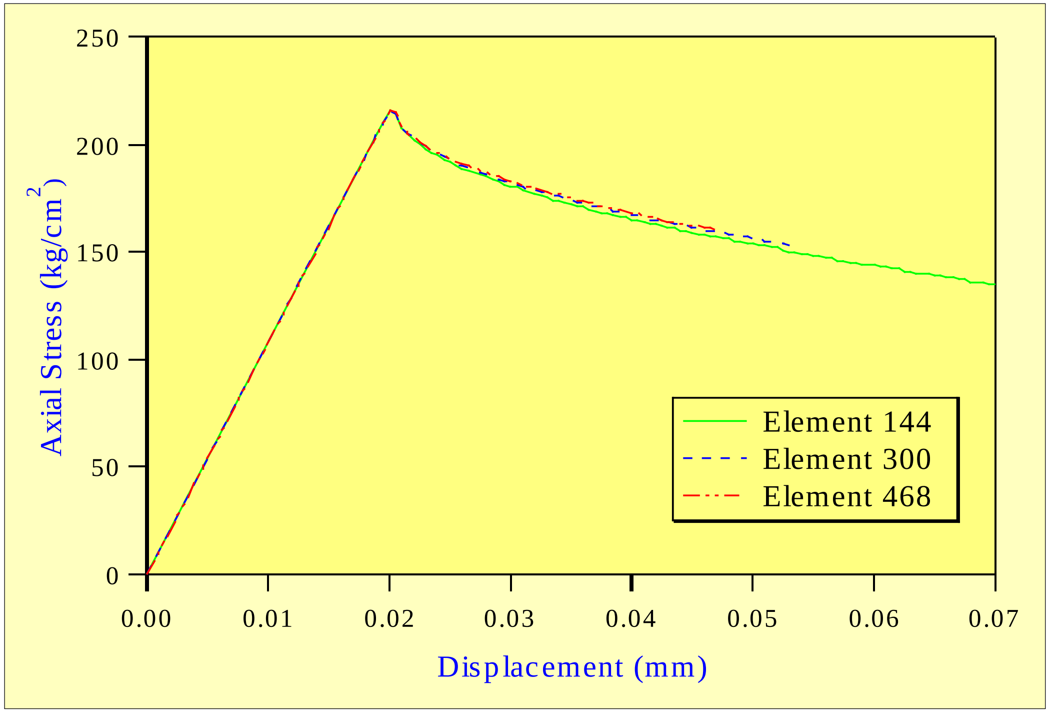

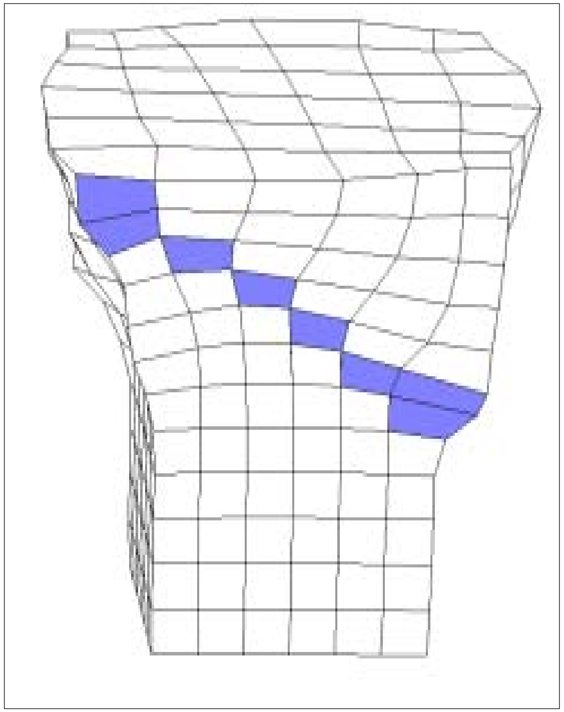

- Comparison with experimental result

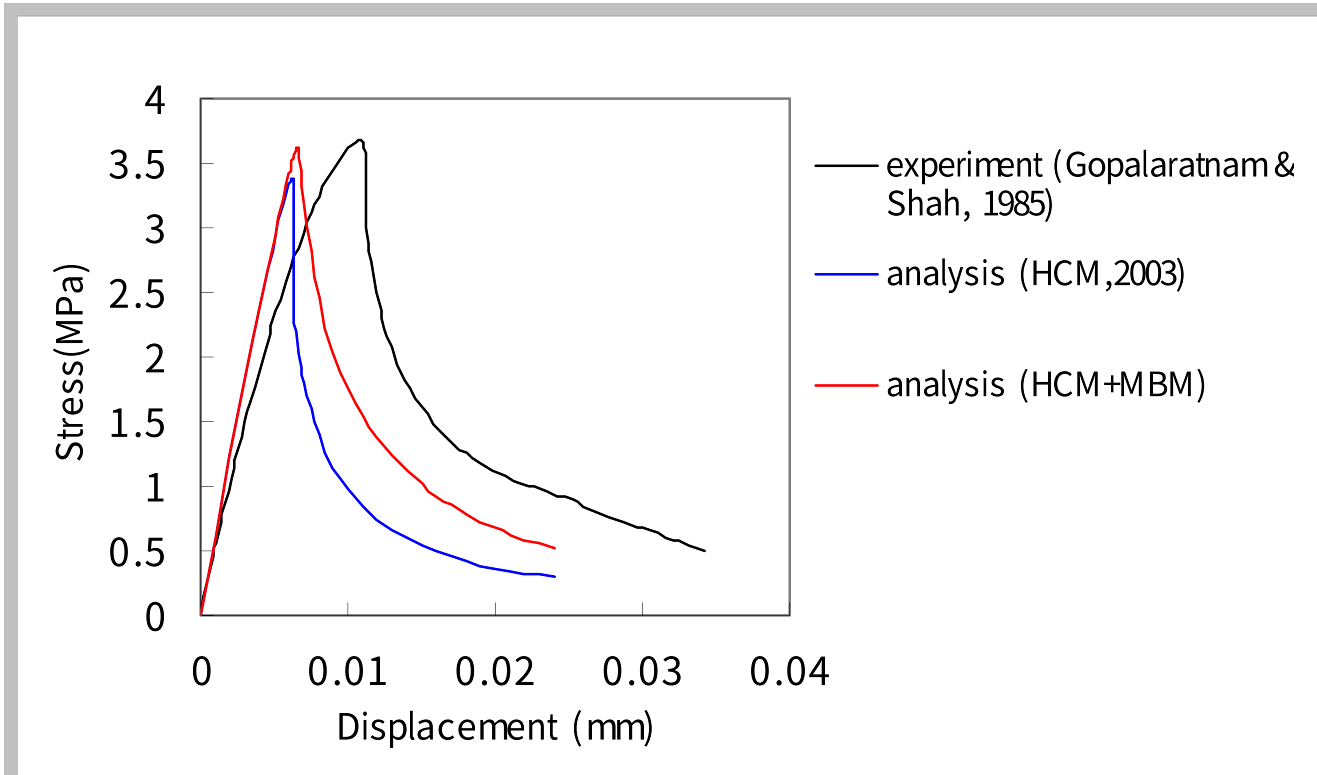

➢ Mesh sensitivity check for tension

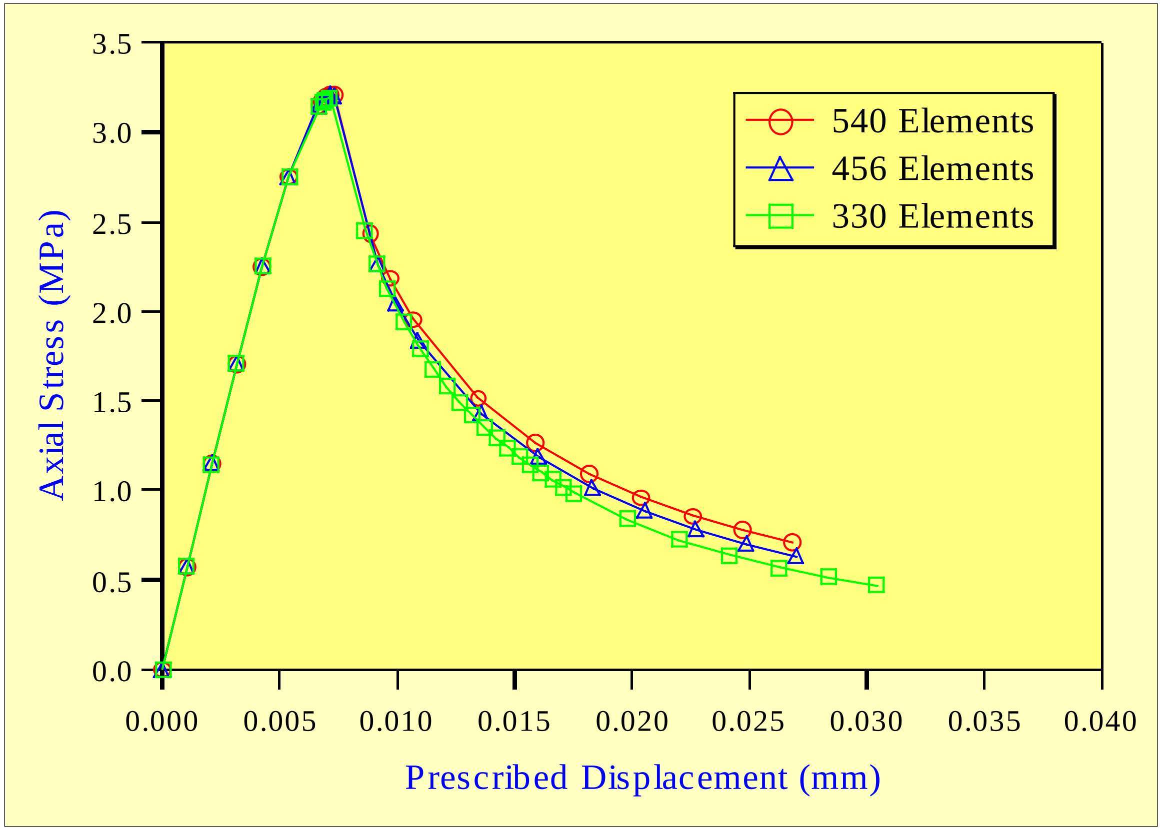

➢ Tension failure with damage

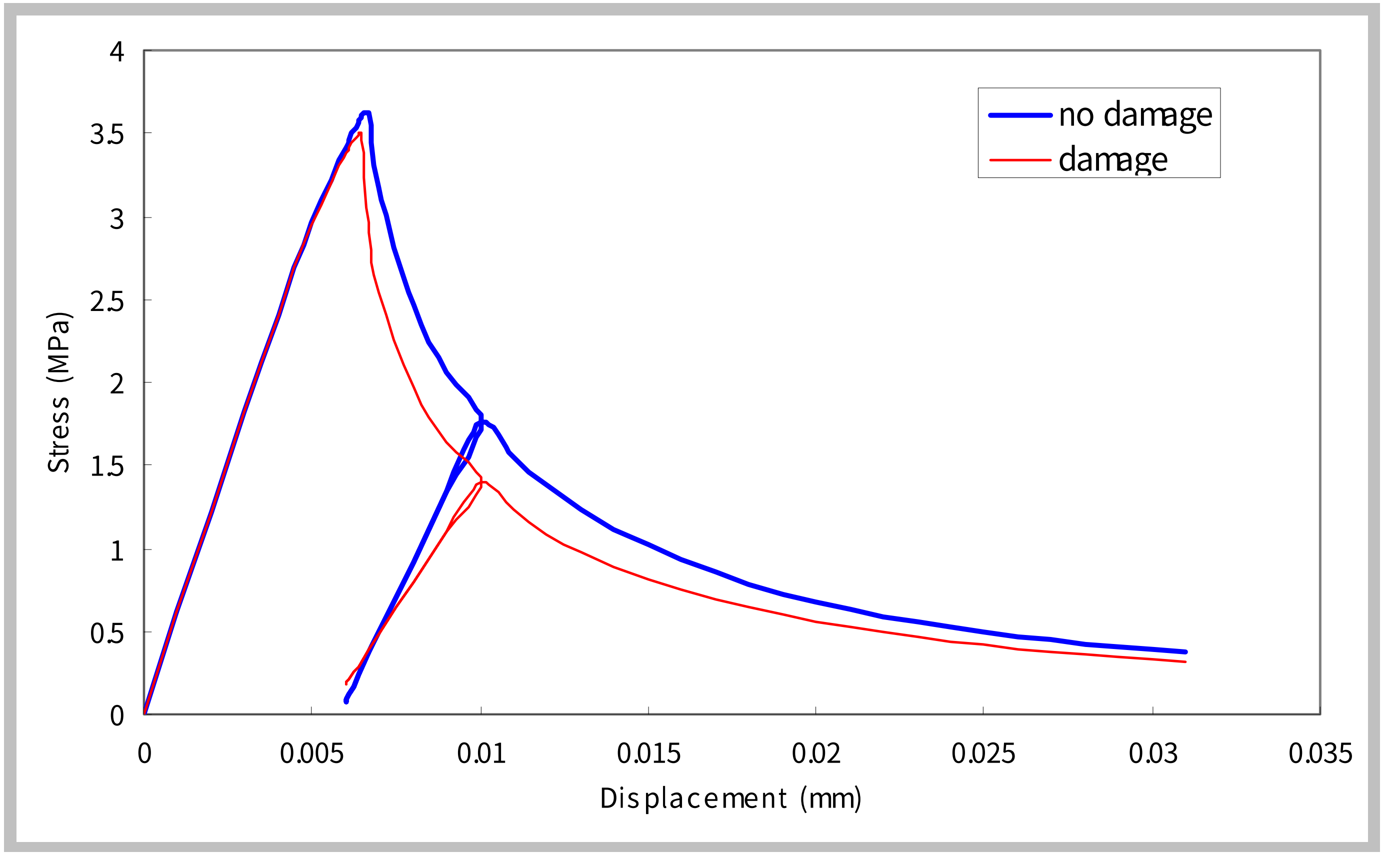

Flexural failure

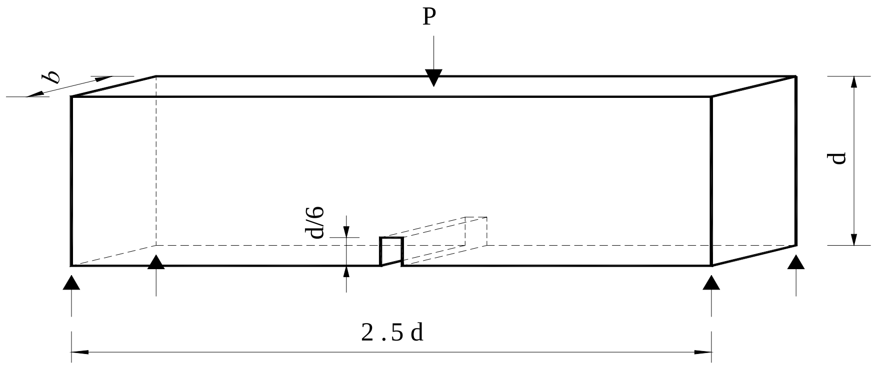

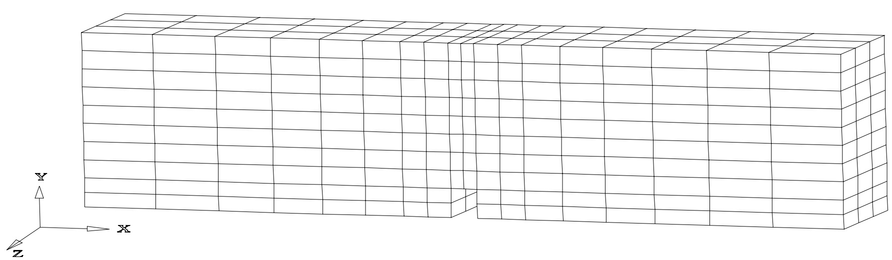

- 528 elements
- 2977 nodes

Specimen (mm)	*Notch (mm)*	$f_t\,(MPa)$	$E_c\,(GPa)$	ν_c	$K_N\,(GPa/m)$	$K_S\,(GPa/m)$
190.5×76.2×38	**6.5×12.7**	**2.97**	**28.06**	**0.2**	**2,680**	**1,680**

➢ Results

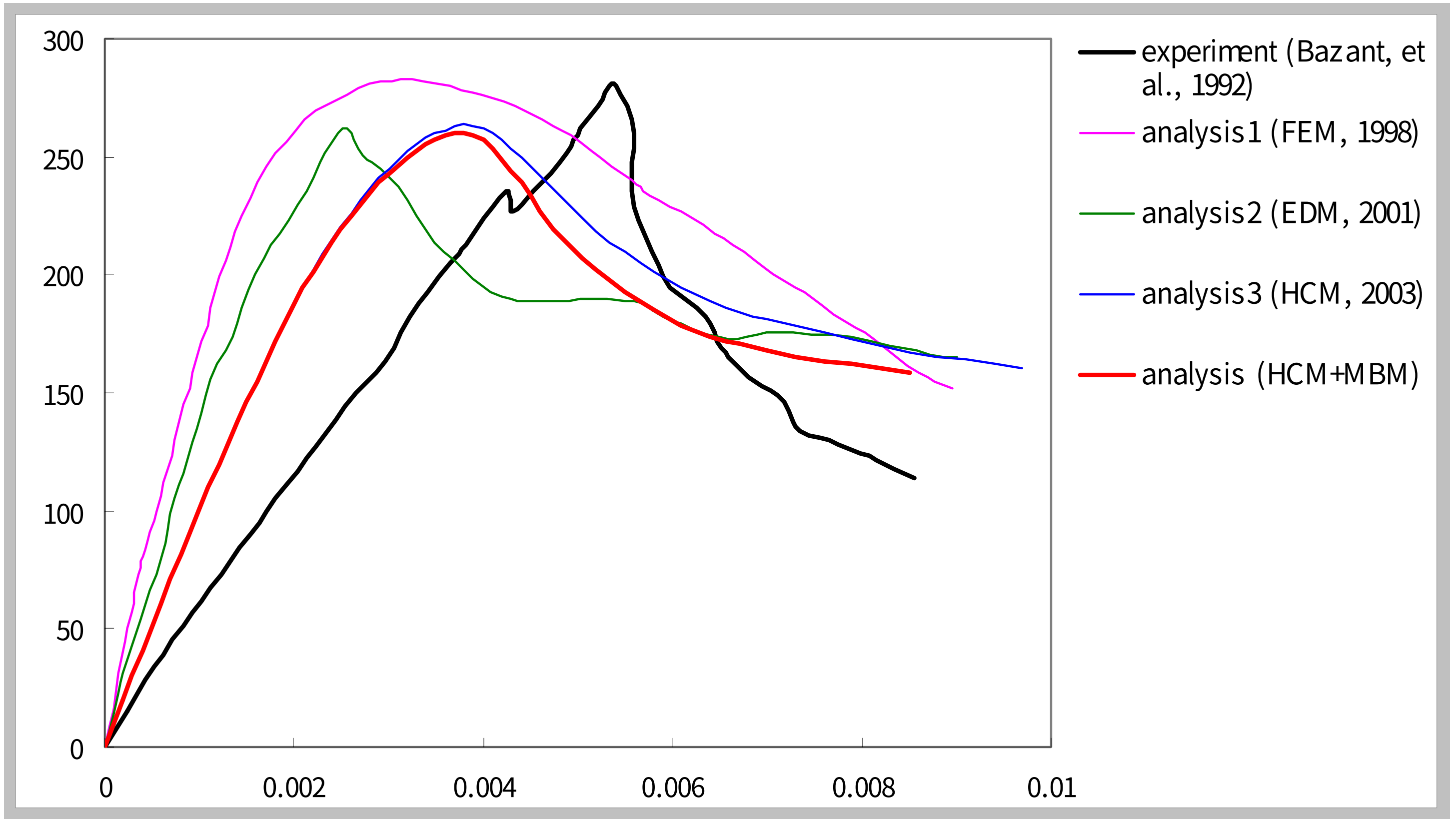

300
250
200
150
100
50
0
0
0.002
0.004
0.006
0.008
0.01
experiment (Bazant, et al., 1992)
analysis1 (FEM, 1998)
analysis2 (EDM, 2001)
analysis3 (HCM, 2003)
analysis (HCM+MBM)

RC panel of simulating RCCV wall subjected to biaxial tension

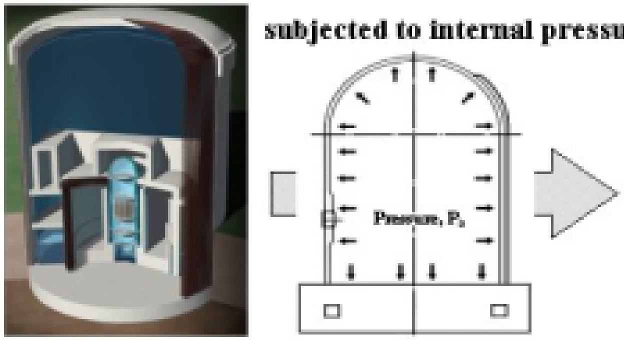

RCCV Structure

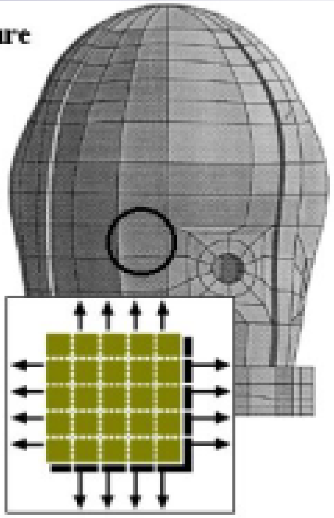

RC containment wall element subjected to biaxial tension

RC panel specimen

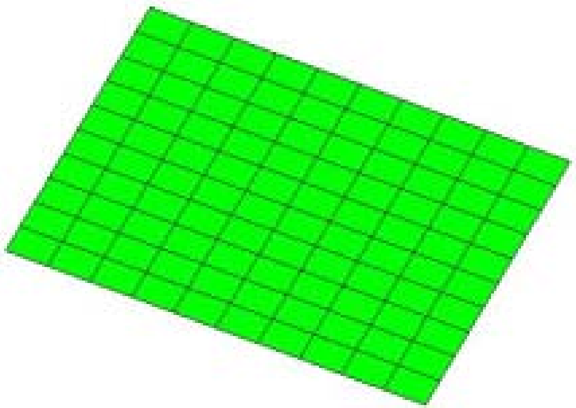

Modeling as shell element

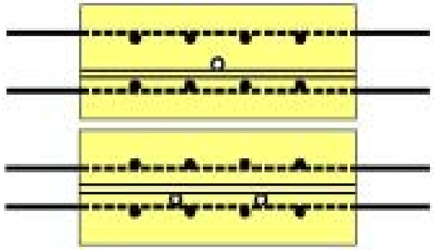

Layered shell element

Specification < HICT and KAERI, 2001 >

- Compressive strength of concrete (σ_c) : 41.9MPa
- Tensile strength of concrete (σ_t) : 2.87MPa
- Modulus of elasticity of concrete (E_c) : 23828MPa
- Yield strength of reinforcement (σ_y) : 410MPa
- Modulus of elasticity of reinforcement (E_s) : 205744MPa

FEM MESH and Boundary condition

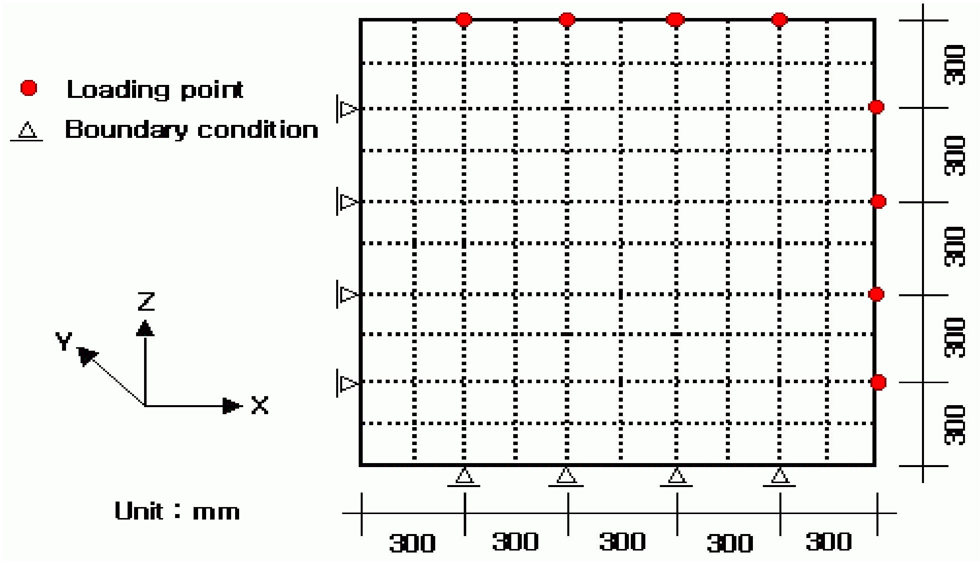

RC panel is discretized as 10 x 10 mesh

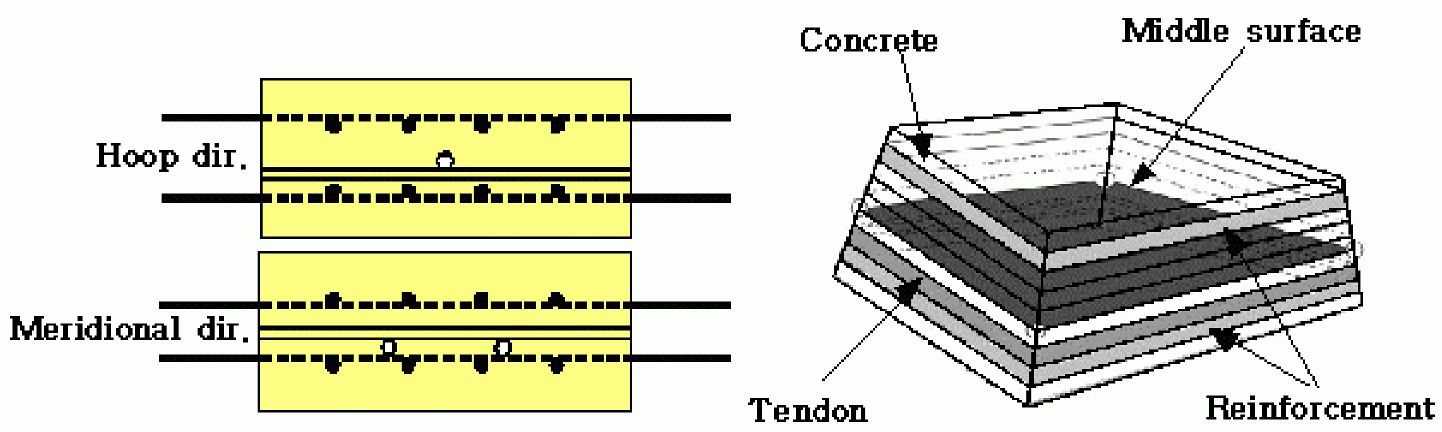

Stress-strain curve of rebars

Hoop direction

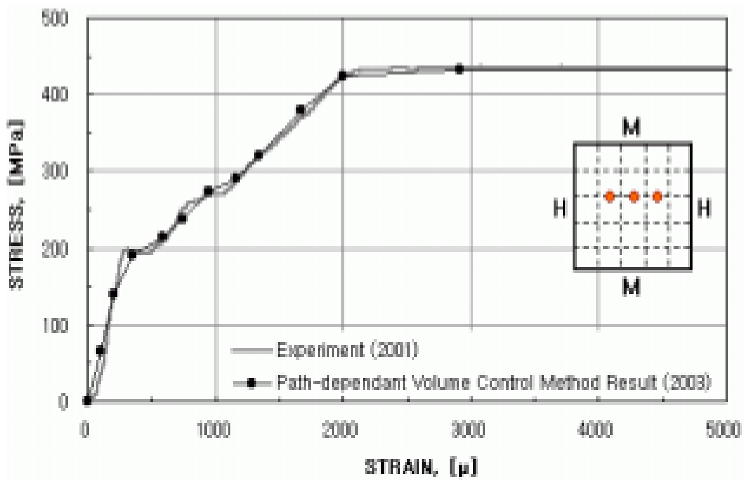

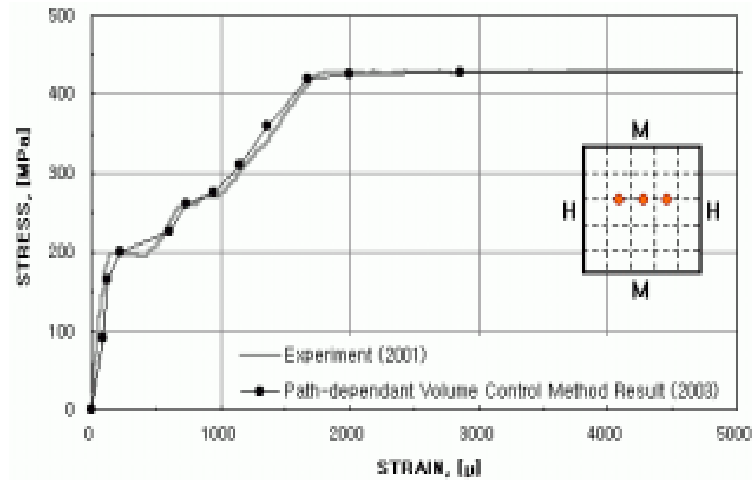

Meridional direction

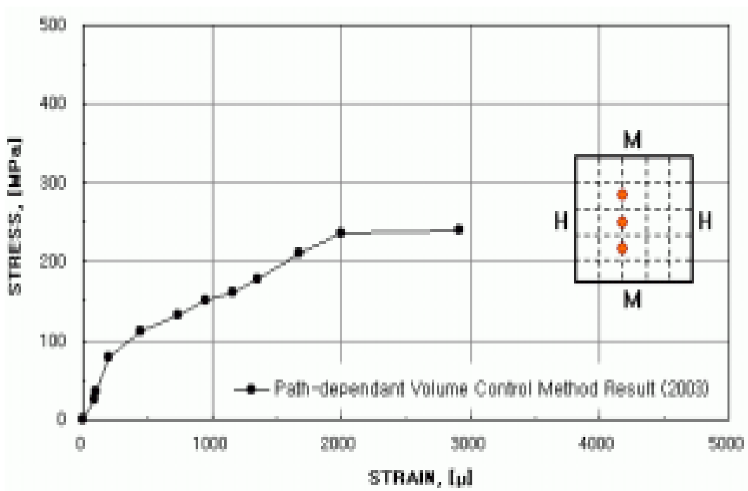

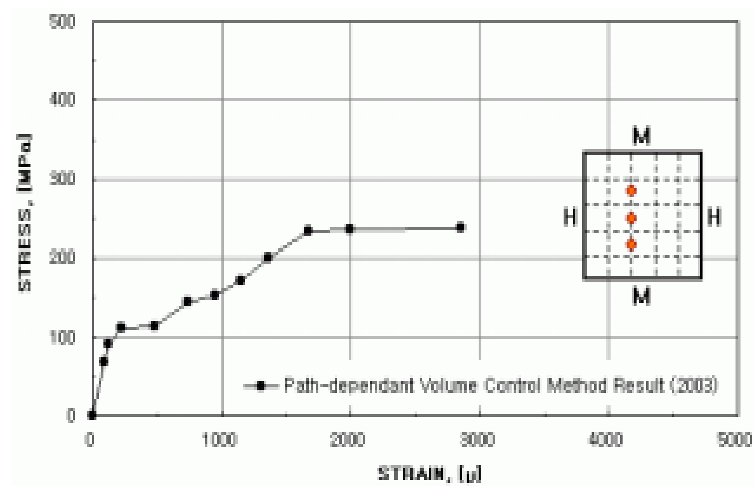

Top of RC panel

Bottom of RC panel

Stress-strain curve of rebars

Hoop direction

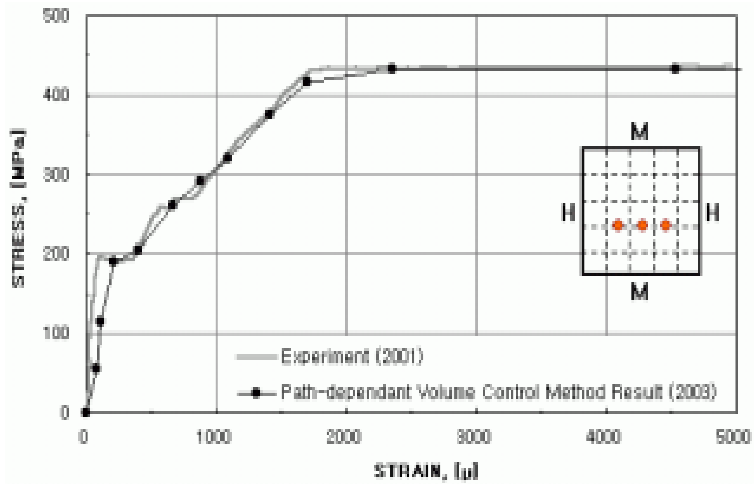

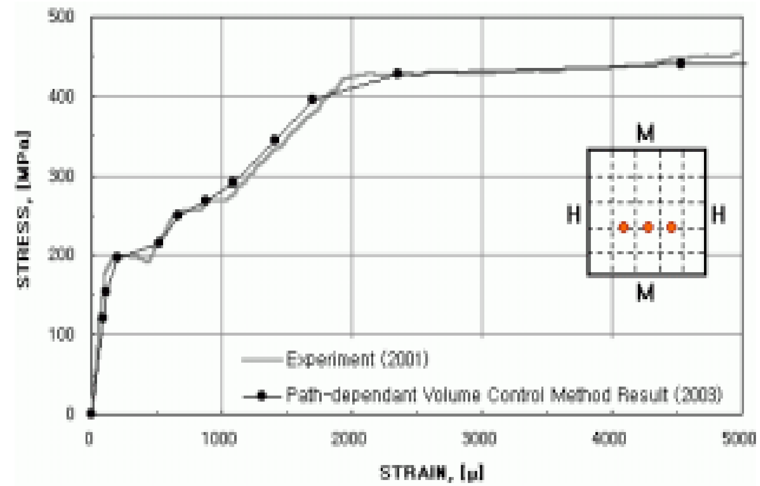

Meridional direction

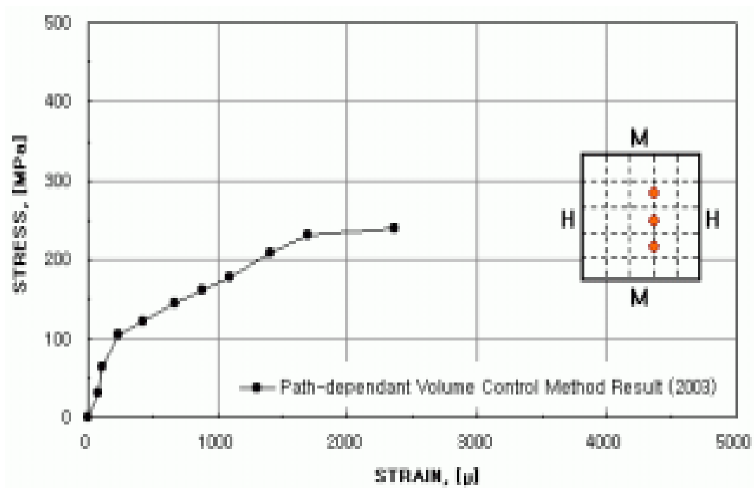

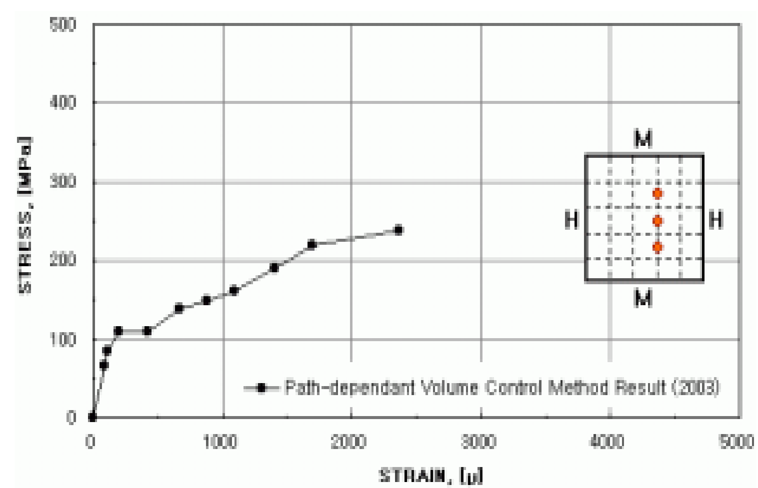

Top of RC panel

Bottom of RC panel

Stress-strain curve of rebars

Hoop direction

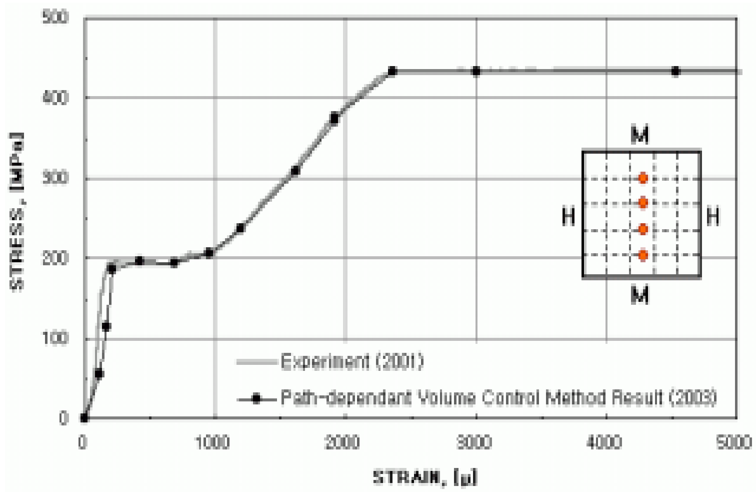

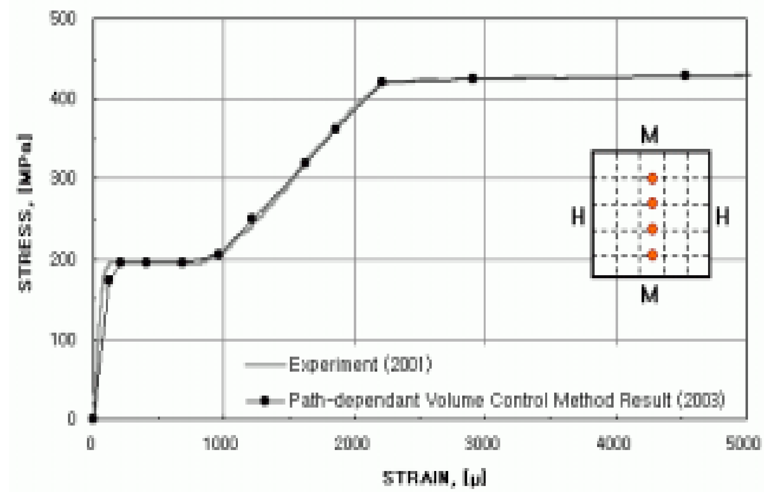

Meridional direction

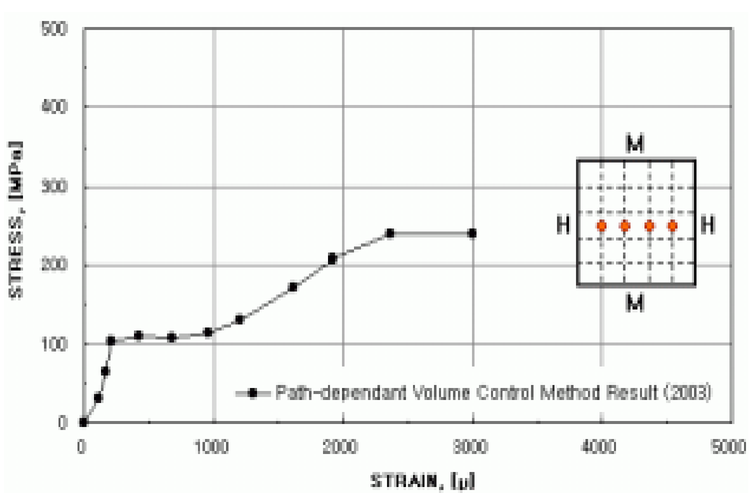

Top of RC panel

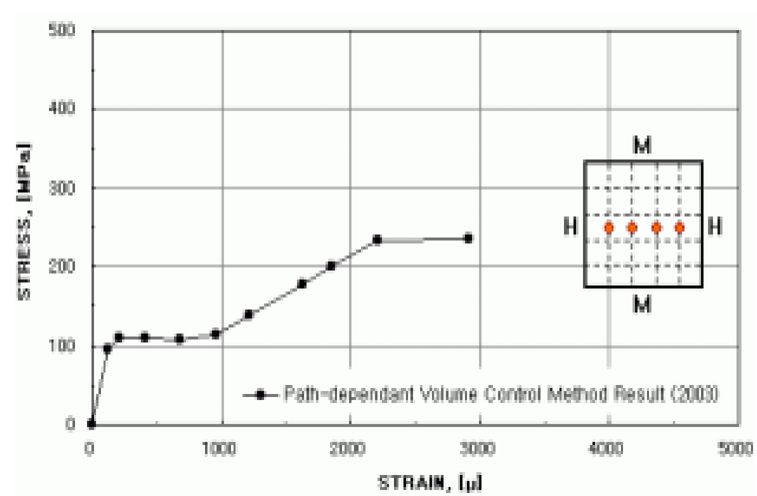

Bottom of RC panel

Crack patterns of RC panel

Top of RC panel by experiment

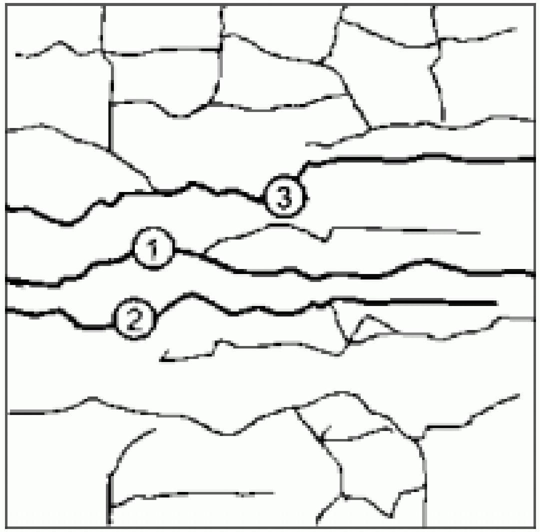

Top of RC panel by volume control analysis

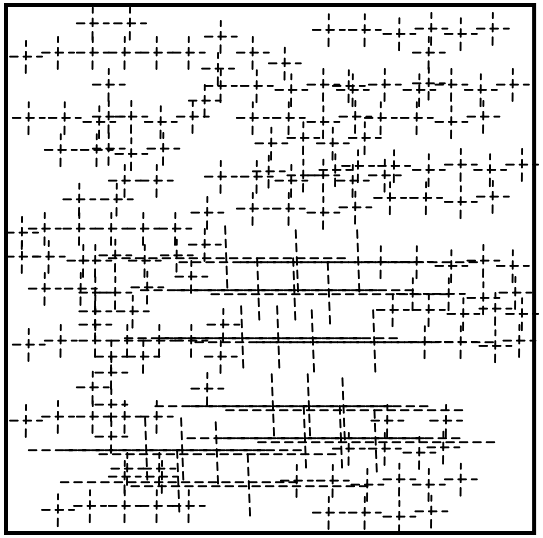

Bottom of RC panel by experiment

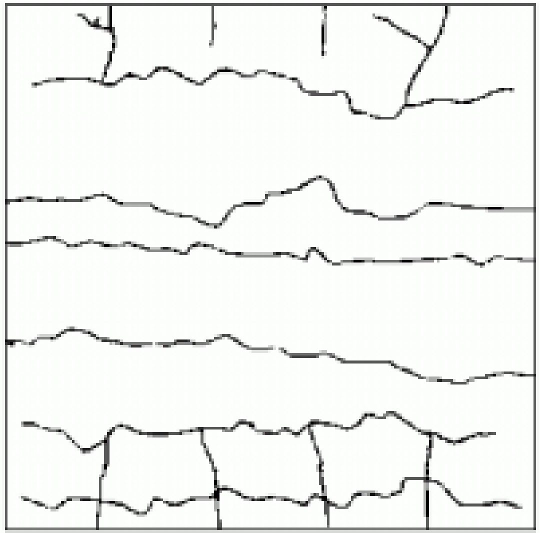

Bottom of RC panel by volume control analysis

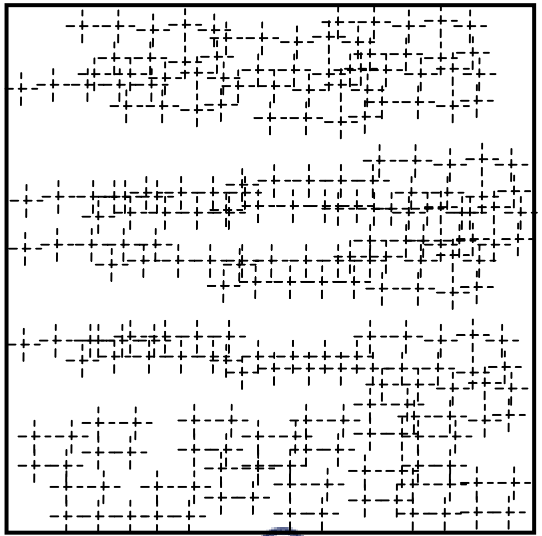

Deformed shape of RC panel

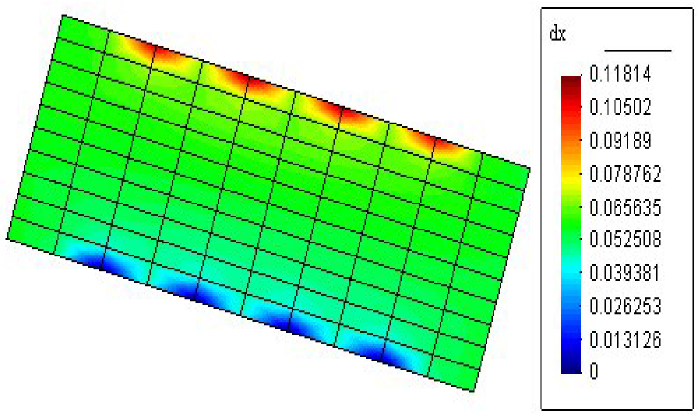

Hoop dir. displacement. at 1st crack occurrence

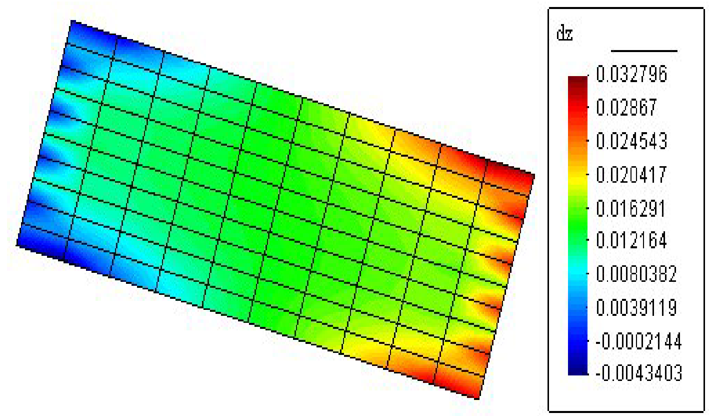

Meridional dir. displacement at 1st crack occurrence

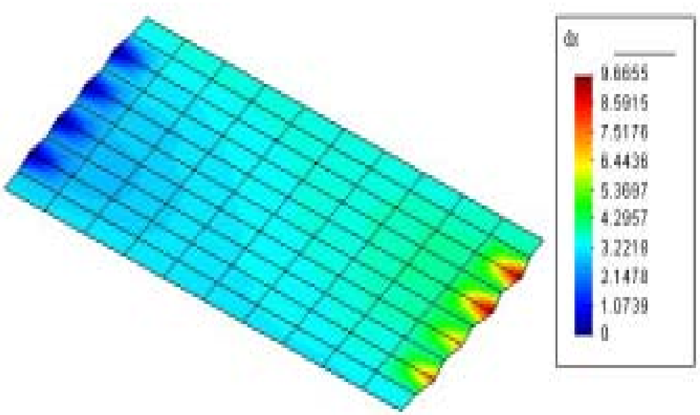

Hoop dir. displacement. at rebar yielding

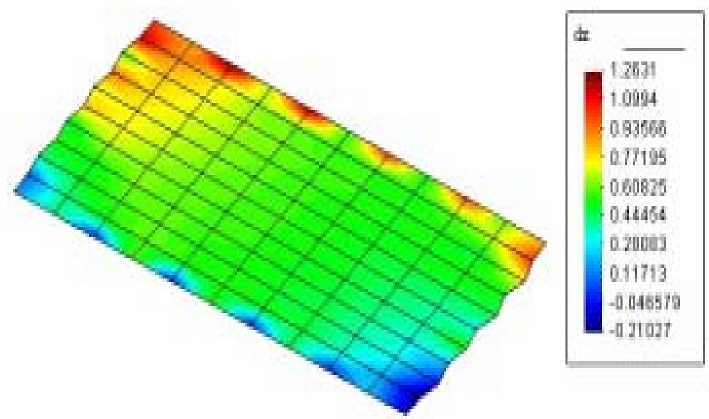

Meridional dir. displacement at rebar yielding

RCCV subjected to internal pressure

Specification < SNL, 2001 >

- Compressive strength of concrete (σ_c) : 46.0MPa
- Tensile strength of concrete (σ_t) : 3.45MPa
- Modulus of elasticity of concrete (E_c) : 33,100MPa
- Poisson's ratio of concrete (ν_c) : 0.20
- Yield strength of reinforcement (σ_y) : 450.0MPa
- Modulus of elasticity of reinforcement (E_s) : 214,000MPa
- Poisson's ratio of reinforcement (ν_s) : 0.30

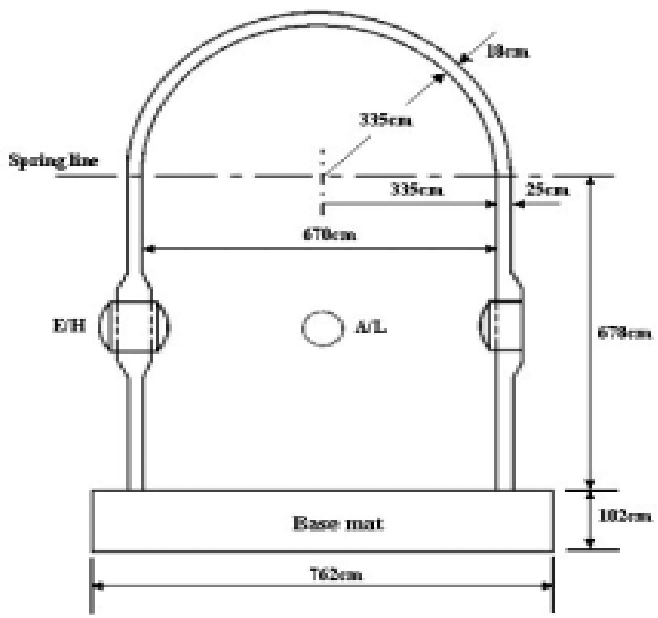

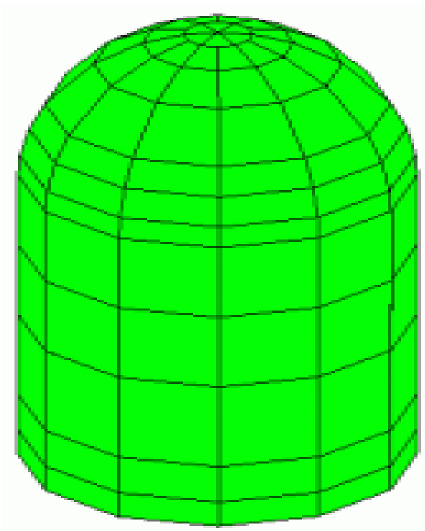

Modeling with or without considering foundation

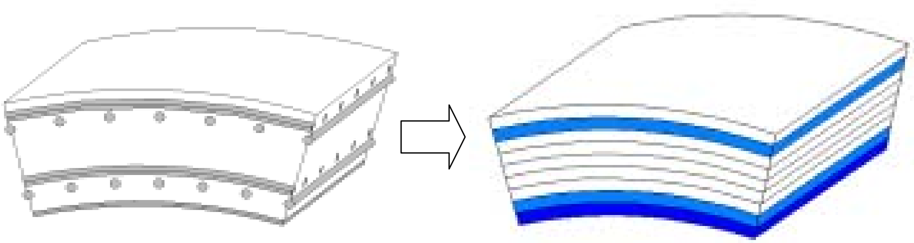

Layered shell element

Global behaviors

Radial displacement – Pressure relationship at mid-height

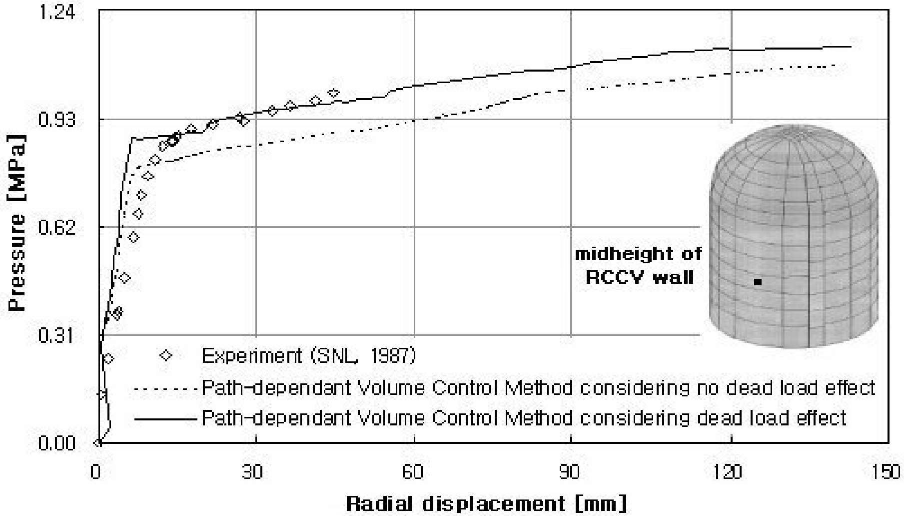

Vertical displacement – Pressure relationship at spring-line

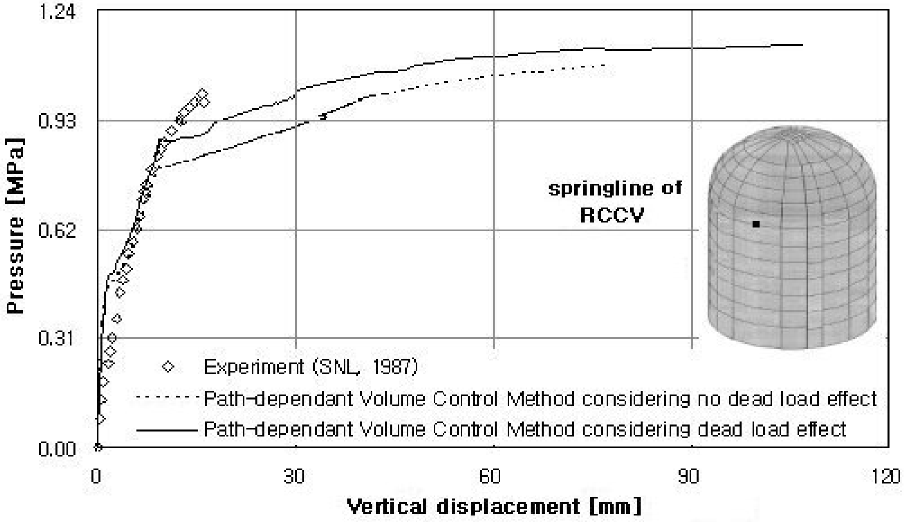

Crack patterns of RCCV

1.0Pd (0.31MPa)

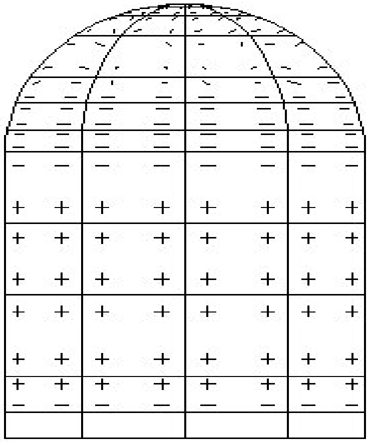

2.0Pd (0.62MPa)

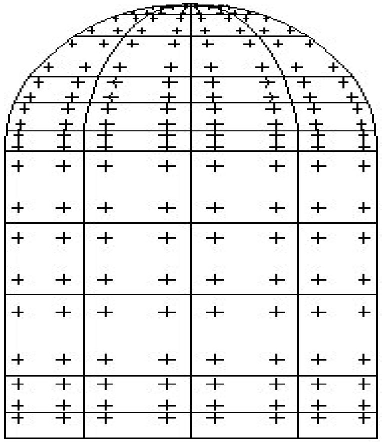

3.0Pd (0.93MPa)

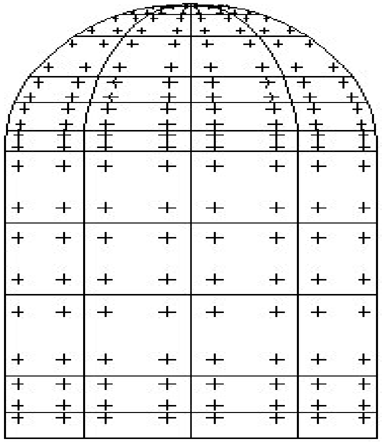

Deformed shape of RCCV

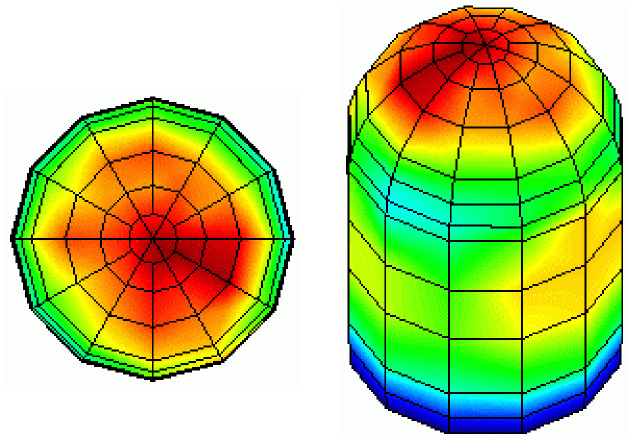

1.0Pd (0.31MPa)

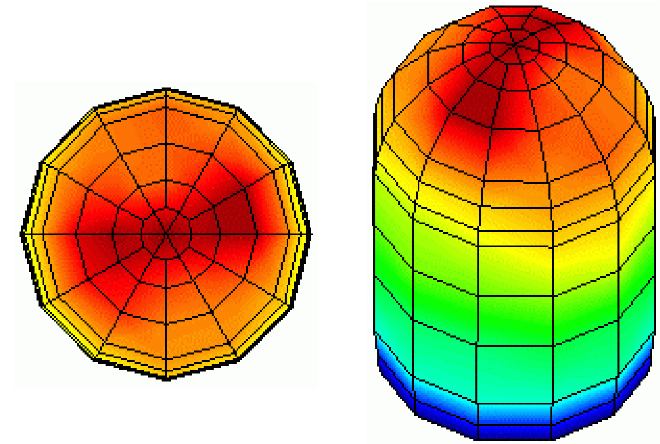

2.0Pd (0.62MPa)

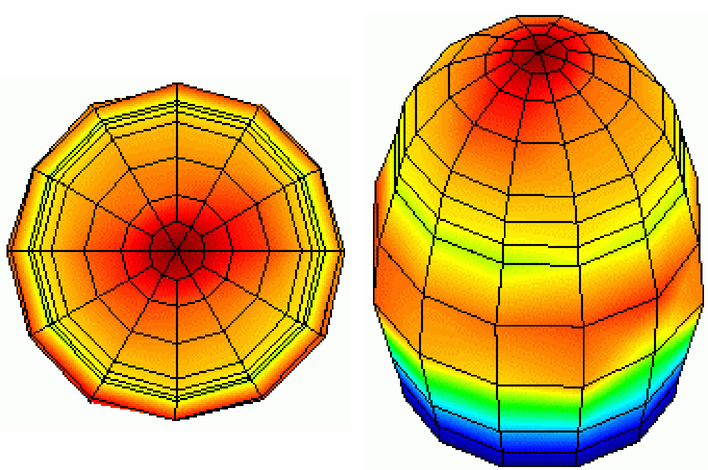

3.0Pd (0.93MPa)

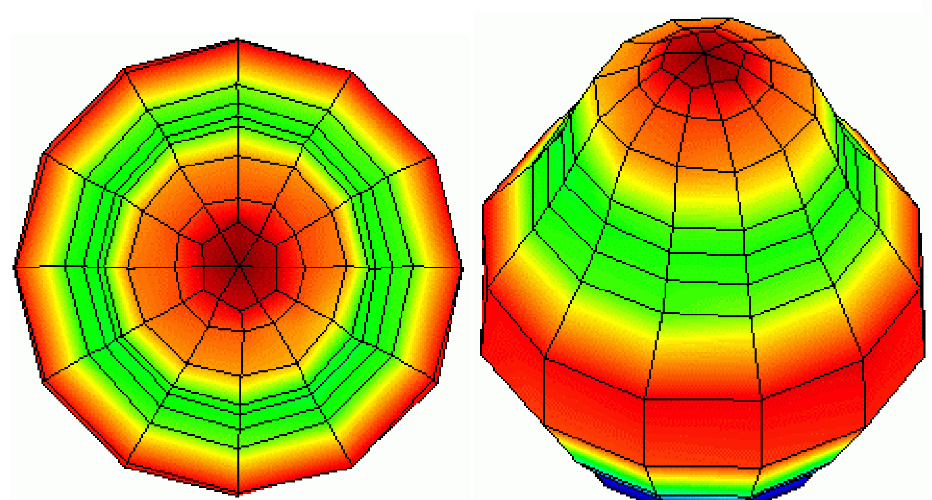

Ultimate pressure

RC tank subjected to reversed cyclic loading

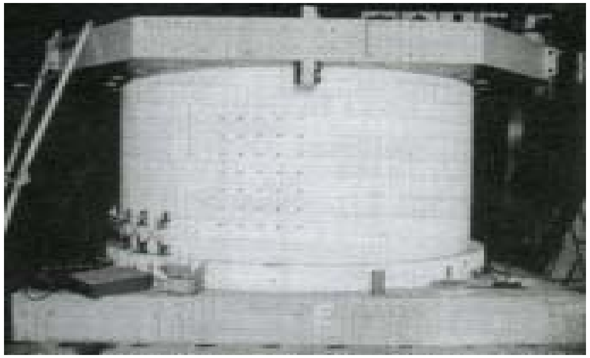

Specification < Harada et al., 2001 >

- Compressive strength of concrete (σ_c) : 28.0MPa
- Tensile strength of concrete (σ_t) : 2.20MPa
- Modulus of elasticity of concrete (E_c) : 22,600MPa
- Yield strength of reinforcement (σ_y) : 384.0MPa
- Modulus of elasticity of reinforcement (E_s) : 183,000MPa

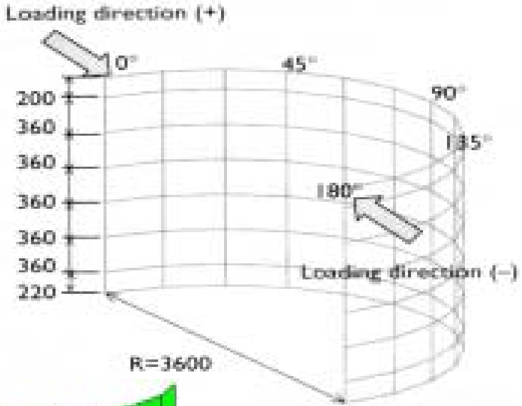

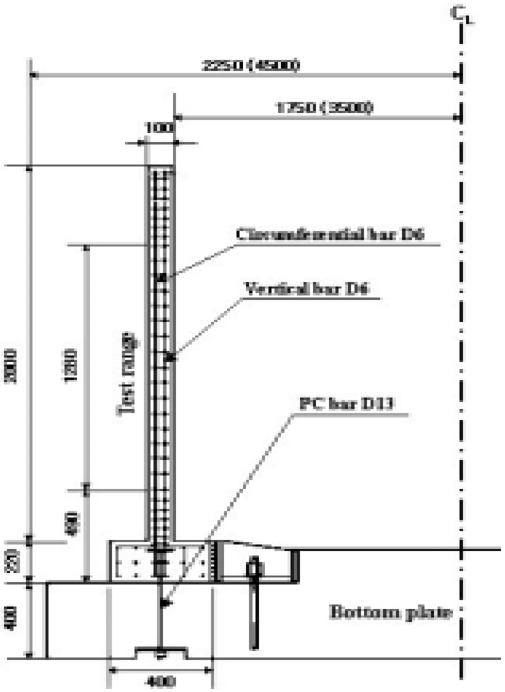

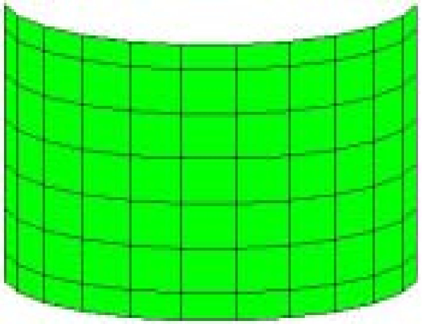

Modeling as shell element

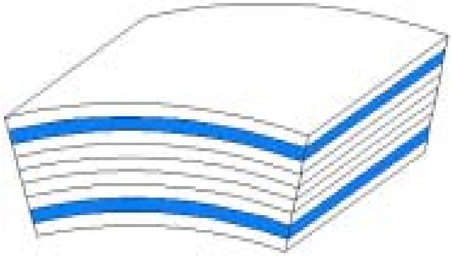

Layered shell element

Relative horizontal displacement - load curve

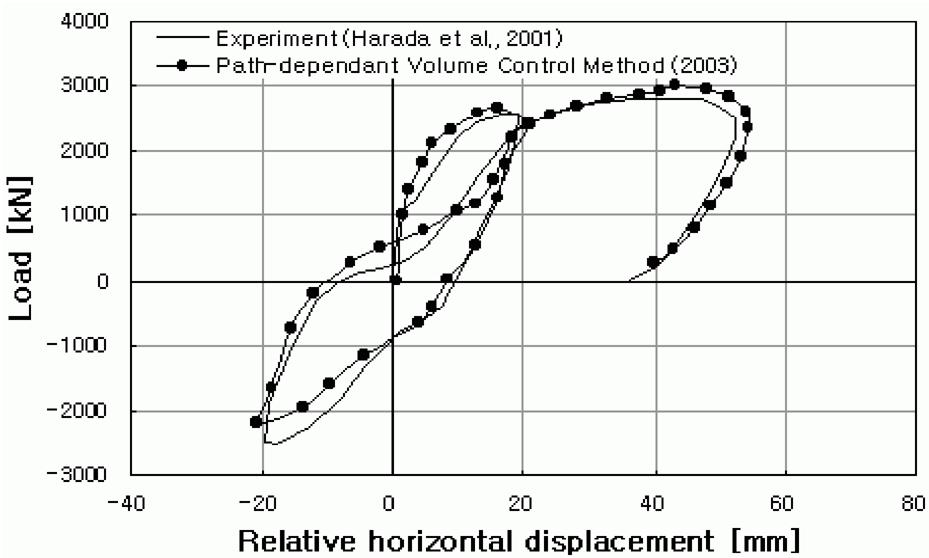

Comparison experiment result with path-dependant volume control result

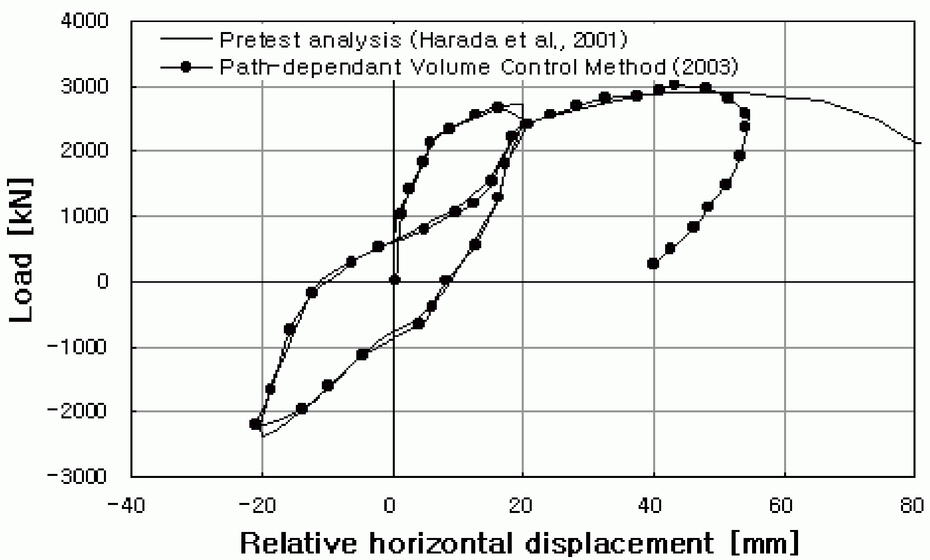

Comparison path-dependant volume control result with pre-test analysis result

Crack status of RC tank

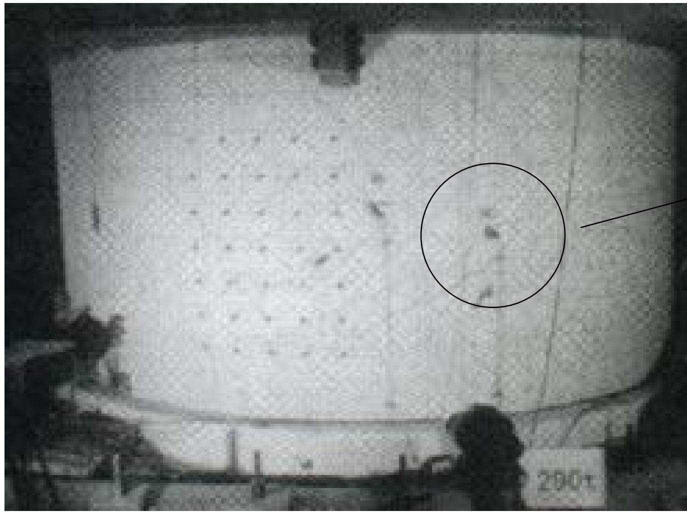

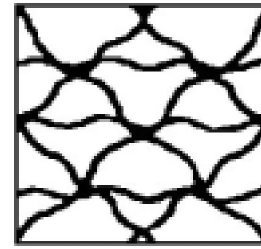

Multi-directional cracks occurrence
due to reversed cyclic loading

Crack status of RC tank by experiment

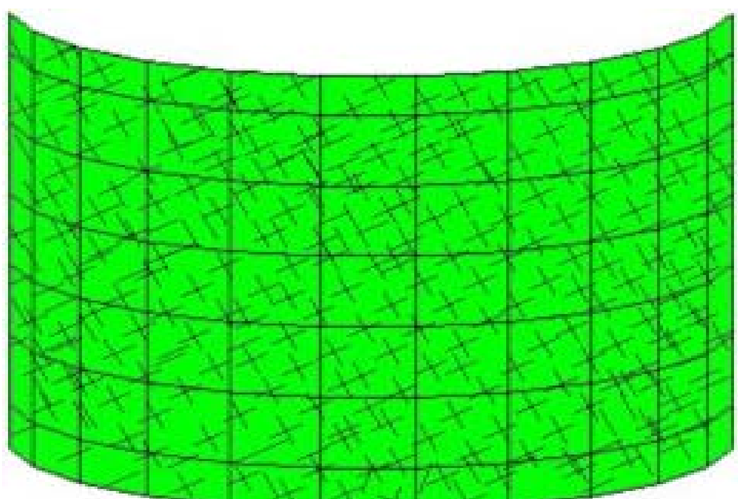

Crack status of RC tank by volume control analysis

Deformed shape of RC tank

Horizontal load = 3,037 kN

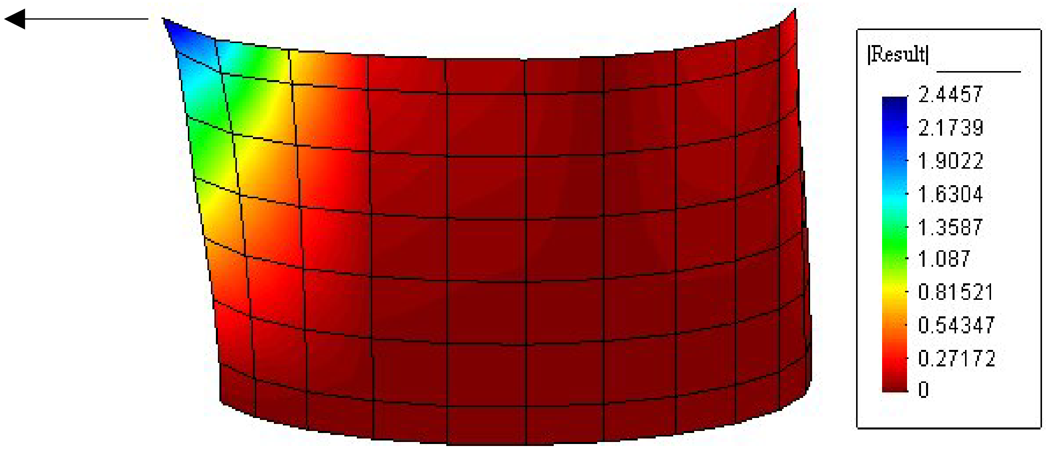

Horizontal load = -2,200 kN

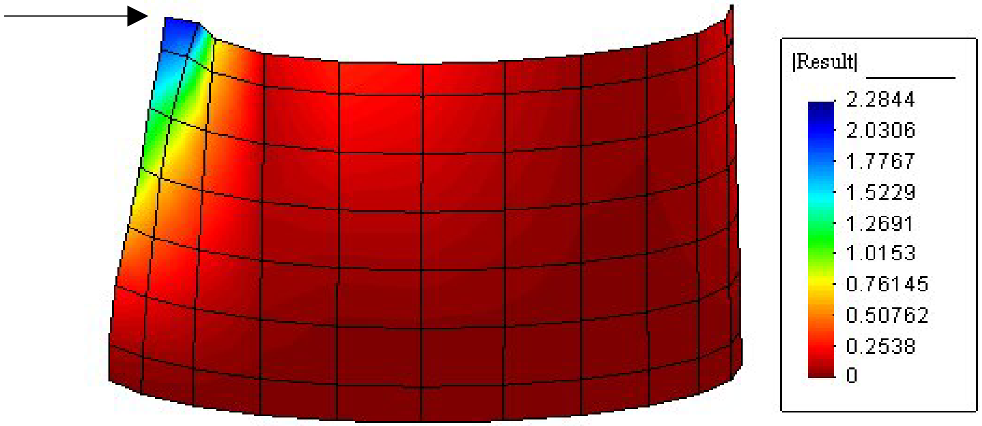

RC slab subjected to out-of plane cyclic loading

Specification < Irawan, 2001 >

- Compressive strength of concrete (σ_c) : 37.0MPa
- Tensile strength of concrete (σ_t) : 3.70MPa
- Yield strength of reinforcement (σ_y) : 380.0MPa
- Modulus of elasticity of reinforcement (E_s) : 206,000MPa

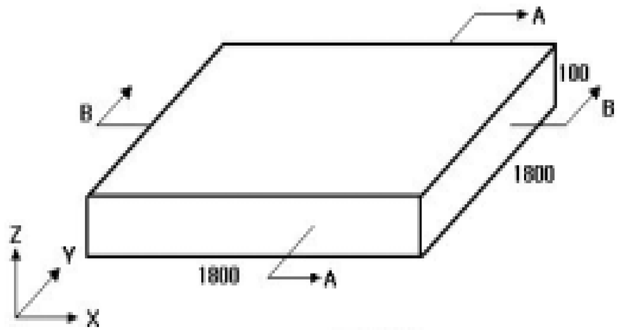

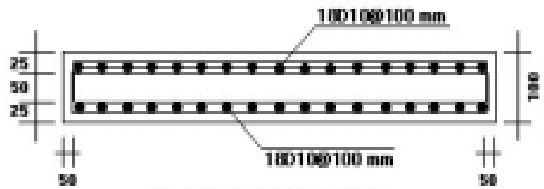

A – A Section (IS1 and IS2)

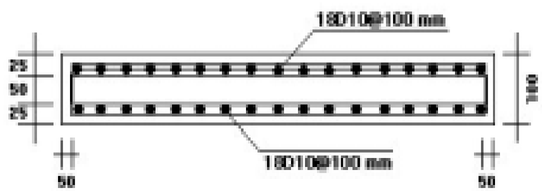

B – B Section (IS1)

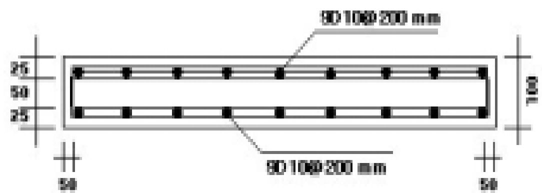

B – B Section (IS2)

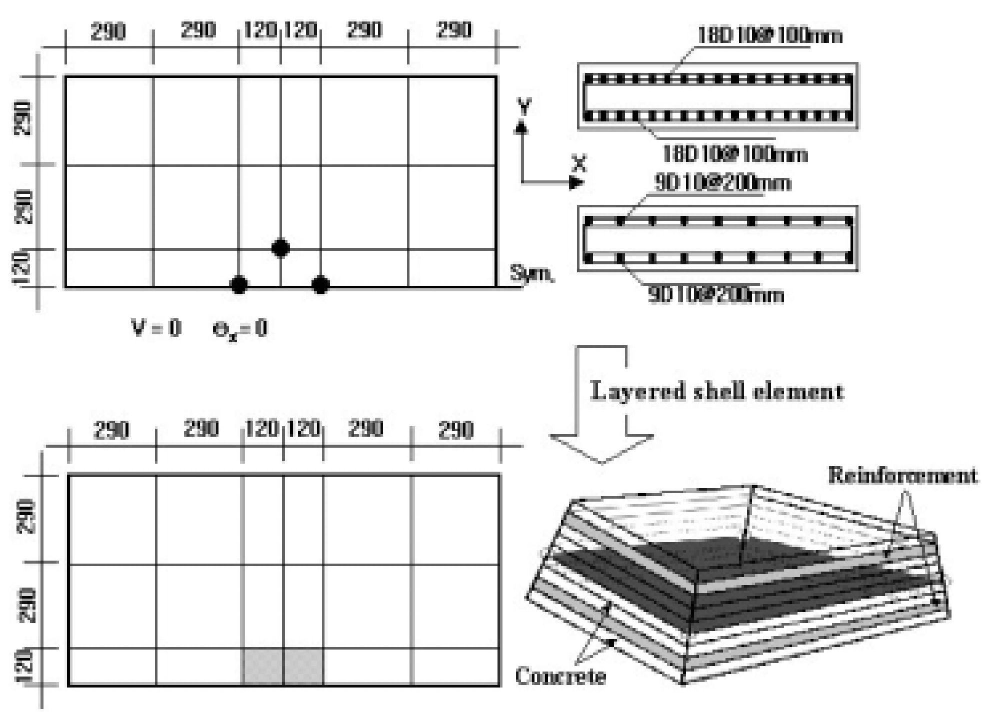

Central displacement - load curve

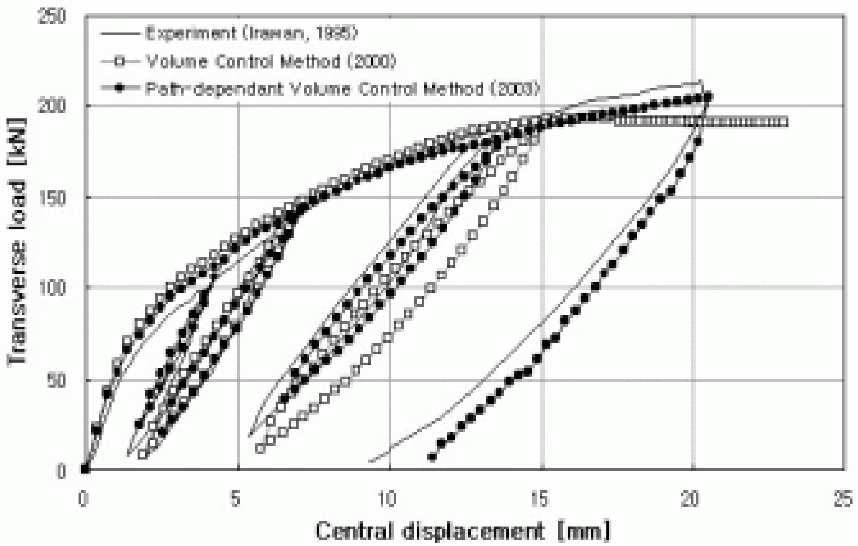

Comparison existing volume control result with path-dependant volume control result (IS1)

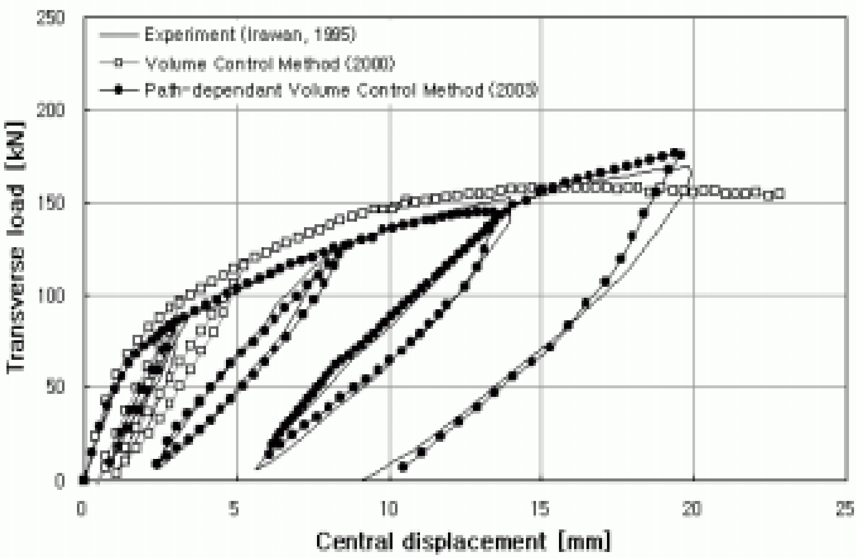

Comparison existing volume control result with path-dependant volume control result (IS2)

Analysis result according to number of layered shell element

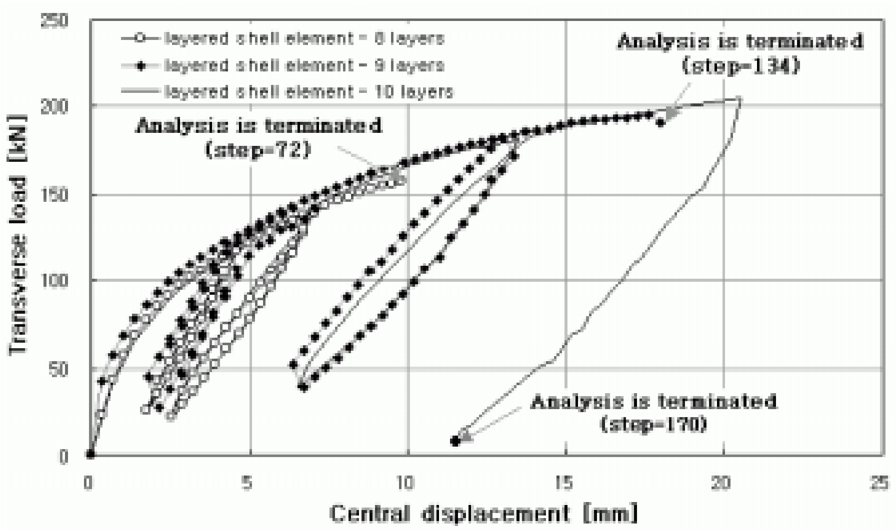

Analysis result according to number of layered shell element

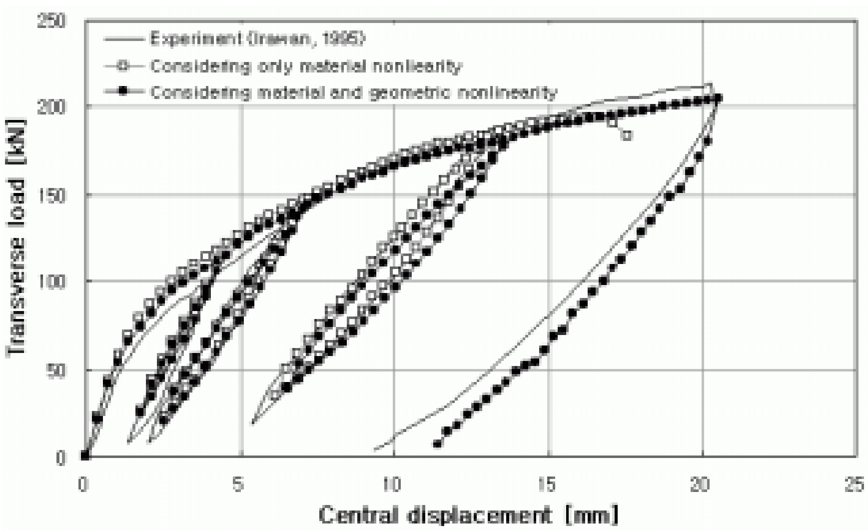

Crack status of RC slab

Specimen IS1 : vertical load = 193 kN

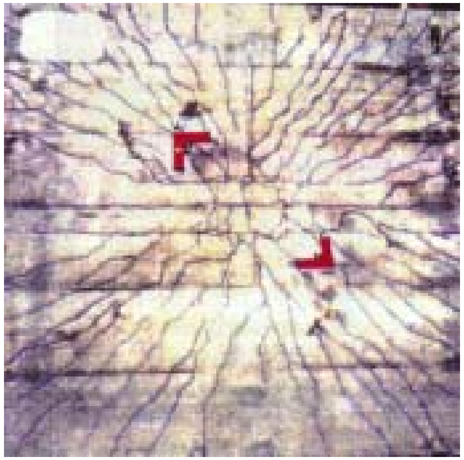

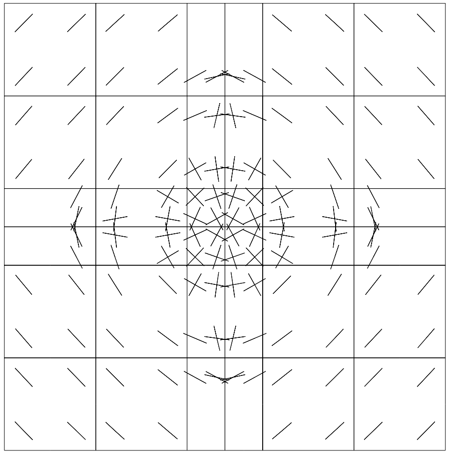

Specimen IS2 : vertical load = 193 kN

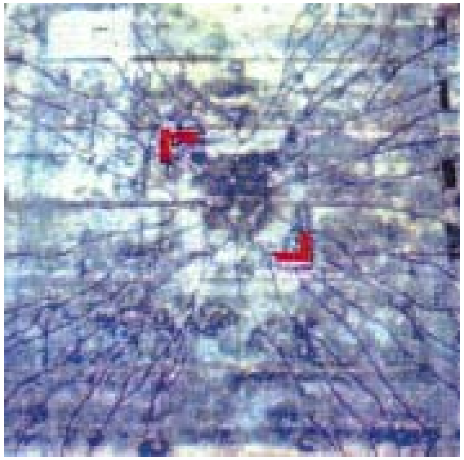

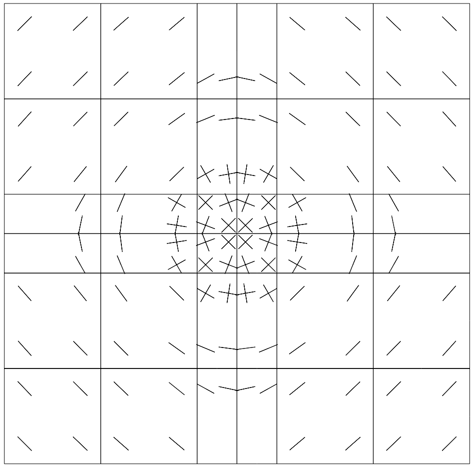

Deformed shape of RC slab

Specimen IS1 : vertical load = 178 kN

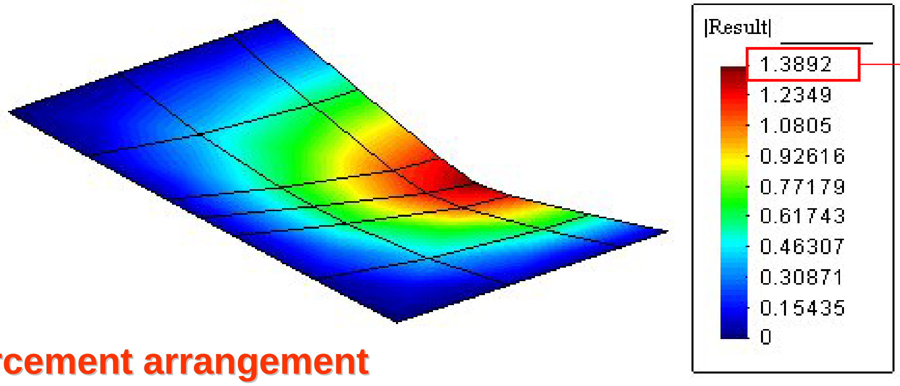

Isotropic reinforcement arrangement

Specimen IS2 : vertical load = 144 kN

Stiffness of IS1 > Stiffness of IS2
Due to reinforcement arrangement

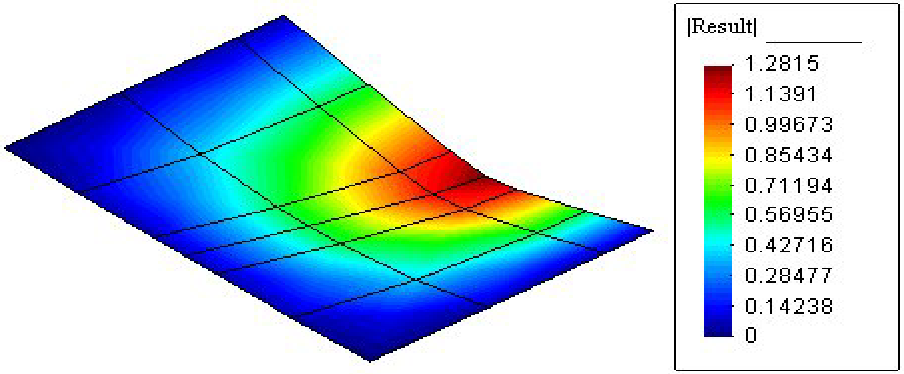

Anisotropic reinforcement arrangement

RC box culvert subjected to cyclic loading

Specification < Irawan, 1995 >

- Compressive strength of concrete (σ_c) : 50.0MPa
- Yield strength of reinforcement (σ_y) : 500.0MPa

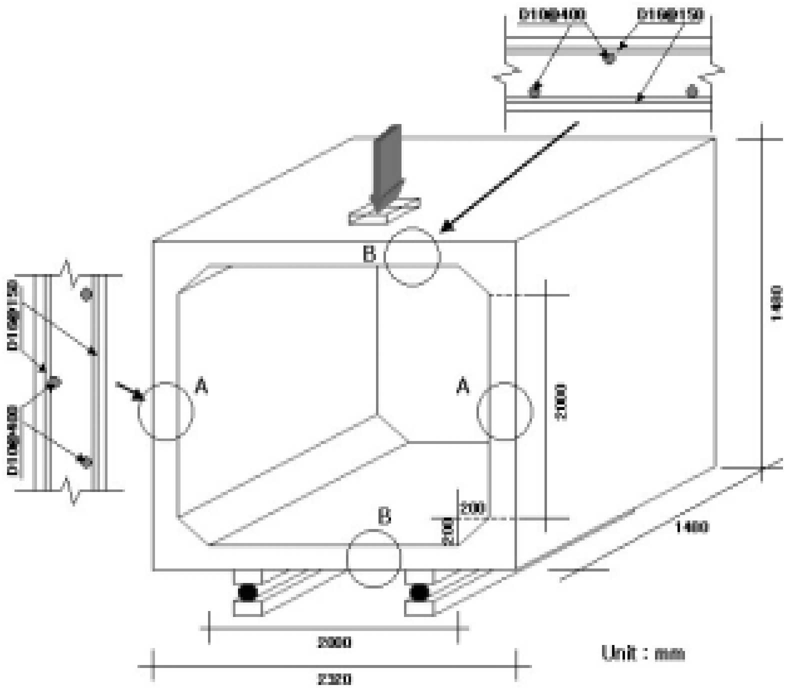

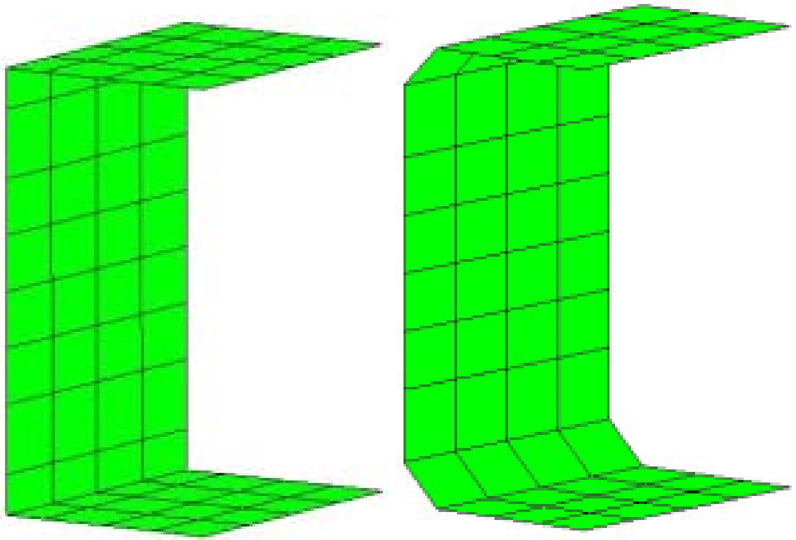

Modeling with and without considering haunch

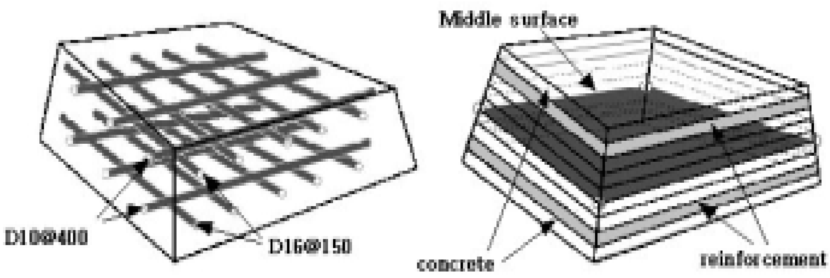

Layered shell element

Load-deflection curve of RC box culvert

Static failure load : 48 tonf

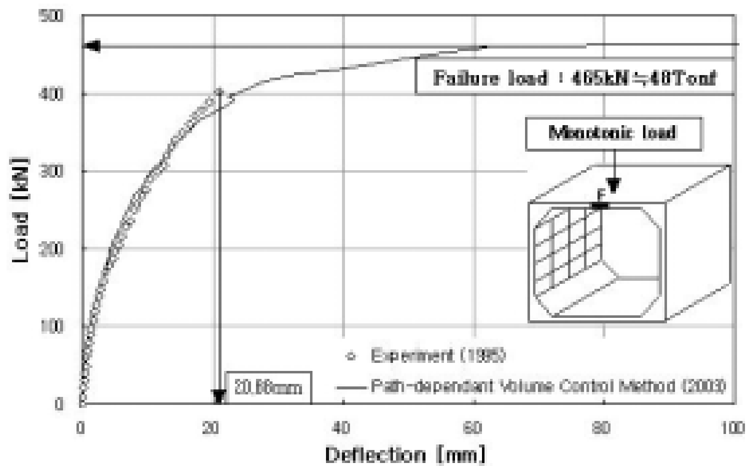

Model of considering without considering haunch

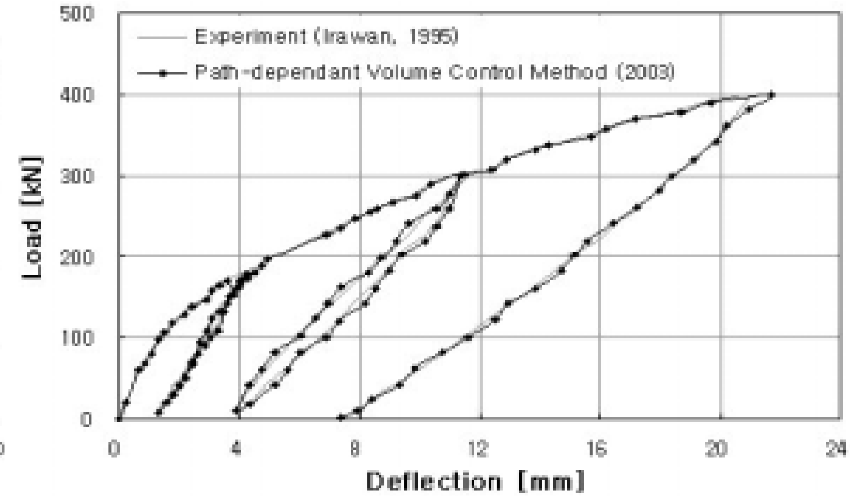

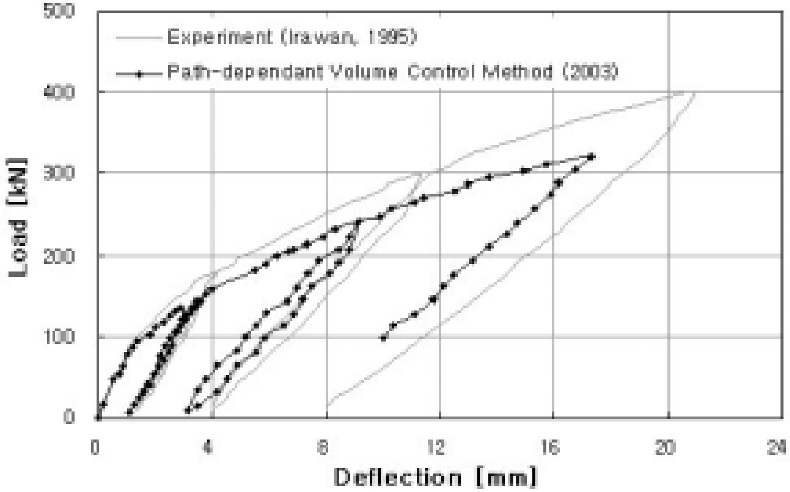

Model of considering with haunch is reinforced concrete layer

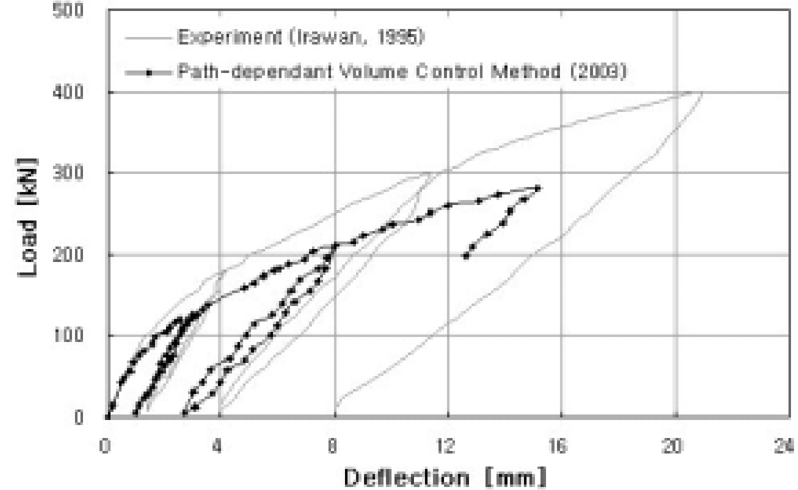

Model of considering with haunch is plain concrete layer

Crack status of RC box culvert

Wall of RC box culvert

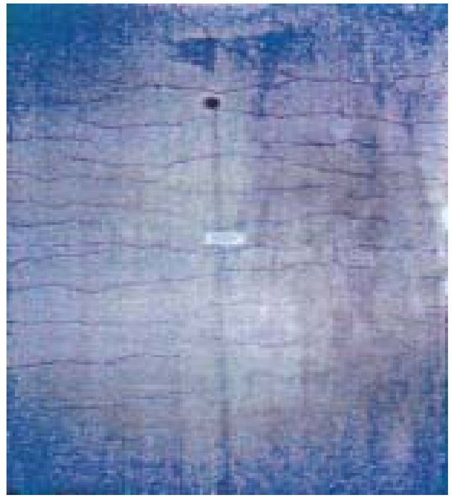

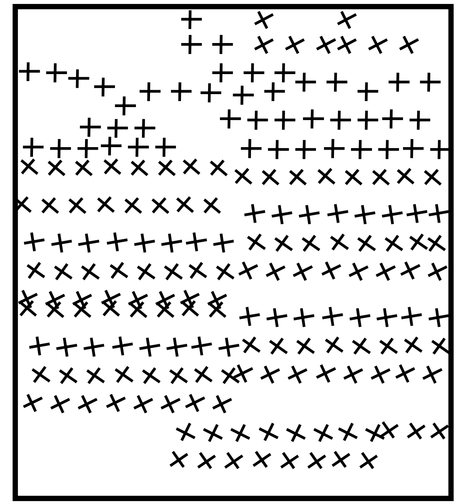

Top slab and wall of RC box culvert

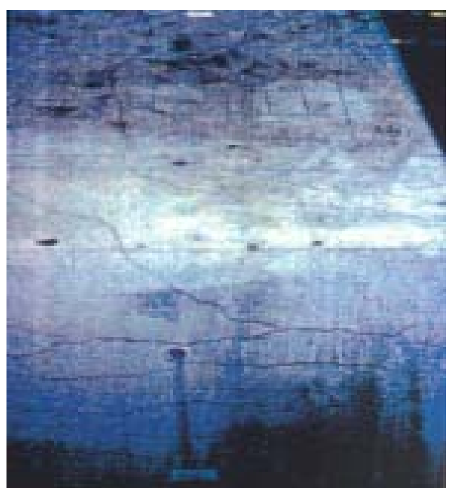

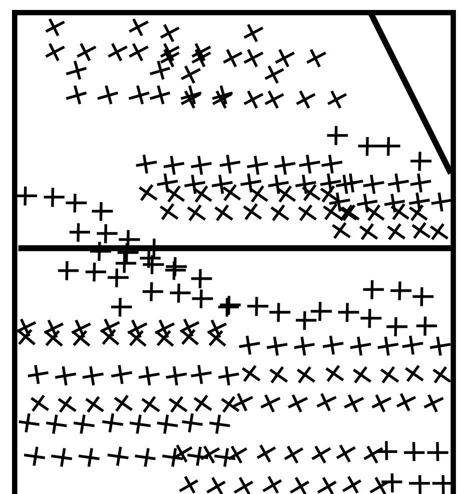

Deformed shape of RC box culvert

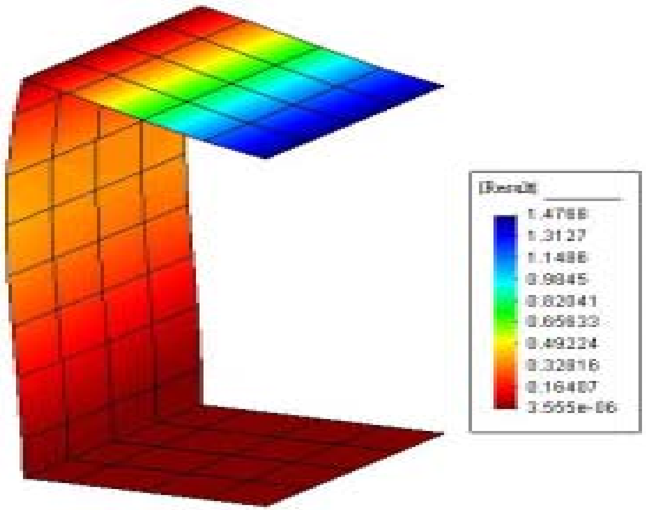

Model of considering without haunch

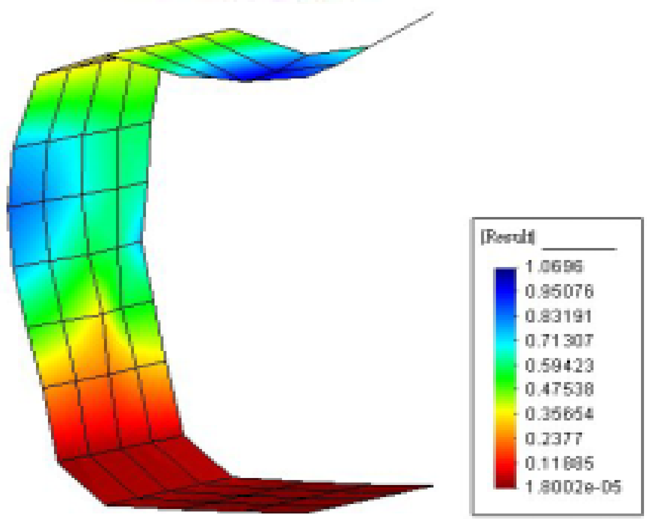

Model of considering with haunch is reinforced concrete layer

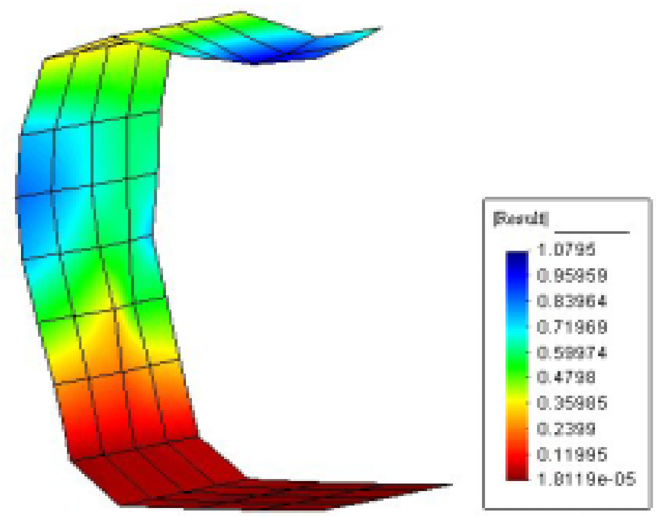

Model of considering with haunch is plain concrete layer

RC hollow column under lateral loading

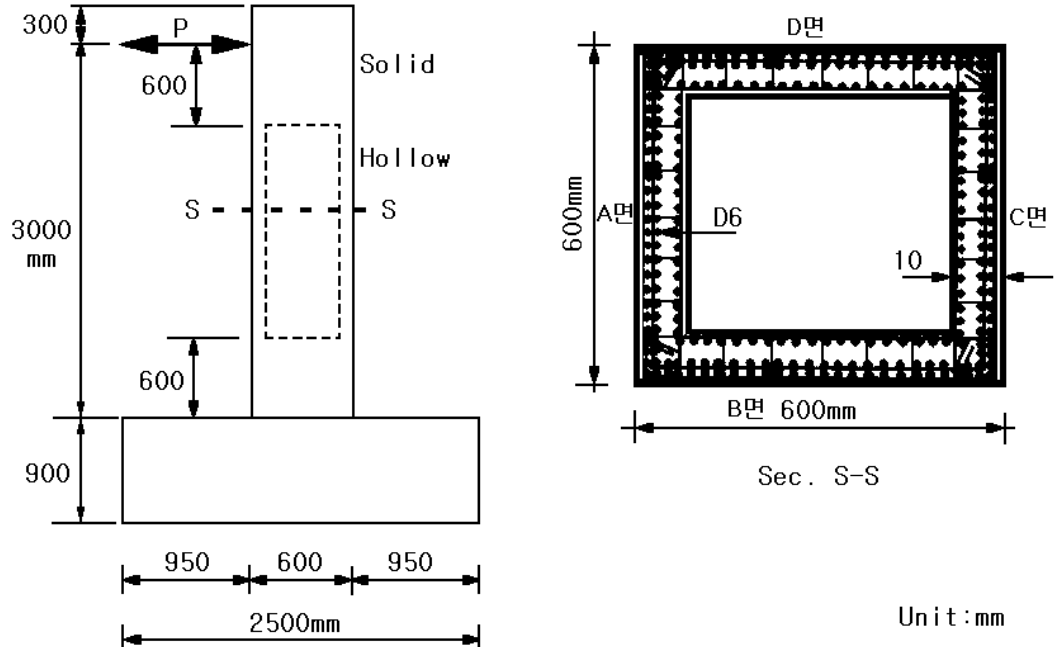

Concrete		Reinforcement	
f_c	76.5 MPa	f_y	350 MPa
E_c	31.4 GPa	f_u	421 MPa
ν	0.21	E_s	200 MPa
f_t	2.63 MPa		

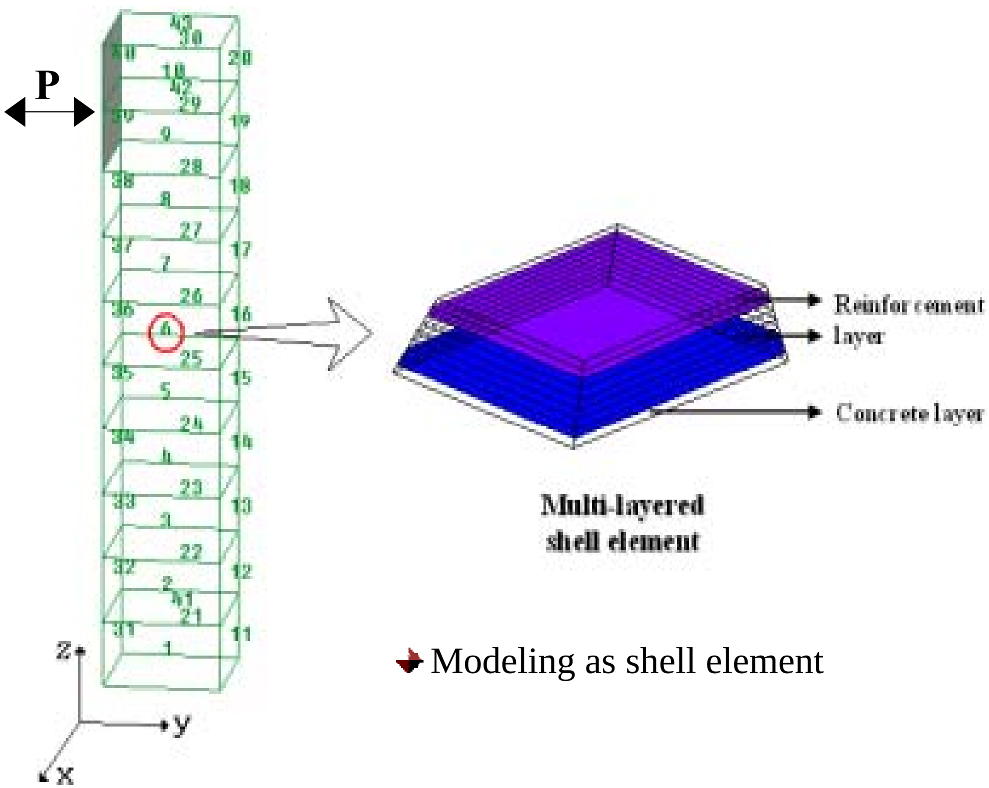

Modeling as shell element

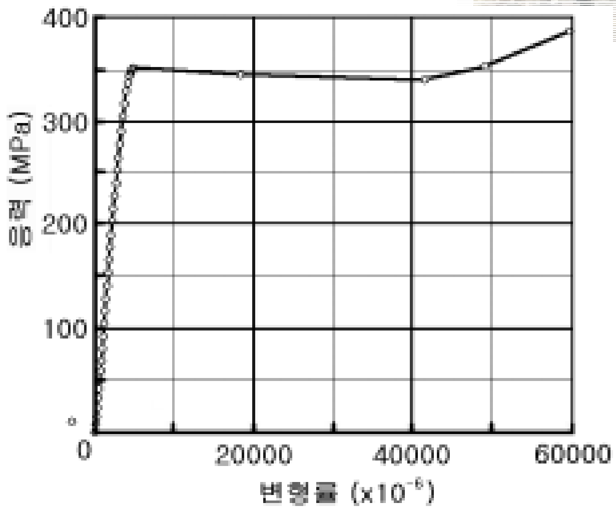

(a) Steel

Stress-strain curve of concrete and reinforcing steel

(Masukawa et al., 1997)

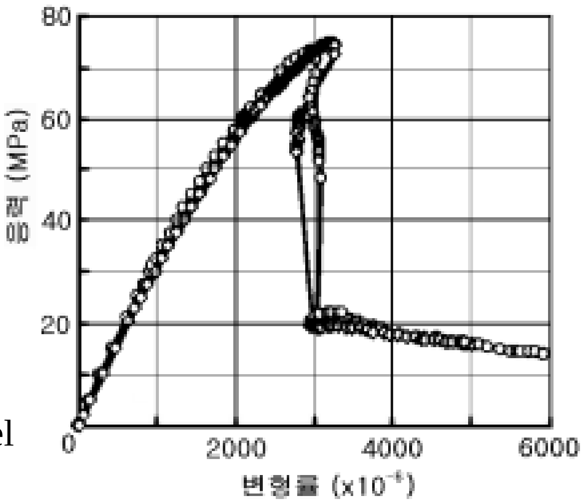

(b) Concrete

Load-displacement curve

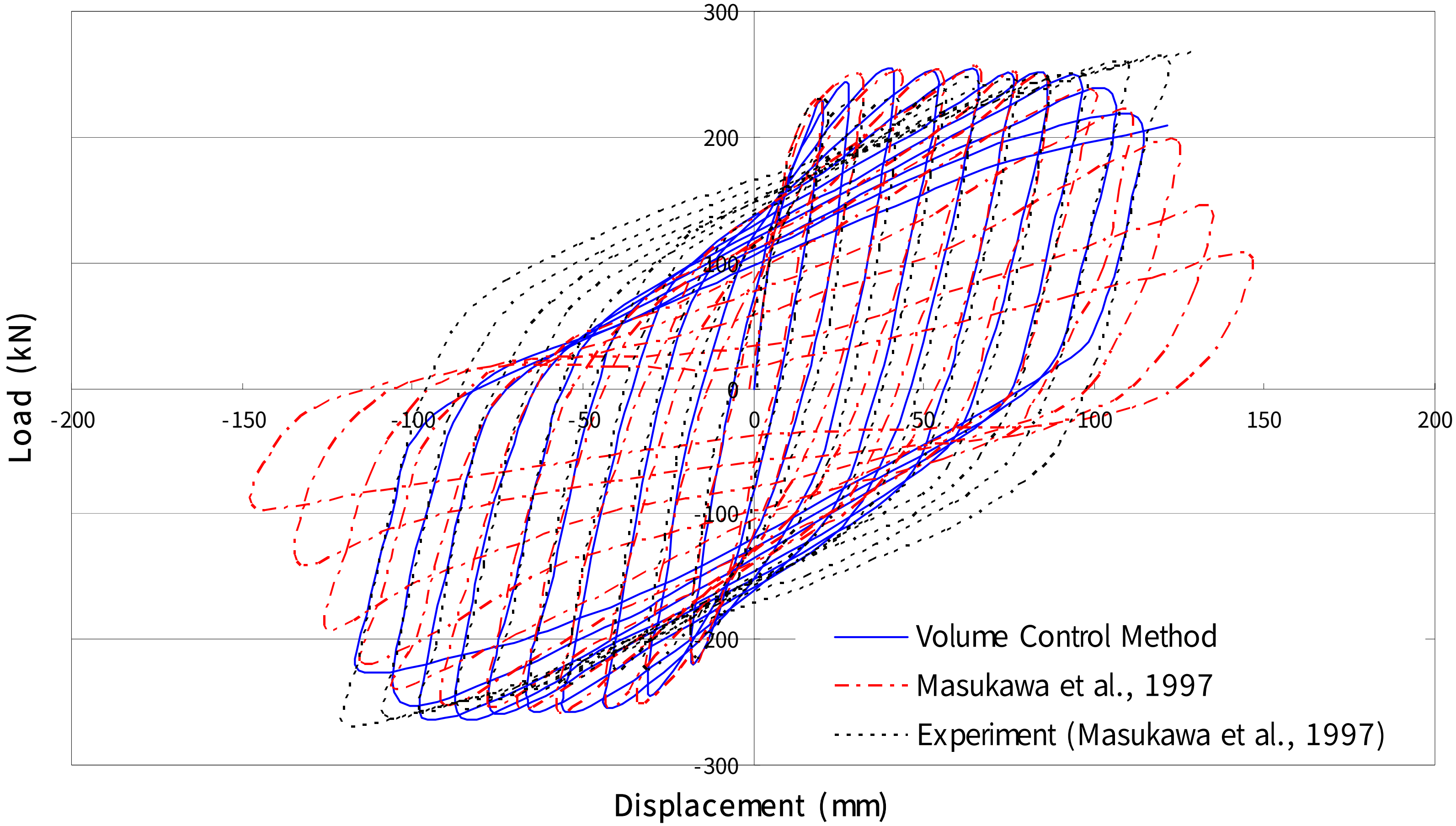

Masukawa et al., “Development of RC column members in use of high strength reinforcement”, Proceedings of JCI, Vol. 19, No. 2, pp. 557-564, 1997

Contour

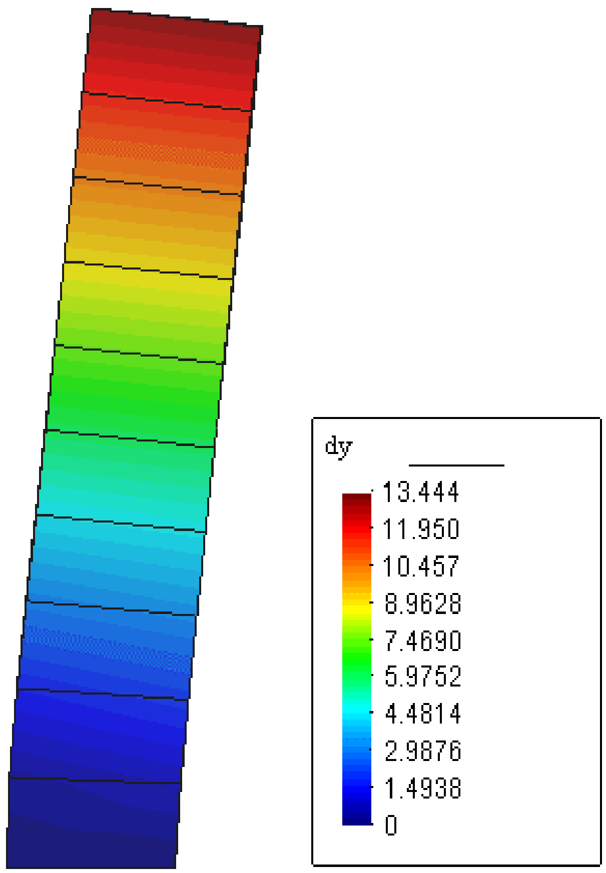

(a) At final compression

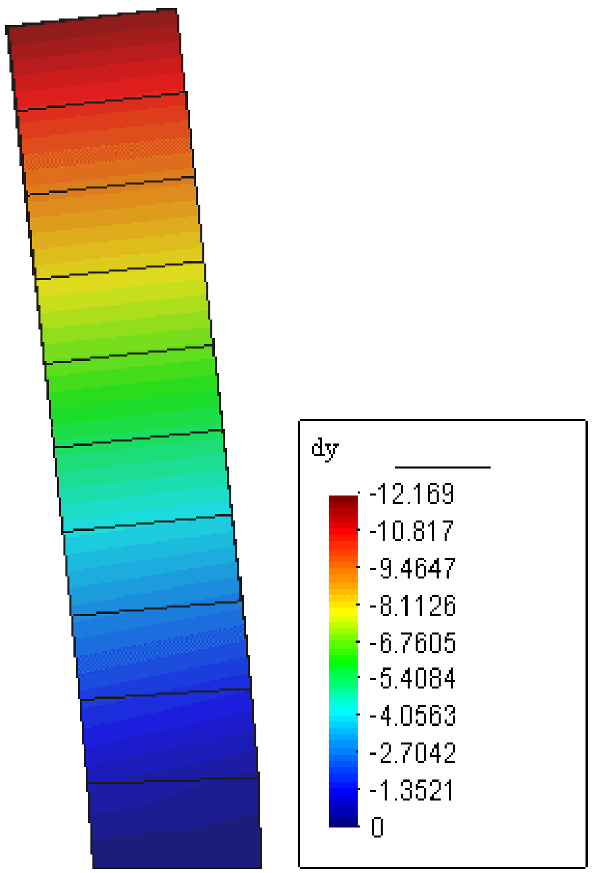

(a) At final tension

Crack patterns

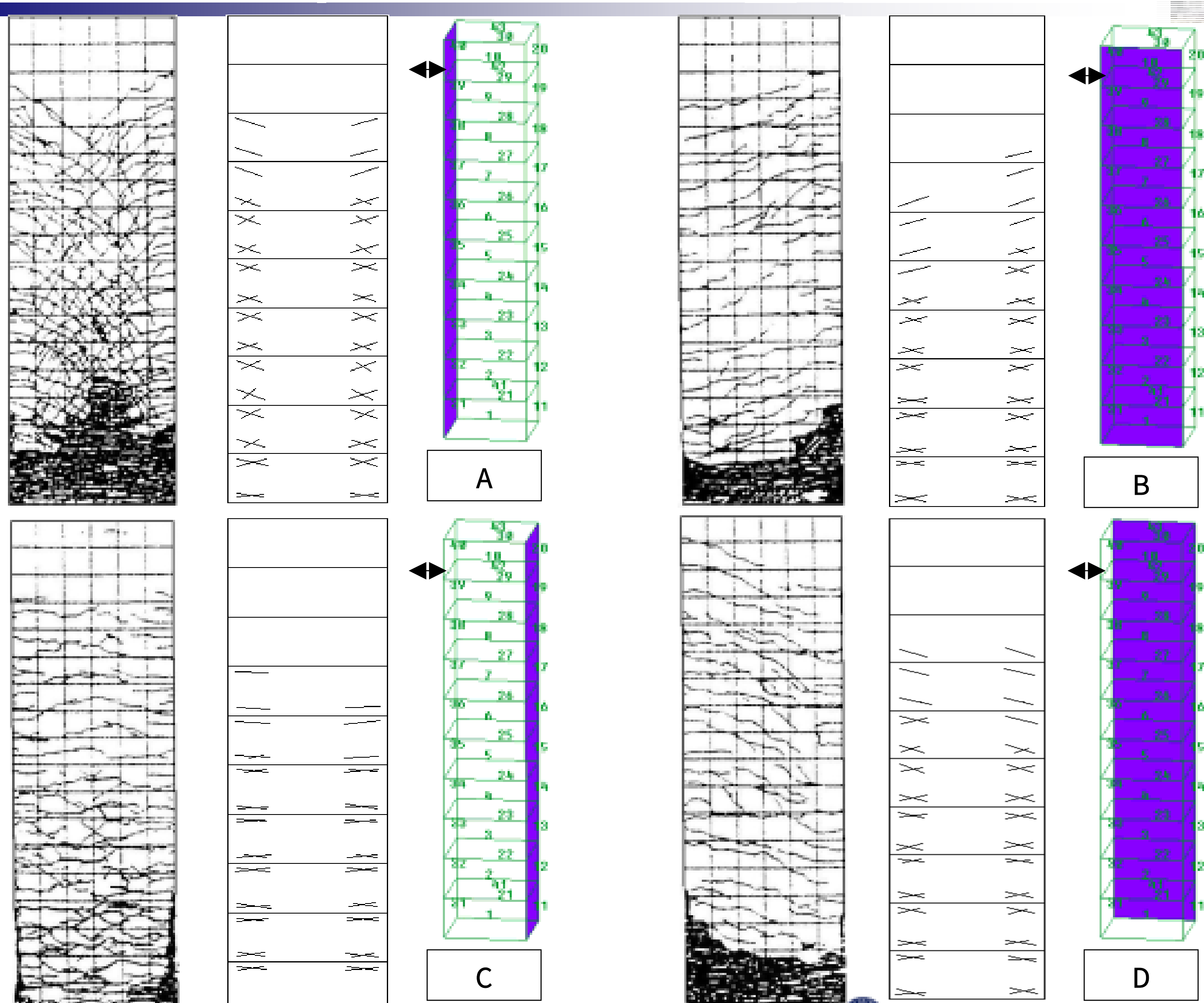

Analysis of 1/4 prestressed concrete containment vessel(PCCV)

Sandia National Laboratories, Albuquerque, New Mexico,2000

Tendon layout

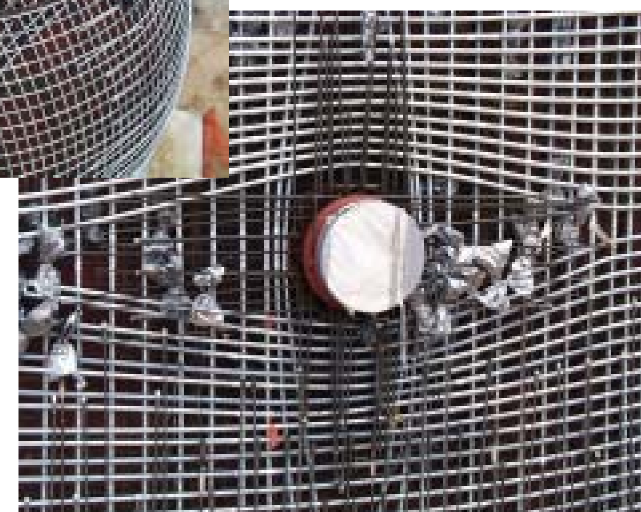

Unbonded tendon

Characteristics of Model Test and Analysis

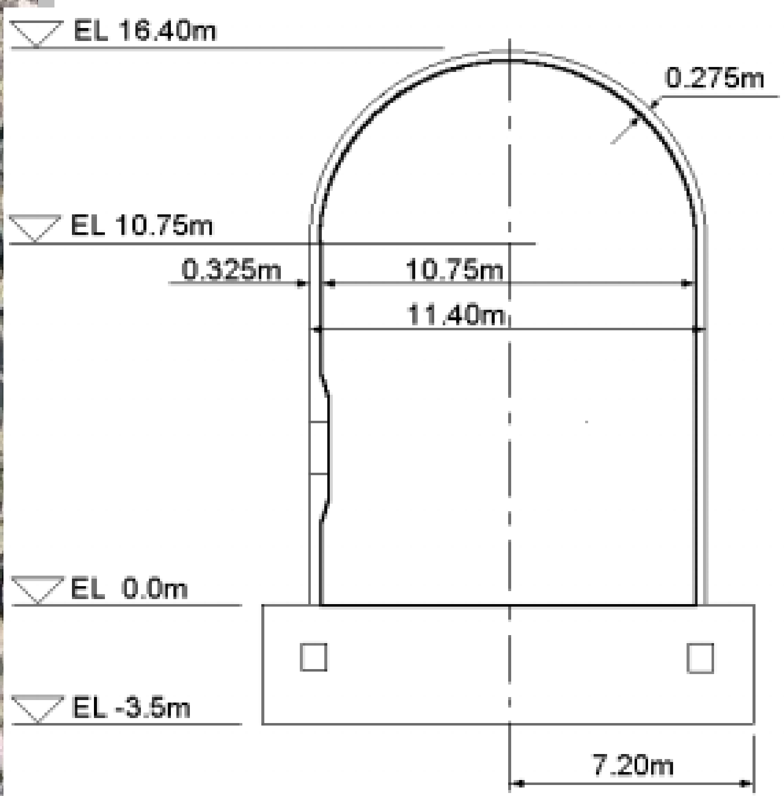

1/4 Scale PCCV model

- The first model test to satisfy material and design details of design code (ASME Sec. III, Div.2)
  - limit state test (LST) and structural failure mechanism test (SFMT)
  - Large scale model including openings and steel liners
- 3D finite element modeling including tendons, rebars and openings using DIANA
  - Pre-test analysis
  - Post-test analysis
- Introduction of volume control technique

Model Tests (Failure Test due to Internal Pressure)

- Limit state test (LST)
  - Pressurized by nitrogen gas
  - Structural soundness test & leakage test
  - $1.5P_d$, $2.0P_d$, $2.5P_d$ and $3.3P_d$

    (P_d = 0.39 MPa)
  - Functional failure due to leakage was occurred at $3.3P_d$ due to tearing of liner

- Structural failure mechanism test (SFMT)
  - Pressurized by water
  - Structural failure at $3.6P_d$

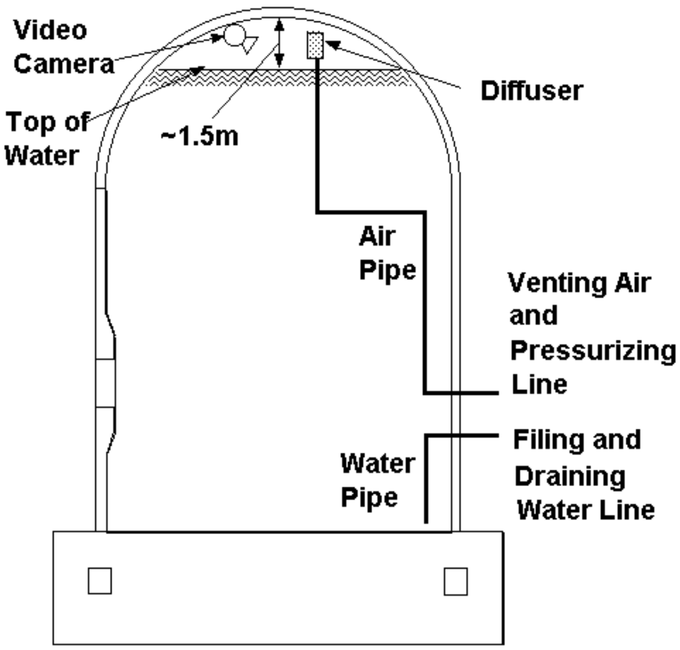

Structural Failure Mechanism Test (SFMT)

LST test result

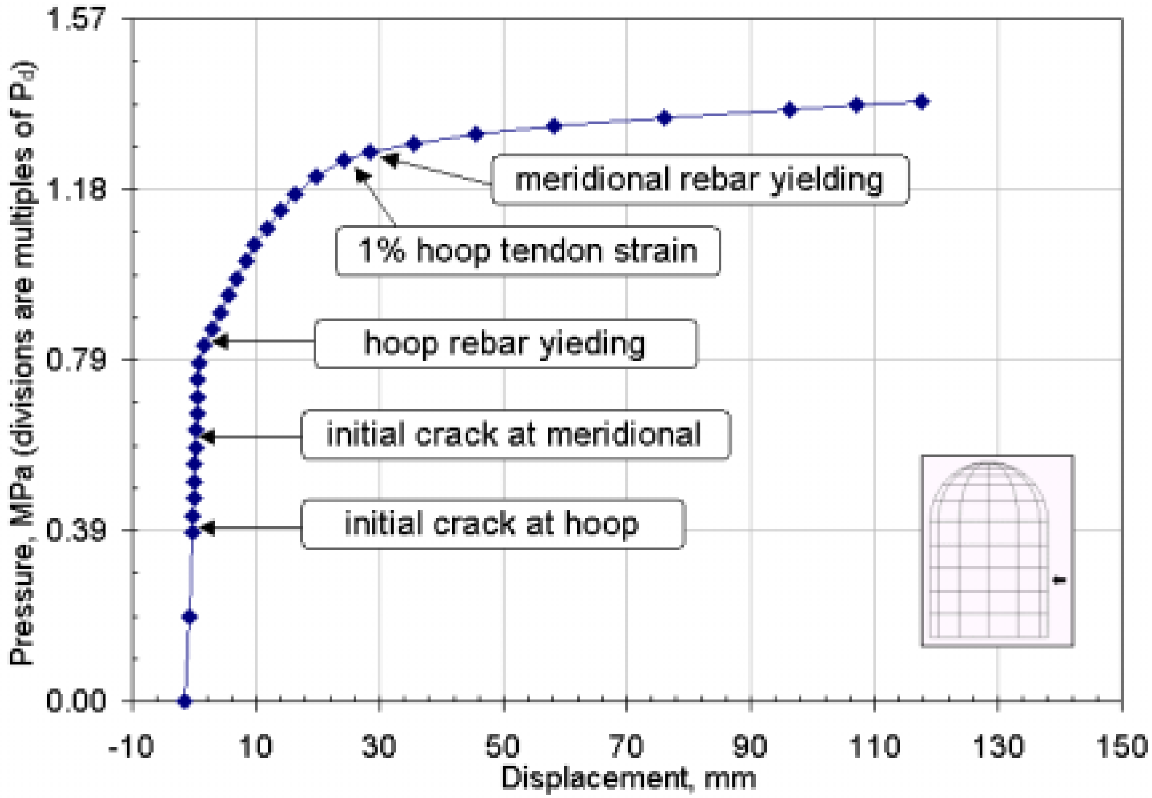

-Hoop directional deformations govern PCCV behaviors

Test result and comparison with the analytical results

Deformation profile at 135° section (magnified ×100)

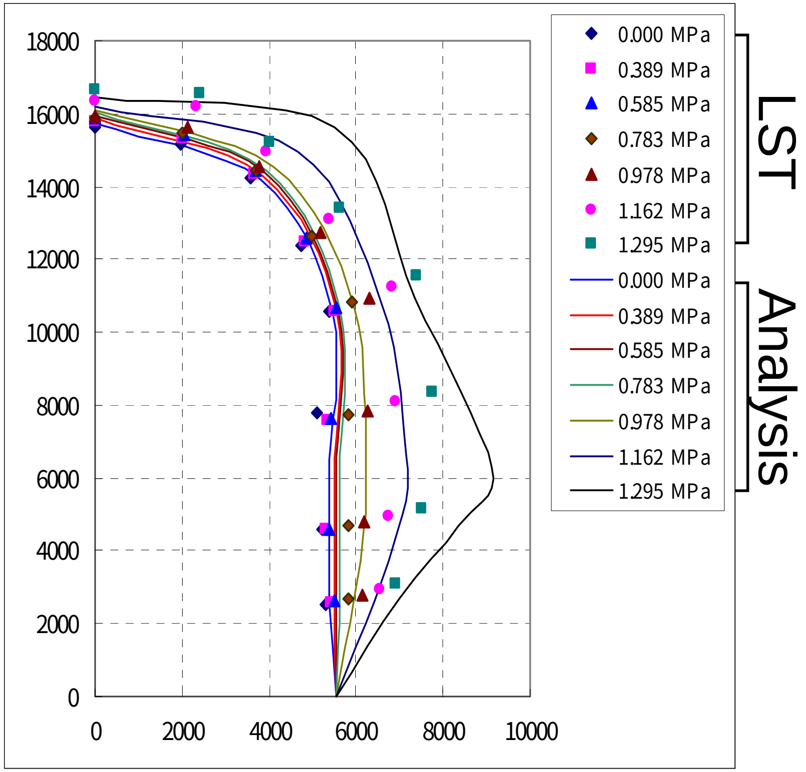

- For higher pressure, analysis generally predicts larger deformations than those by the test
- The analysis comparably well predicts the global behavior

LST results

Pressure/Pd	Leakage Rate*	Observation
1.5	0.5	no leakage
2.0		no evidence of distress
2.5	1.6	liner strain: 2% evidence of liner tear
3.0		difficult to increase pressure
3.1	100	
3.3		
Final	900	

* volume change (%) per day (V/Day)

**Permissible leakage rate for design pressure:

(pressurized water reactor with steel liner) 0.1% V/Day

Comparison

- **Deformations**

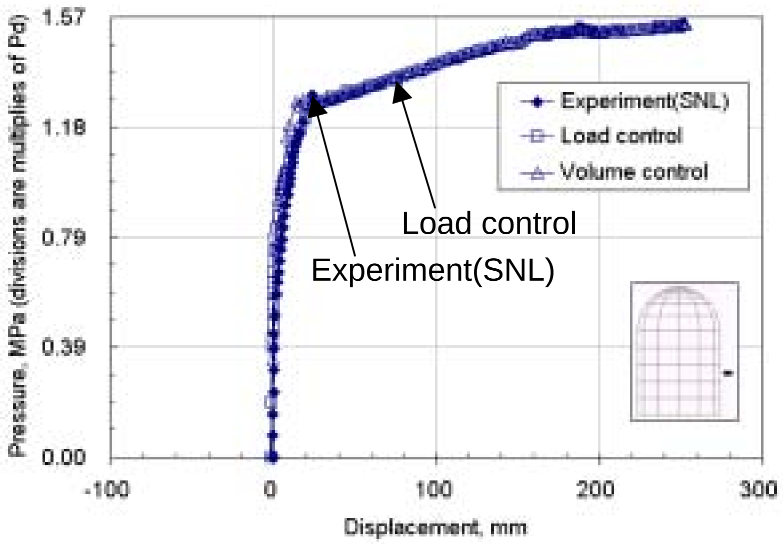

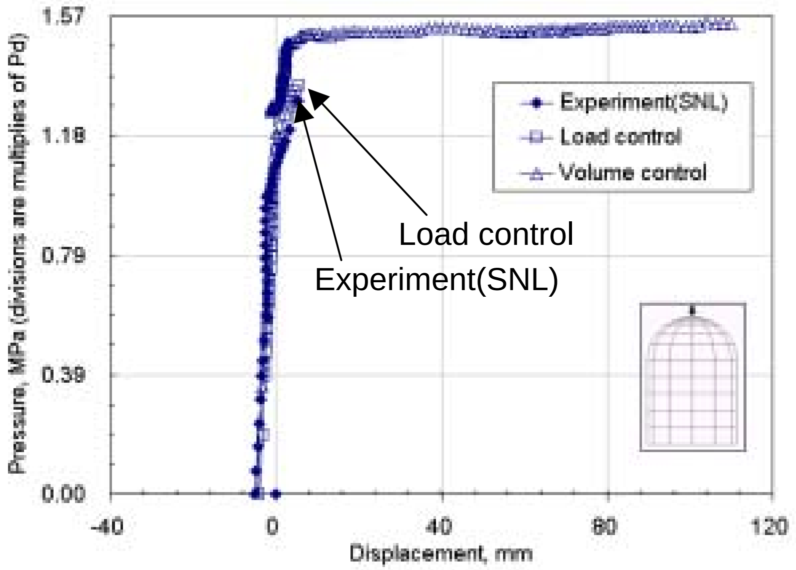

Radial displ. at midheight

Vertical displ. at dome apex

- More stable solution is possible with volume control technique

Rebar stains

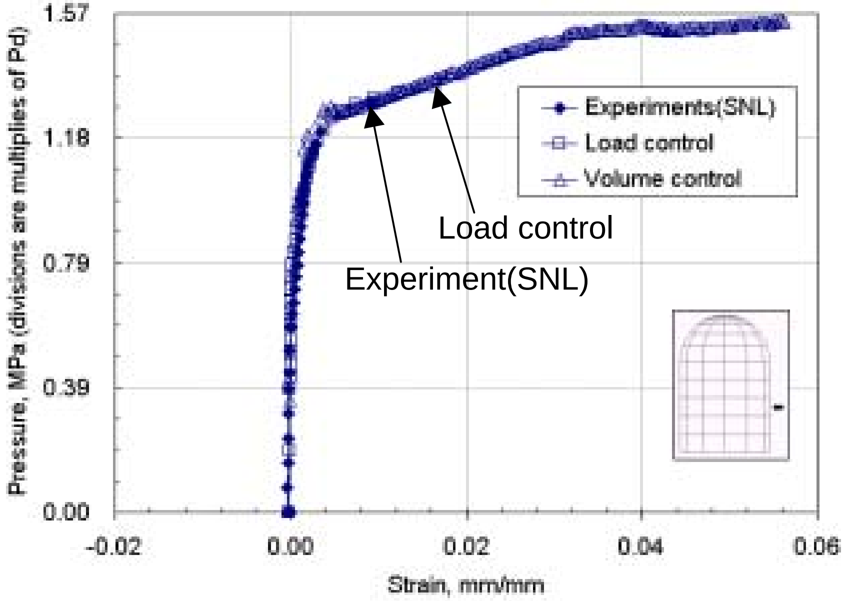

Outer rebar hoop strain at midheight

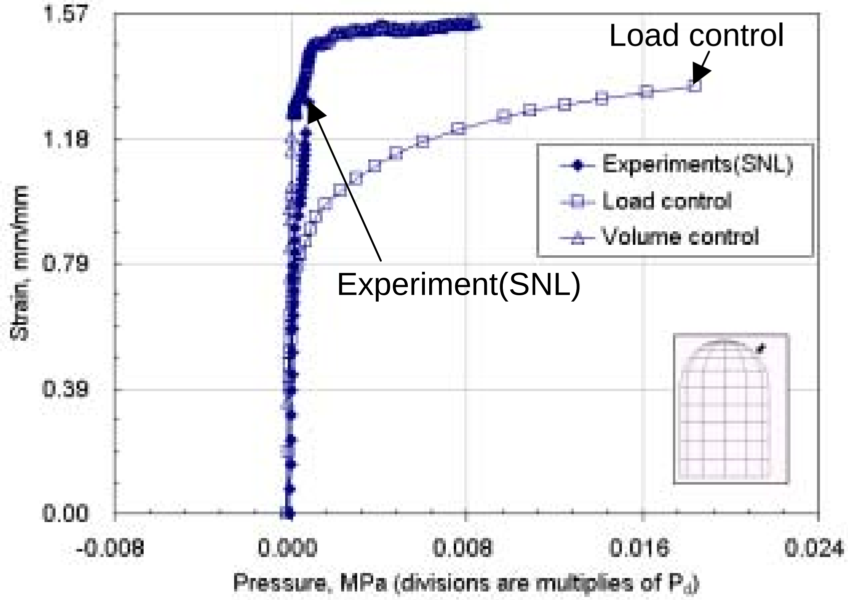

Outer rebar hoop strain at dome 45°

Conclusions and future work

- For the failure analysis of RC shell structures using FEM, both material and structural instability problems can be solved effectively by the homogenized crack model and the volume control technique.
- In-plane constitutive laws of cracked concrete and modified Barcelona model can be useful for the modeling of the layered RC shell element and ECC repaired layers.
- Failure analysis or performance evaluation of the deteriorated RC shell structures repaired with the ECC layers is now under carried out.

Thank you for
your kind attention!

song@yonsei.ac.kr